

## ANNEXE 8

Modélisation hydrodynamique





HYDRODYNAMIC AND SEDIMENT DYNAMICS  
MODELING  
ANSE DU MOULIN

BAIE-COMEAU



HYDRODYNAMIC AND SEDIMENT DYNAMICS MODELING  
ANSE DU MOULIN

BAIE-COMEAU

Presented to

ALCOA

By

GENIVAR inc.

SEPTEMBER 2012

111-21002-00



## **TEAM WORK**

---

### **ALCOA**

Project Manager, Alcoa Remediation Team : Larry McShea

Environmental Representative  
– AADM Project Team : Jean-Pierre Barry

### **ANCHOR QEA**

Project Leader : Marc Mahoney

### **GENIVAR inc.**

Project Leader : Steve Renaud, ing., M. Sc.

Project Manager : Nicolas Guillemette, ing., M. Sc.

Modeling Lead : Pierre Dupuis, ing., M. Sc.  
Vincent Métivier, ing. Jr, M. Sc.

Oceanographer : Marc Pelletier, M. Sc.

---

### **Référence à citer :**

GENIVAR. 2013. *Hydrodynamic and sediment dynamics modeling*. Anse du Moulin. Baie-Comeau. Rapport de GENIVAR à 111-21002-00 (ALCOA). 62 p.





# TABLE OF CONTENTS

	<i>Page</i>
Team Work .....	i
Table of contents .....	iii
List of table .....	v
List of figures .....	v
List of appendix.....	vii
1. introduction .....	1
2. Site Characteristics.....	3
2.1 Wave Exposure .....	3
2.2 Bathymetry .....	3
2.3 Tides.....	3
3. Offshore Wave Climate .....	7
3.1 Wind data .....	7
3.2 Fetch Analysis .....	11
3.3 Offshore Wave Climate .....	11
4. Wave Transformation .....	17
4.1 Wave Model .....	17
4.2 Wave Refraction.....	17
5. Near Shore Wave Climate.....	21
5.1 Wave Validation .....	21
5.2 ADM Wave Characteristics.....	21
5.2.1 Wave Rose and Seasonal Statistics .....	21
5.2.2 Storm Events and Extreme Wave Heights .....	26
6. Sediment Stability and Circulation Patterns in ADM.....	29
6.1 Sediment Stability.....	29
6.1.1 Theory and Approach.....	29
6.1.2 Hydrodynamic conditions .....	30
6.1.3 Sediment Stability Mapping.....	31
6.2 Current Velocities and Directions in the ADM .....	36
6.2.1 Instantaneous Current Measurements – ADCP Transects .....	36

## **TABLE OF CONTENTS**

6.2.2	Surface Current Measurements – Drogue Tracks .....	43
6.2.3	Average Current Measurements – ADCP Moorings .....	45
6.2.4	Bathymetry Comparison 2007-2011 .....	47
6.2.5	Bathymetry Comparison 2011-2012 .....	48
6.2.6	General Discussion .....	49
7.	Modeling of Dredging Activities with DREDGE .....	53
7.1	Model Description and Approach .....	53
7.1.1	General Description and Model Limitations .....	53
7.1.2	Detailed Model Approach.....	54
7.2	Application of DREDGE in ADM .....	55
7.2.1	Assumptions and Model Limits .....	55
7.3	Results .....	58
8.	Discussions and Recommendations .....	61
8.1	Hydrodynamic and Sediment Stability .....	61
8.2	Dredging Operations .....	63
9.	REFERENCES.....	65

## **LIST OF TABLE**

		<b>Page</b>
Table 1	Tide Chart Data for Baie-Comeau (CHS, 2011).....	3
Table 2	Wind Statistics for the Baie-Comeau Airport Meteorological Station from 1970 to 2011. ....	10
Table 3	Deep Water Wave Distribution for Baie-Comeau from 1970 to 2011.....	13
Table 4	Extreme Offshore Wave Height (Hm0) by Direction for Baie-Comeau from 1970 to 2011. ....	14
Table 5	STWAVE Inputs and Outputs Wave Parameters – Wave Refraction Analysis. ....	18
Table 6	Near Shore Wave Distribution at the Entrance of ADM from 1970 to 2011. ....	24
Table 7	Storm Events Characteristics from 1968 to 2011 for the Baie Comeau Region. ....	26
Table 8	Extreme Near Shore Wave Height (Hm0) by Direction (Mean Water Level, 0.0m).....	27
Table 9	Selected Hydrodynamic Conditions for the Sediment Stability Assessment in ADM. ....	31
Table 10	Meteorological and Hydraulic Conditions Observed in ADM on October 4 <sup>th</sup> , 5 <sup>th</sup> and 7 <sup>th</sup> 2011.....	37
Table 11	Profile Characteristics Measured on October 4 <sup>th</sup> 2011 with the ADCP. ....	37
Table 12	Profile Characteristics Measured on October 5 <sup>th</sup> and 7 <sup>th</sup> 2011 with the ADCP. ....	41
Table 13	Water Depth and Median Grain Size for each scenario under study. ....	55
Table 14	Input Data used for the DREDGE model.....	57
Table 15	Dredge Results obtained for each scenario under study. ....	59

## **LIST OF MAP**

		<b>Page</b>
Map 1	Site Location and Area Under Study.....	4
Map 2	Bathymetry of Baie des Anglais. ....	5
Map 3	Location of the two Acoustic Doppler Current Profiler (ADCP) Deployed During the 2011 Site Survey. ....	22

## **LIST OF FIGURES**

	<b>Page</b>
Figure 1	Location of the Baie Comeau Airport Meteorological Station.....7
Figure 2	Wind data Measurements at the Baie-Comeau Airport Station from 1965 to 2011. ....8
Figure 3	Wind Rose at Baie-Comeau Station from 1970 to 2011 (all months). ....9
Figure 4	Radials and Effective Fetch Distances used to Generate the Offshore Wave Climate. ....11
Figure 5	Deep water Wave Rose at Baie-Comeau from 1970 to 2011. ....12
Figure 6	Extreme Offshore Wave Height (Hm0) by Direction. ....15
Figure 7	Refraction Pattern at the Entrance of ADM for Deep Water Waves Coming from the South (Hs = 1.06 m; Tp = 6s). ....19
Figure 8	Near Shore Wave Rose at the Entrance of ADM from 1970 to 2011.....23
Figure 9	Monthly Near Shore Wave Roses from 1970 to 2011.....25
Figure 10	Extreme Near Shore Wave Height (Hm0) by Direction (Mean Water Level, 0.0 m). ....27
Figure 11	Extreme Wave Conditions in ADM. (Hm0 = 3.64 m; Tp = 7.8s; Direction From = East, Water Level = 3.1 m).....28
Figure 12	Median Sediment Grain Size (D50, mm) at the Seabed Surface of Anse du Moulin. ....32
Figure 13	Critical Bed Shear-Stress (Pa) in Anse du Moulin. ....32
Figure 14	Sediment Stability under a Wave Height of 1.2 m (24 hrs/year) from the East combined with a Mean Water Level (MWL). ....34
Figure 15	Sediment Stability under a Wave Height of 1.4 m (6 hrs/year) from the East combined with a Mean Water Level (MWL). ....34
Figure 16	Sediment Stability under a Wave Height of 1.8 m (1 hrs/year) from the East combined with a Mean Water Level (MWL). ....35
Figure 17	ADCP Transect Locations and ID (letters) Used to Measure Instantaneous Current Magnitudes and Directions on October 4th, 5th and 7th 2011. ....36
Figure 19	Wave-Induced Currents in ADM, October 4th 2011 (Hm0 = 0.9 m; Tp = 4.0s). ....40
Figure 20	ADCP Profiles Measured October 5th and 7th 2011 Along Transect A and B in Anse du Moulin. ....42
Figure 21	Drogue Model Used During the 2011 Field Work. ....43
Figure 22	Drogue Tracks Released in Anse du Moulin on October 4th, 5th and 7th 2011 with Associated Meteorological and Hydraulic Conditions. ....44
Figure 23	Averaged Surface and Bottom Current Magnitudes Measured by Hydro-1 from October 8th to November 23rd 2011.....46

## ***LIST OF FIGURES***

Figure 24	Location of ADCPs and currents induced by waves on April 23rd 2012 ( $H_{m0} = 2.04\text{m}$ ; $T_p = 5.8\text{s}$ ; Direction from East). ....	47
Figure 25	Difference in Elevation Obtained by the Comparison of the Bathymetric Data Measured in 2007 and 2011. ....	51
Figure 25-B	Difference in Elevation Obtained by the Comparison of the Bathymetric Data Measured in 2011 and 2012. ....	52
Figure 26	Dredging Area Considered for the Modeling. ....	56

## ***LIST OF APPENDIX***

Appendix 1	Historical high wind speeds recorded at the Baie-Comeau station during winter
Appendix 2	Validation of the wind-wave model
Appendix 3	Historical storm events
Appendix 4	Modeling approach – Model setup & Input parameters
Appendix 5	Dredge modeling results



# 1. INTRODUCTION

---

GENIVAR Inc. (GENIVAR) was mandated by ALCOA to complete an Environmental and Social Impact Assessment Study (ESIA) to address Anse du Moulin contaminated sediment. Preliminary remedial options include; sediment removal (dredging) to a confinement disposal facility (CDF), sediment capping with uncontaminated material and monitored natural recovery (MNR).

The specific objective of this hydrodynamic study is to develop an understanding of the hydrodynamic and sediment transport behaviour in Anse du Moulin (ADM) to assess the potential impacts (applicable mitigation measures) on the marine environment and to support the engineering feasibility study regarding future remediation works. Based on previous reports, circulation patterns within the Anse du Moulin are mainly driven by wave motion with a moderate influence from tides.

The first part of this report focuses on the description of the near shore wave climate at the entrance of Anse du Moulin. The second part focuses on the sediment stability and circulation patterns to support the engineering feasibility study as well as the assessment of the environmental impacts regarding the remediation works.

GENIVAR's scope of work for this Hydrodynamic Study includes the following items:

- Analyse existing data such as bathymetry, offshore winds and historical storm events;
- Evaluate the offshore wave climate (deep water) based on measured wind speeds and directions;
- Transform the offshore waves using a numerical model to predict the near shore wave climate;
- Validate the wave model and assess its adequacy based on measured wave characteristics collected during the 2011 survey;
- Evaluate the near shore wave climate at the entrance of Anse du Moulin including frequency of exceedence, seasonal trends and extreme values;
- Assess the sediment stability in ADM under different hydrodynamic conditions;
- Review current measurements and circulation patterns in ADM;
- Assess the environmental impacts of the dredging works.





## 2. SITE CHARACTERISTICS

---

### 2.1 Wave Exposure

The Anse du Moulin study area is located in the South West part of Baie des Anglais on the Baie-Comeau shoreline (Map 1). The site is partially protected to the South West by the Pointe-Lebel and to the North East (NE) by the Pointe Saint-Pancrace resulting to a direct wave exposure from the East North East (ENE) to South (S).

### 2.2 Bathymetry

Part of the survey carried out in 2011 by GENIVAR was to collect bathymetric data within ADM. These measurements were combined with a large data set provided by the Canadian Hydrographic Service (CHS, 2011) to complete the offshore bathymetric coverage. This information is required as input data to properly simulate the propagation of offshore waves toward Anse du Moulin. Marine charts were also used to complete some areas not covered by the combined data set. Map 2 shows the bathymetric map.

### 2.3 Tides

The CHS (2011) provides the following tide chart for Baie-Comeau (Table 1). The water elevations are provided in meters for both Datum: Charts Datum (CD) and Mean Water Level (MWL, referred as the geodetic Datum, IGLD85).

Table 1 Tide Chart Data for Baie-Comeau (CHS, 2011).

		CD (m)	MWL (m)
Higher High Water	Mean Tide	3,4	1,6
	Large Tide	4,2	2,4
Mean Water Level		1,8	0,0
Lower Low Water	Mean Tide	0,5	-1,3
	Large Tide	-0,1	-1,9
Extreme recorded	Low Water	-0,9	-2,7
	High Water	4,9	3,1
Range	Mean Tide	3,0	1,2
	Large Tide	4,3	2,5



Sediment Rehabilitation  
of Anse du Moulin, Baie des Anglais, Baie-Comeau  
Hydrodynamic and Sediment Dynamics Modeling

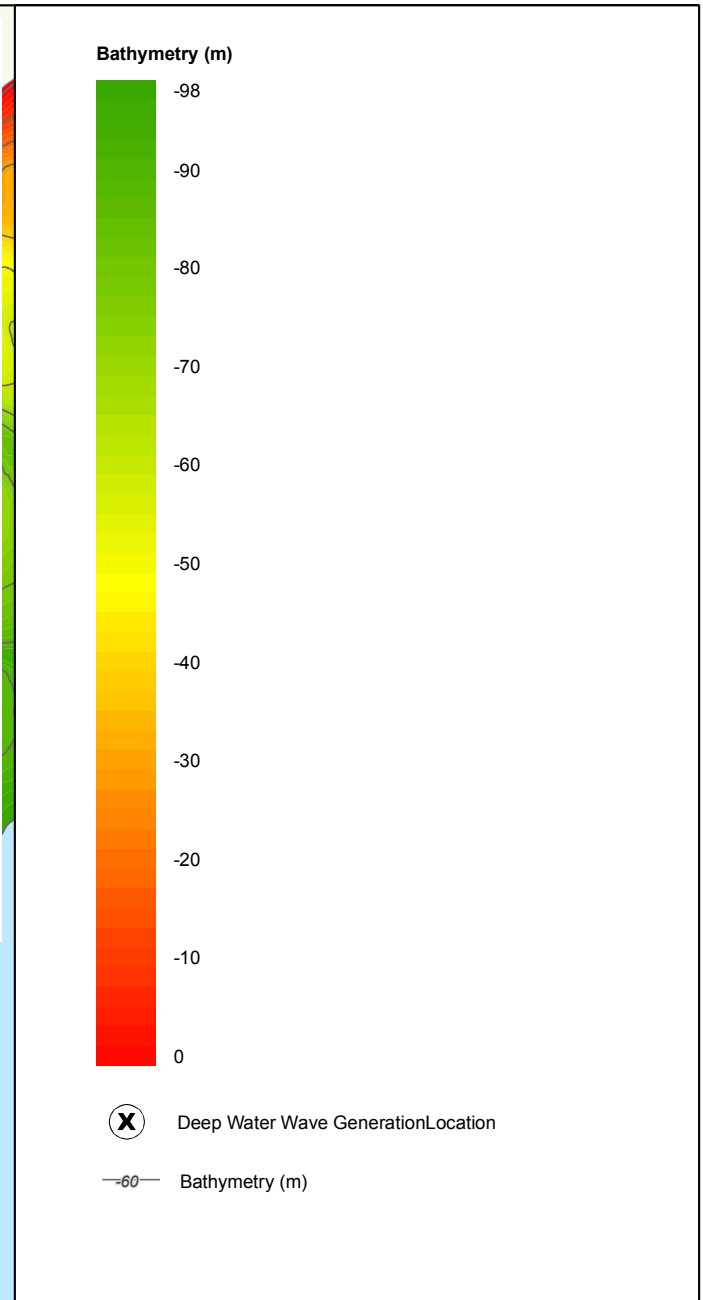
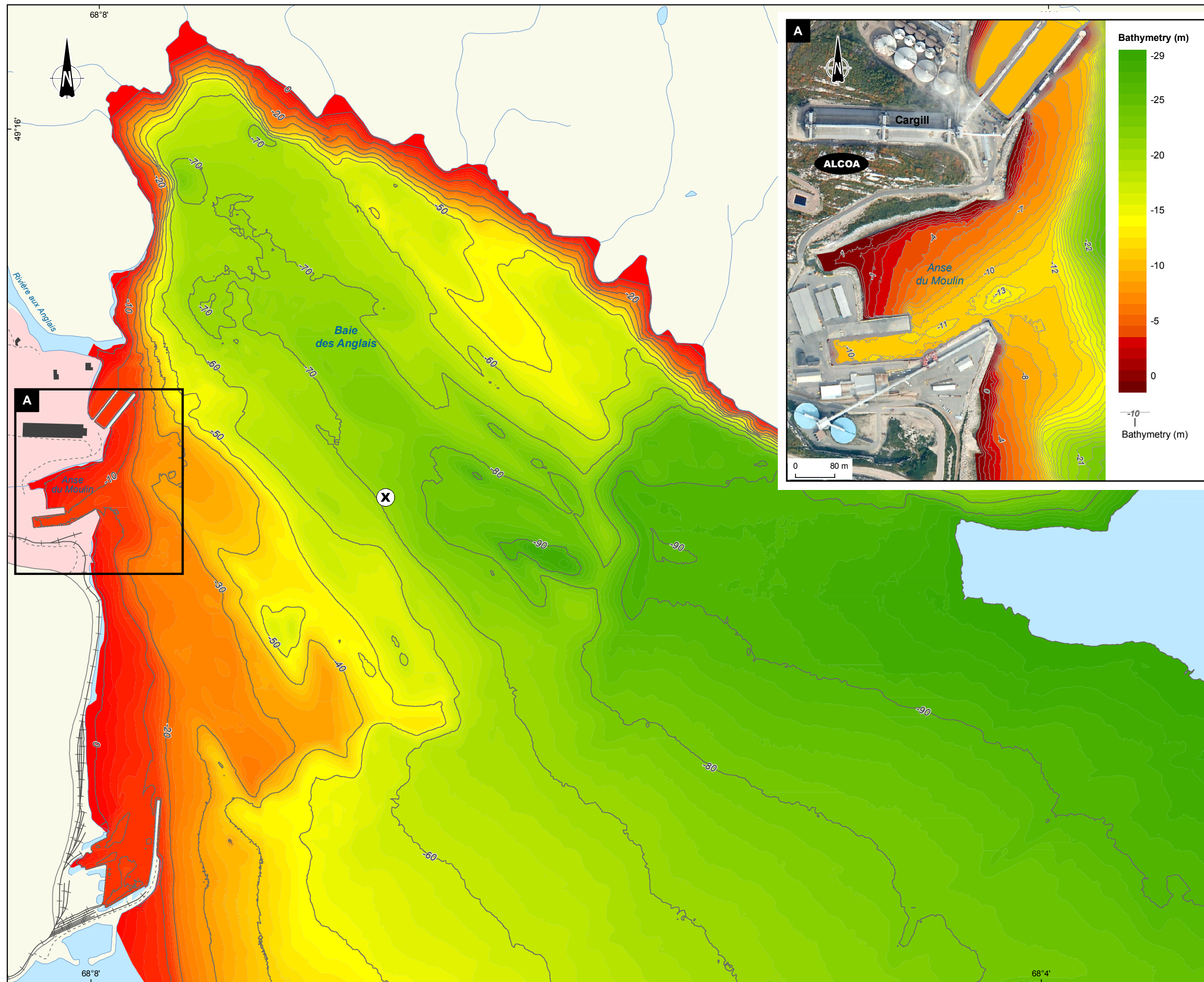
Map 1  
**Site Location**


Sources:  
BDTO, 1:20,000, MRNF Québec, 2002  
Mapping: GENIVAR, gei  
File: 111\_21002\_RY\_geq\_c1\_loc\_120227\_AN.mxd

0 700 1400 m  
MTM, Zone 6, NAD83

February 2012  
111-21002-00

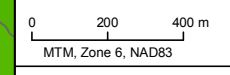




 Sediment Rehabilitation of Anse du Moulin,  
Baie des Anglais, Baie-Comeau  
Hydrodynamic and Sediment Dynamics Modeling

Map 2  
**Bathymetry of Baie des Anglais**

**Sources:**  
BDTQ, 1:20,000 MRNF Québec, 2002 (22F08101-22F08102-22F01201-22F01202)  
Bathymetry, GENIVAR Hydraulique, 2012  
File: 111\_21002\_RY\_geq\_c2\_BathyBAnglais\_120228\_AN.mxd



February 2012



111-21002-00



### 3. OFFSHORE WAVE CLIMATE

---

#### 3.1 Wind data

Wind data from Baie-Comeau Airport (# 7040442; # 7040440) meteorological station were used to generate the offshore deep water wave climate. The location of the Baie-Comeau station (Figure 1) is the nearest of the study area and is considered representative of ADM wind exposure. The station is at an elevation of 21.6 m above Mean Water Level (MWL) and its distance from the shoreline is appropriated to represent overwater wind velocities without any correction factor. The hourly wind data are available from 1965 to 2012 for this station.

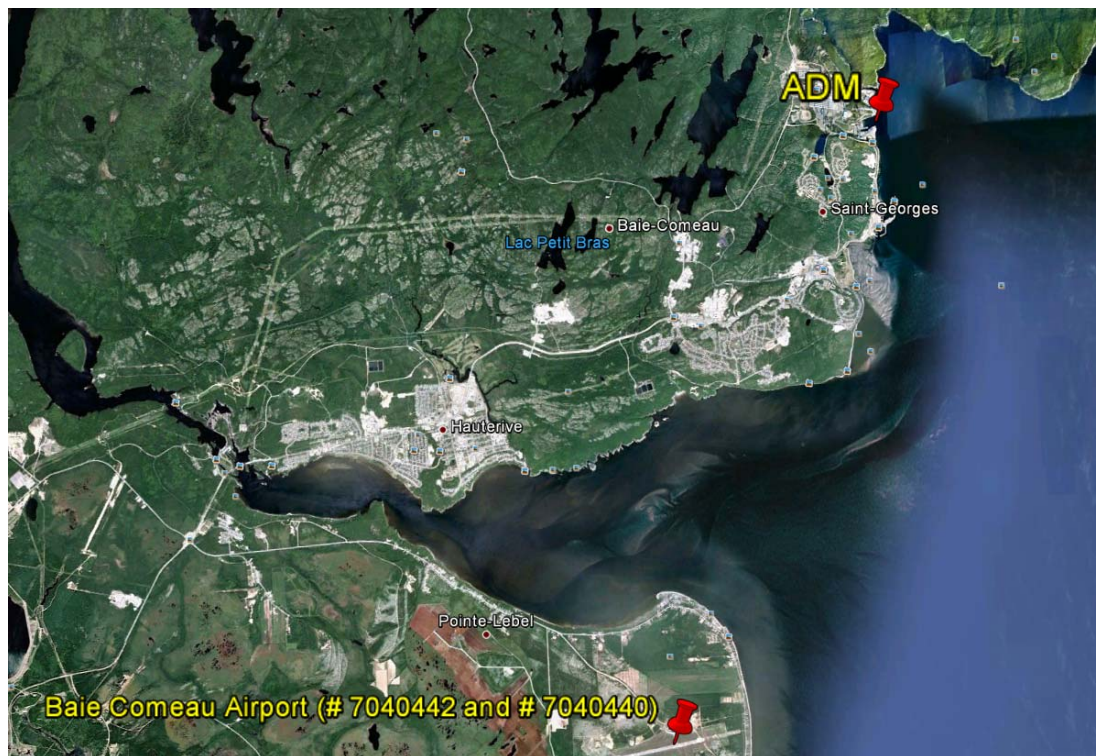


Figure 1 Location of the Baie Comeau Airport Meteorological Station.

Wind data were analysed during the ice-free period for the study area, in order to generate a representative wave climate at ADM. When ice covers the St-Lawrence estuary, peak wind speeds measured near the shoreline are deemed higher than wind speeds measured during the ice-free period. In fact, the ice cover can significantly decrease the energy transferred from wind to water which result in peak wind measurements during winter (outliers) comparatively to the ice free period. Therefore, use of such wind speeds in a wind-wave model hindcast may result in an overestimation of wave heights. Figure 2 shows the complete wind data set for Baie-Comeau Airport station including peak values considered as outliers.

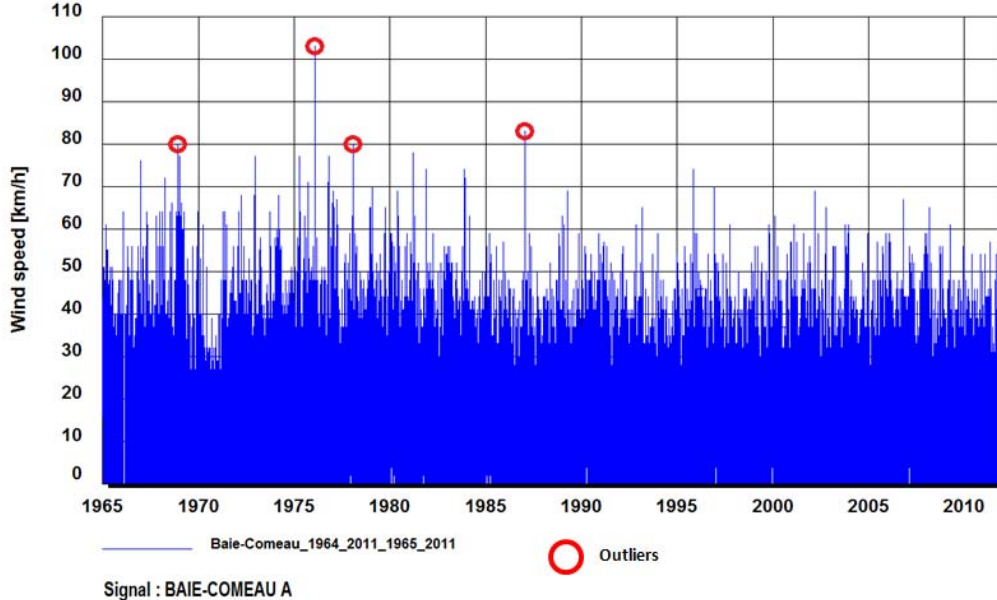


Figure 2 Wind data Measurements at the Baie-Comeau Airport Station from 1965 to 2011.

Based on more than 45 years of measurements from the Baie-Comeau meteorological stations, wind speeds range most of the time between 0 and 75 km/h. Figure 2 shows that only four events with wind measurements over 80 km/h were collected during this same period. The investigation of these 4 outliers reveals that wind measurements were collected during winter when there was a significant amount of ice in the St-Lawrence River near Baie Comeau area. Appendix 1 provides the historical ice charts issued by the Canadian Coast Guard (CCG) showing ice concentration and distribution observed during these specific events. Since ice charts were not available before 1970, only 3 events were documented in Appendix 1.

Based on the information provided by historical and recent ice charts from the CCG, supplemented by discussion with locals, there has been little to no ice cover in recent years in the Baie-Comeau region. Therefore all wind data (January 1<sup>st</sup> to December 31<sup>st</sup>) from 1970 to 2011 were retained, excluding only winter months associated to wind peak events of 1976, 1978 and 1987 (see Appendix 1).

Section 5.1 and Appendix 2 of the current report provide the wave calibration analysis and the assessment of the model adequacy using both wind data sets from the Baie-Comeau and Mont-Joli meteorological stations. Comparison between in-situ wave measurements and predicted waves reveals that the Baie-Comeau wind data set provides a better adequacy when compared to the Mont-Joli station.

Figure 3 and Table 2 show the wind rose and associated statistics for the Baie-Comeau station.

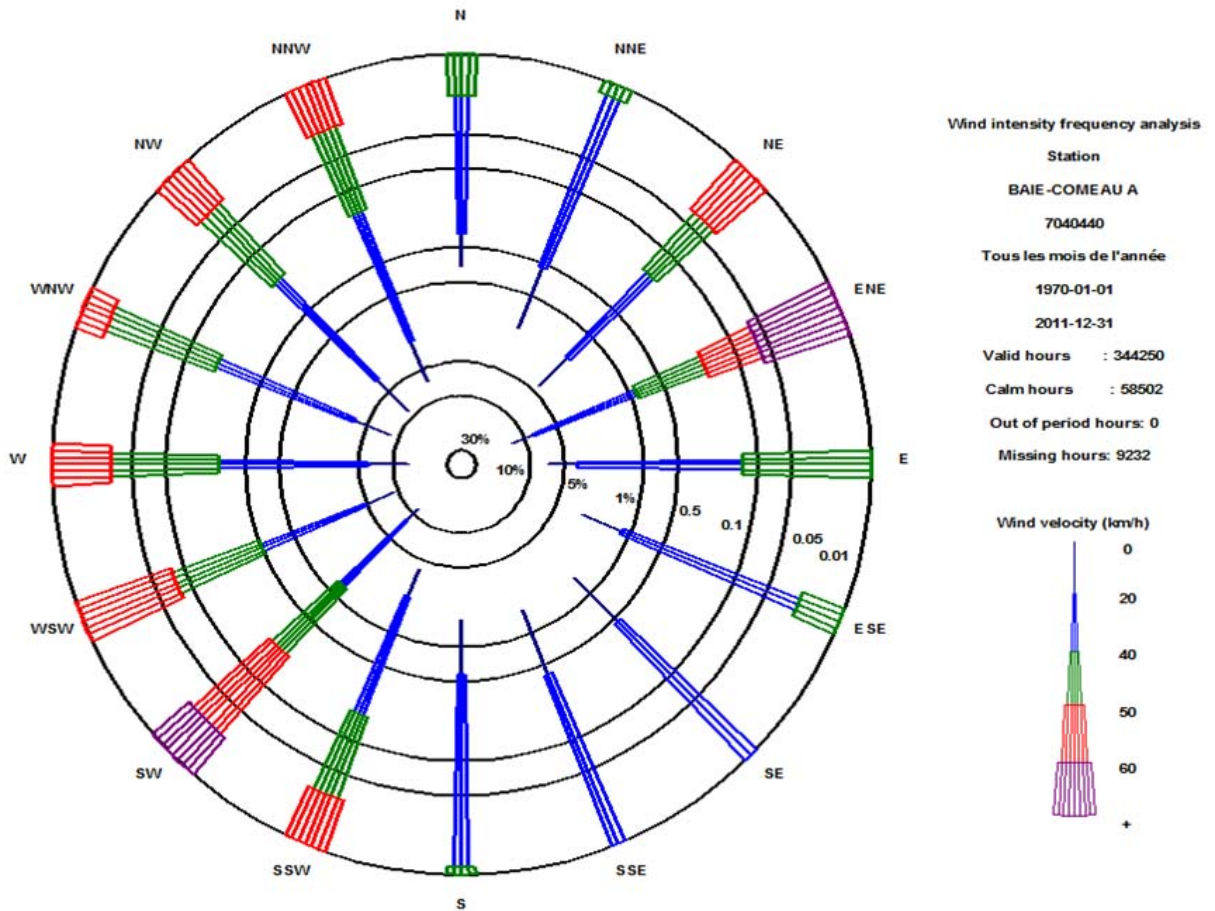


Figure 3 Wind Rose at Baie-Comeau Station from 1970 to 2011 (all months).

Table 2 Wind Statistics for the Baie-Comeau Airport Meteorological Station from 1970 to 2011.

Wind Speed (km/h)	Direction From													TOTAL						
	N	NNE	NE	ENE	E	ESE	SE	SSE	S	SSW	SW	WSW	W	WNW	NW	NNW	Total	%	%Cumul	%Exceed.
0 - 5	2181	1089	1154	1689	1040	706	636	826	630	812	1023	1283	2439	1613	1784	1647	20552	5.97	5.97	100.00
5 - 10	5501	2652	4134	7453	4362	2673	1871	1991	1884	2847	5041	6640	11842	8007	8897	6503	82298	23.91	29.88	94.03
10 - 15	3537	1299	2813	8023	4595	2200	1295	1395	1392	2681	5280	6835	11149	5761	6518	4534	69307	20.13	50.01	70.12
15 - 20	3040	1048	2559	9861	5760	2082	977	975	1139	3099	7288	6676	9873	5670	5734	4428	70209	20.40	70.40	49.99
20 - 25	1459	489	1761	8173	4318	1251	372	317	550	2309	7170	4326	5712	3829	3498	2626	48160	13.99	84.39	29.60
25 - 30	482	175	861	3879	1749	428	124	70	157	1029	4429	2160	2461	1739	1429	1008	22180	6.44	90.84	15.61
30 - 35	238	102	746	3284	1103	246	65	30	94	700	4357	1834	1774	1217	1007	679	17476	5.08	95.91	9.16
35 - 40	53	37	329	1586	354	69	12	10	25	341	2475	990	627	437	409	315	8069	2.34	98.26	4.09
40 - 45	24	6	157	741	87	13	4	2	10	146	1285	459	249	156	195	147	3681	1.07	99.33	1.74
45 - 50	3	1	63	268	14	4	2	1	5	53	445	175	72	41	56	75	1278	0.37	99.70	0.67
50 - 55	0	1	44	201	3	0	0	0	0	25	193	56	26	15	28	11	603	0.18	99.87	0.30
55 - 60	0	0	18	97	3	0	0	0	0	22	64	23	12	3	12	6	260	0.08	99.95	0.13
60 - 65	0	0	2	57	1	0	0	0	0	2	24	9	2	3	2	1	103	0.03	99.98	0.05
65 - 70	0	0	4	38	0	0	0	0	0	1	3	2	1	0	2	0	51	0.02	99.99	0.02
70 - 75	0	0	1	13	0	0	0	0	0	0	1	0	0	0	0	0	15	0.00	100.00	0.01
75 - 80	0	0	0	7	0	0	0	0	0	0	0	0	0	0	0	0	8	0.00	100.00	0.00
80 - 85	0	0	0	0	0	0	0	0	0	0	0	0	0	0	0	0	0	0.00	100.00	0.00
85 - 90	0	0	0	0	0	0	0	0	0	0	0	0	0	0	0	0	0	0.00	100.00	0.00
90 - 95	0	0	0	0	0	0	0	0	0	0	0	0	0	0	0	0	0	0.00	100.00	0.00
95 - 100	0	0	0	0	0	0	0	0	0	0	0	0	0	0	0	0	0	0.00	100.00	0.00
100 - 105	0	0	0	0	0	0	0	0	0	0	0	0	0	0	0	0	0	0.00	100.00	0.00
105 - 110	0	0	0	0	0	0	0	0	0	0	0	0	0	0	0	0	0	0.00	100.00	0.00
110 - 115	0	0	0	0	0	0	0	0	0	0	0	0	0	0	0	0	0	0.00	100.00	0.00
115 - 120	0	0	0	0	0	0	0	0	0	0	0	0	0	0	0	0	0	0.00	100.00	0.00
120 - 125	0	0	0	0	0	0	0	0	0	0	0	0	0	0	0	0	0	0.00	100.00	0.00
125 - 130	0	0	0	0	0	0	0	0	0	0	0	0	0	0	0	0	0	0.00	100.00	0.00
130 - 135	0	0	0	0	0	0	0	0	0	0	0	0	0	0	0	0	0	0.00	100.00	0.00
135 - 140	0	0	0	0	0	0	0	0	0	0	0	0	0	0	0	0	0	0.00	100.00	0.00
140 - 145	0	0	0	0	0	0	0	0	0	0	0	0	0	0	0	0	0	0.00	100.00	0.00
145 - 150	0	0	0	0	0	0	0	0	0	0	0	0	0	0	0	0	0	0.00	100.00	0.00
Total	16518	6899	14646	45370	23389	9672	5358	5617	5886	14067	39078	31468	46239	28491	29572	21980	344250			
Total (%)	4.80	2.00	4.25	13.18	6.79	2.81	1.56	1.63	1.71	4.09	11.35	9.14	13.43	8.28	8.59	6.38	100			



### 3.2 Fetch Analysis

The radials are defined as the unobstructed distance that wind can travel over water in a constant direction. Radials for each degree were calculated for Baie Comeau from a specific point offshore designated as the deep water wave generation location. The geographical coordinates of this point are 260 180 E and 5 457 050 O (MTM, SCoPQ - zone 6). Map 2 shows the location of this point (see section 2.2).

The effective fetches were computed for each degree to obtain the fetch distribution. Figure 4 shows the radials (blue lines) and the effective fetch distribution (red envelope) used to generate the offshore wave climate. Note that the fetch evaluation method can be strictly used with the wave hindcast model described in section 3.3 and cannot be substituted with another fetch evaluation method.

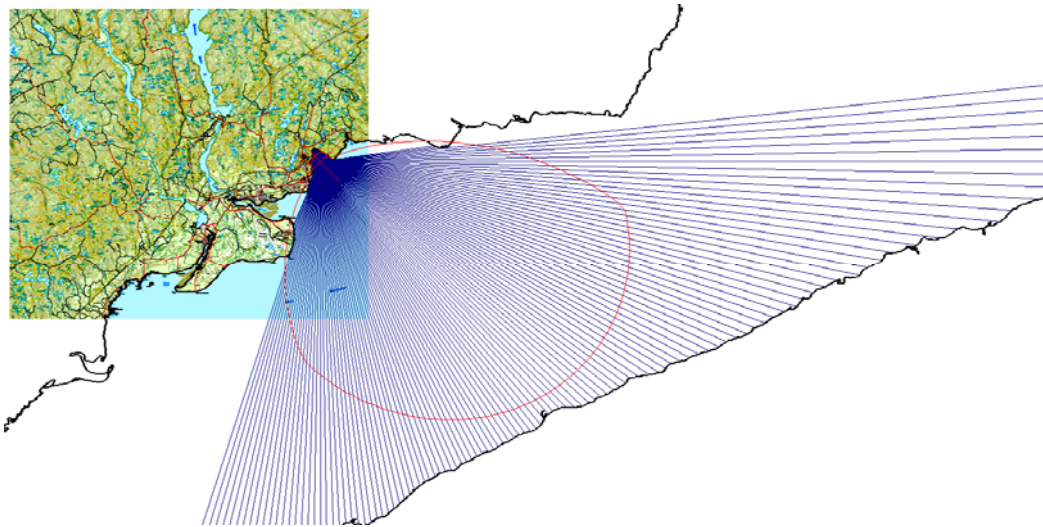


Figure 4 Radials and Effective Fetch Distances used to Generate the Offshore Wave Climate.

### 3.3 Offshore Wave Climate

The GENIVAR wind-wave hindcast model was used to generate the offshore wave climate based on wind data from the Baie-Comeau Airport station. The fetch analysis described in the previous section gives the specific geographical location for which the deep water wave climate was generated.

Figure 5 and Table 3 show the deep water wave rose and associated wave distribution.

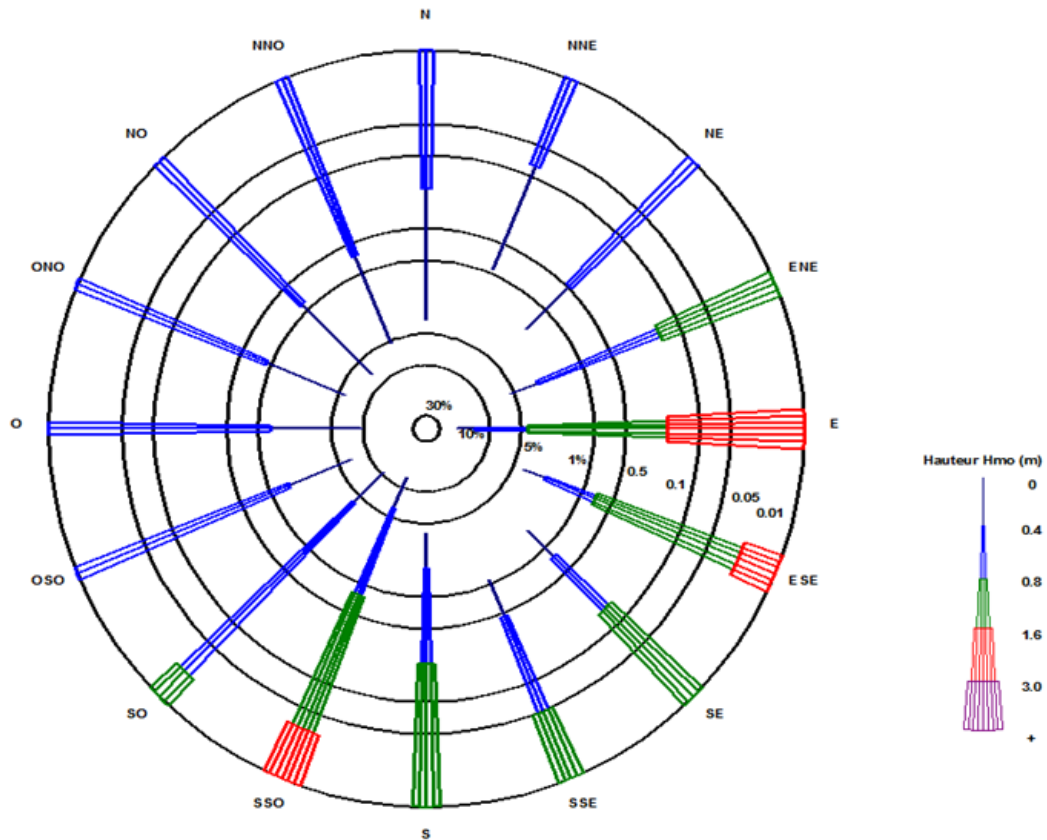


Figure 5 Deep water Wave Rose at Baie-Comeau from 1970 to 2011.

The percentage of “calm water” can be defined from Table 3 for wave heights less than 0.4 m including the winter months (0.2-0.4 m interval and lower). For the Baie-Comeau region, 85.2% of the total hours measured between 1970 and 2011 are characterized as “calm”.

Best fit for the extreme wave heights were found for Log-Pearson Type III or Log-Normal distribution laws. Returns periods for extreme wave height were estimated based on the offshore wave characteristics for each direction. Table 4 and Figure 6 summarize the results.

Table 3 Deep Water Wave Distribution for Baie-Comeau from 1970 to 2011.

Wave Height H <sub>m0</sub> (m)	Direction From																TOTAL			
	N	NNE	NE	ENE	E	ESE	SE	SSE	S	SSW	SW	WSW	W	WNW	NW	NNW	Total	%	%Cumul	%Exceed.
0 - 0.2	12191	2954	4681	9235	22399	5735	3334	2332	7916	23096	22232	18523	29248	17558	22961	16483	220878	61.55	61.55	100.00
0.2 - 0.4	748	274	1554	6551	19963	3676	1540	1128	4270	13996	13041	5071	4636	3124	2893	2262	84727	23.61	85.16	38.45
0.4 - 0.6	4	5	131	3061	14062	2158	636	366	1562	5368	1818	427	125	70	113	110	30016	8.36	93.52	14.84
0.6 - 0.8	0	0	9	400	7675	1249	314	131	475	1589	76	15	2	1	9	0	11945	3.33	96.85	6.48
0.8 - 1.0	0	0	0	125	4409	727	139	31	218	697	3	0	0	0	1	0	6350	1.77	98.62	3.15
1.0 - 1.2	0	0	0	34	1907	375	66	9	79	298	0	0	0	0	0	0	2768	0.77	99.39	1.38
1.2 - 1.4	0	0	0	13	865	173	23	4	33	126	0	0	0	0	0	0	1237	0.34	99.73	0.61
1.4 - 1.6	0	0	0	0	382	50	7	0	16	55	0	0	0	0	0	0	510	0.14	99.88	0.27
1.6 - 1.8	0	0	0	0	180	22	4	0	5	45	0	0	0	0	0	0	256	0.07	99.95	0.12
1.8 - 2.0	0	0	0	0	79	11	0	0	0	7	0	0	0	0	0	0	97	0.03	99.98	0.05
2.0 - 2.2	0	0	0	0	27	3	0	0	0	6	0	0	0	0	0	0	36	0.01	99.99	0.03
2.2 - 2.4	0	0	0	0	15	0	0	0	0	2	0	0	0	0	0	0	17	0.00	99.99	0.02
2.4 - 2.6	0	0	0	0	13	0	0	0	0	2	0	0	0	0	0	0	15	0.00	99.99	0.01
2.6 - 2.8	0	0	0	0	12	0	0	0	0	0	0	0	0	0	0	0	12	0.00	100.00	0.01
2.8 - 3.0	0	0	0	0	6	0	0	0	0	0	0	0	0	0	0	0	6	0.00	100.00	0.00
3.0 - 3.2	0	0	0	0	2	0	0	0	0	0	0	0	0	0	0	0	2	0.00	100.00	0.00
3.2 - 3.4	0	0	0	0	1	0	0	0	0	0	0	0	0	0	0	0	1	0.00	100.00	0.00
3.4 - 3.6	0	0	0	0	2	0	0	0	0	0	0	0	0	0	0	0	2	0.00	100.00	0.00
3.6 - 3.8	0	0	0	0	0	0	0	0	0	0	0	0	0	0	0	0	0	0.00	100.00	0.00
3.8 - 4.0	0	0	0	0	0	0	0	0	0	0	0	0	0	0	0	0	0	0.00	100.00	0.00
4.0 - 4.2	0	0	0	0	0	0	0	0	0	0	0	0	0	0	0	0	0	0.00	100.00	0.00
4.2 - 4.4	0	0	0	0	0	0	0	0	0	0	0	0	0	0	0	0	0	0.00	100.00	0.00
4.4 - 4.6	0	0	0	0	0	0	0	0	0	0	0	0	0	0	0	0	0	0.00	100.00	0.00
4.6 - 4.8	0	0	0	0	0	0	0	0	0	0	0	0	0	0	0	0	0	0.00	100.00	0.00
4.8 - 5.0	0	0	0	0	0	0	0	0	0	0	0	0	0	0	0	0	0	0.00	100.00	0.00
5.0 - 5.2	0	0	0	0	0	0	0	0	0	0	0	0	0	0	0	0	0	0.00	100.00	0.00
5.2 - 5.4	0	0	0	0	0	0	0	0	0	0	0	0	0	0	0	0	0	0.00	100.00	0.00
5.4 - 5.6	0	0	0	0	0	0	0	0	0	0	0	0	0	0	0	0	0	0.00	100.00	0.00
5.6 - 5.8	0	0	0	0	0	0	0	0	0	0	0	0	0	0	0	0	0	0.00	100.00	0.00
5.8 et plus	0	0	0	0	0	0	0	0	0	0	0	0	0	0	0	0	0	0.00	100.00	0.00
<b>Total</b>	12943	3233	6375	19419	71999	14179	6063	4001	14574	45287	37170	24036	34011	20753	25977	18855	358875			
<b>Total (%)</b>	3.61	0.90	1.78	5.41	20.06	3.95	1.69	1.11	4.06	12.62	10.36	6.70	9.48	5.78	7.24	5.25	100			

**Note 1:** H<sub>m0</sub> is defined as the Characteristic Wave Height or Zero Moment Wave Height:  $H_{m0} = 4\sigma$ , where  $\sigma$  is the variance of the signal.

**Note 2:** Wave hours (358875) can be larger than wind hours (344250, see Table 2) because wave heights are attenuated over time even if the corresponding measured wind speeds are 0 km/h.

Table 4 Extreme Offshore Wave Height (Hm0) by Direction for Baie-Comeau from 1970 to 2011.

Direction From	Return Periods											
	2		5		10		25		50		100	
	Hmo (m)	Tp (s)	Hmo (m)	Tp (s)	Hmo (m)	Tp (s)	Hmo (m)	Tp (s)	Hmo (m)	Tp (s)	Hmo (m)	Tp (s)
N	0.3	2.2	0.3	2.4	0.4	2.5	0.4	2.6	0.4	2.7	0.5	2.7
NNE	0.2	2.0	0.3	2.3	0.4	2.5	0.4	2.7	0.5	2.8	0.5	2.9
NE	0.4	2.6	0.5	3.0	0.6	3.1	0.7	3.3	0.7	3.4	0.7	3.5
ENE	0.8	3.7	1.0	4.2	1.2	4.4	1.3	4.7	1.4	4.9	1.6	5.1
E	1.9	5.6	2.3	6.2	2.6	6.6	3.0	7.1	3.3	7.5	3.6	7.8
ESE	1.4	4.8	1.6	5.2	1.8	5.4	1.9	5.7	2.0	5.8	2.1	6.0
SE	1.0	4.1	1.2	4.5	1.4	4.8	1.6	5.1	1.7	5.3	1.8	5.5
SSE	0.7	3.4	0.9	3.9	1.1	4.2	1.3	4.6	1.4	4.9	1.6	5.2
S	1.1	4.2	1.4	4.7	1.5	5.0	1.7	5.3	1.8	5.5	2.0	5.7
SSW	1.4	4.9	1.8	5.4	2.0	5.8	2.3	6.1	2.5	6.4	2.7	6.7
SW	0.6	3.1	0.7	3.3	0.7	3.5	0.8	3.6	0.8	3.7	0.9	3.9
WSW	0.5	2.8	0.6	3.1	0.6	3.3	0.7	3.4	0.7	3.5	0.8	3.6
W	0.4	2.6	0.5	2.9	0.5	3.0	0.6	3.2	0.6	3.3	0.7	3.4
WNW	0.4	2.5	0.4	2.7	0.5	2.9	0.6	3.0	0.6	3.2	0.6	3.3
NW	0.4	2.5	0.5	2.9	0.6	3.1	0.7	3.3	0.7	3.5	0.8	3.7
NNW	0.3	2.4	0.4	2.7	0.5	2.9	0.6	3.0	0.6	3.2	0.6	3.3

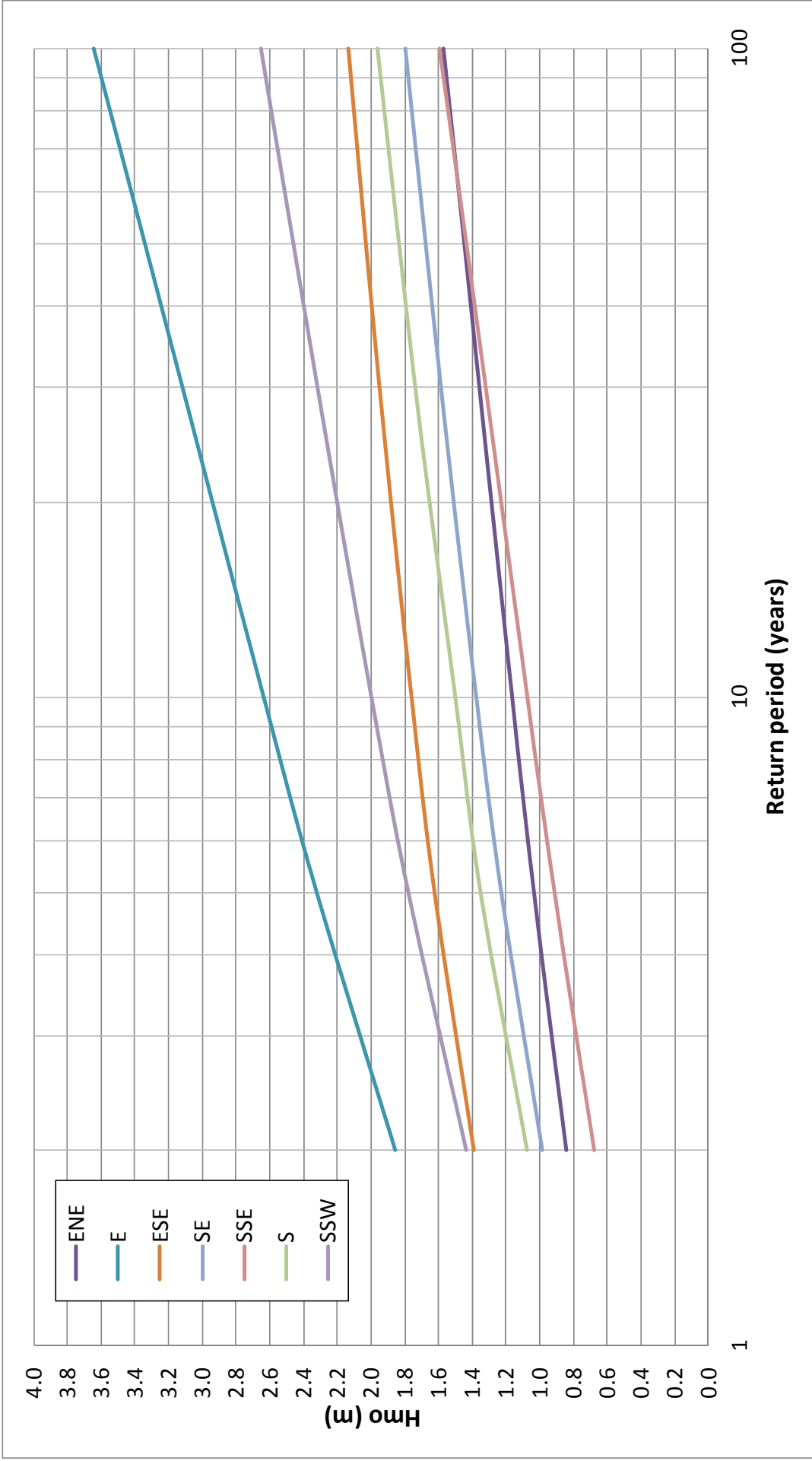


Figure 6 Extreme Offshore Wave Height ( $H_{m0}$ ) by Direction.



## 4. WAVE TRANSFORMATION

---

### 4.1 Wave Model

A numerical wave model was used to transfer the offshore deep water waves toward the entrance of the Anse du Moulin. To evaluate the near shore wave transformation and determine the wave parameters (height and direction) in ADM, the steady-state spectral wave model STWAVE (Smith et al. 2001) was used. STWAVE simulates the wave refraction and shoaling, the wave diffraction and the depth and steepness-induced wave breaking. The wave reflection on structures and shorelines is not simulated with this model. The assumptions made in STWAVE are:

- Mild bottom slope;
- Spatially homogenous offshore wave conditions;
- Steady-state waves;
- Linear wave refraction and shoaling;
- Bottom friction neglected.

STWAVE is a spectral wave model that solves the averaged wave energy over the phase. Thus for applications where near-field reflection on coastal structures is required, a phase-resolving model should be applied. The approximations and assumptions described herein are deemed acceptable to assess the near-shore wave climate at the entrance of ADM.

### 4.2 Wave Refraction

Based on the offshore wave climate, 26 wave simulation cases were computed using the STWAVE model. These simulations intend to establish the refraction coefficients and the refracted directions at the entrance of ADM as transformation datasets to generate the near shore wave climate. All simulations were performed at mean water level. Appendix 4 describes in details the model setup and inputs used to run the STWAVE model.

Table 5 presents the STWAVE wave parameter inputs (scenarios) used to perform the wave refraction analysis with associated outputs at the entrance of ADM.

Finally, wave parameters outputs from STWAVE were extracted directly at the ADCP location known as Hydro 1 (see Map 3, section 5.1.1).

Table 5 STWAVE Inputs and Outputs Wave Parameters – Wave Refraction Analysis.

Offshore - STWAVE Inputs					Entrance of ADM - STWAVE Outputs		
Direction From	Azimuth (degree)	H <sub>m0</sub> (m)	T <sub>p</sub> (s)	Water level (MWL, m)	H <sub>m0</sub> (m)	Refraction Coefficient (K <sub>r</sub> )	Azimuth (degree) (Refracted)
NE	45	0.16	2	0.0	0.13	0.80	55.1
NE	45	0.47	4	0.0	0.35	0.74	62.4
NE	45	1.70	8	0.0	1.26	0.74	88.0
ENE	67.5	0.23	2	0.0	0.21	0.91	71.9
ENE	67.5	0.58	4	0.0	0.50	0.87	75.4
ENE	67.5	1.14	6	0.0	0.89	0.78	82.6
ENE	67.5	1.70	8	0.0	1.26	0.74	88.0
E	90	0.24	2	0.0	0.23	0.96	90.4
E	90	0.58	4	0.0	0.53	0.92	92.7
E	90	1.16	6	0.0	0.96	0.83	97.2
E	90	1.78	8	0.0	1.41	0.79	98.7
E*	90*	4.40*	10*	0.0	3.52	0.78	98.9
ESE	112.5	0.21	2	0.0	0.20	0.95	112.1
ESE	112.5	0.58	4	0.0	0.53	0.92	112.7
ESE	112.5	1.09	6	0.0	0.93	0.85	113.9
SE	135	0.19	2	0.0	0.18	0.95	133.2
SE	135	0.55	4	0.0	0.50	0.91	132.6
SE	135	1.57	6	0.0	1.33	0.85	132.0
SSE	157.5	0.19	2	0.0	0.15	0.79	144.3
SSE	157.5	0.54	4	0.0	0.40	0.74	142.2
SSE	157.5	1.64	6	0.0	1.18	0.72	142.0
S	180	0.19	2	0.0	0.11	0.58	153.5
S	180	0.46	4	0.0	0.25	0.55	151.2
S	180	1.06	6	0.0	0.56	0.53	145.5
SSW	202.5	0.20	2	0.0	0.07	0.33	160.7
SSW	202.5	0.42	4	0.0	0.14	0.33	155.5
SSW	202.5	0.80	6	0.0	0.26	0.32	152.2

**Note:** The wave height of H<sub>m0</sub>=4.4m and T<sub>p</sub>=10s from East has been added for interpolation purpose to complete the matrix of refraction and represents an estimated average wave height excluded of the statistical wave analysis.



Results showed in Table 5 indicate that waves transformed from deep water toward Anse du Moulin have a refracted direction (azimuth) ranging between 55 to 161 degrees (azimuth). In other words, deep water waves from the NE to the SSW are all refracted to a smaller incoming wave sector at the entrance of ADM defined from NE to SSE. Figure 7 shows an example of this refraction pattern at the entrance of ADM for deep water waves coming from the South (the colored legend at the top left corner indicates the wave height, in meter).

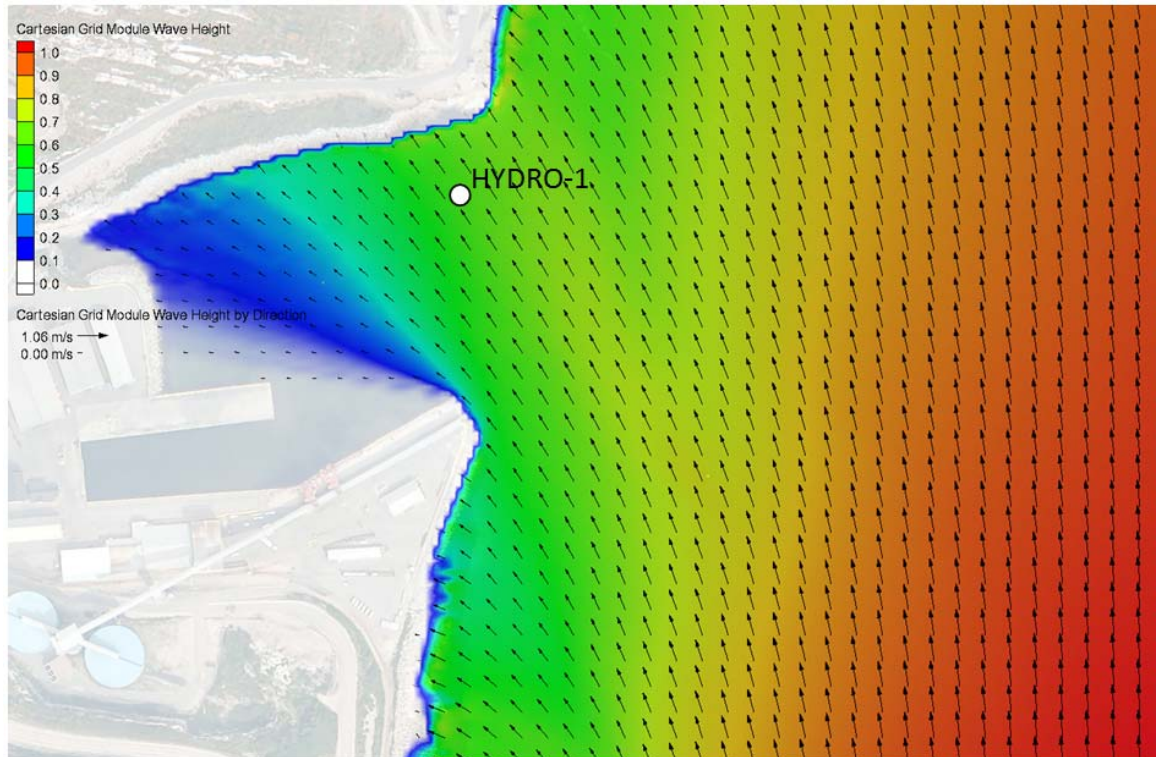


Figure 7 Refraction Pattern at the Entrance of ADM for Deep Water Waves Coming from the South ( $H_s = 1.06$  m;  $T_p = 6$  s).

Finally, using the refraction coefficients and the resulting directions, a new hourly wave climate was calculated at the entrance of ADM for the same observation period (1970 to 2011). The next section describes the near shore wave climate.



## **5. NEAR SHORE WAVE CLIMATE**

---

### **5.1 Wave Validation**

As part of the site survey carried out by GENIVAR in the Fall 2011, two Acoustic Doppler Current Profilers (ADCP) were deployed in ADM from October 7<sup>th</sup> to November 21<sup>st</sup>. Wave heights, periods and directions were measured over this period. Map 3 shows the location of both ADCP deployed in ADM.

Appendix 2 provides the wave validation analysis performed for the current study using the 2011 wave measurements. The wave measurements were used to assess the adequacy of the time series obtained by the combination of the GENIVAR wind-wave hindcast model and STWAVE model. The assessment of the model adequacy was analyzed using both wind data sets from the Baie-Comeau and Mont-Joli meteorological stations. The wave heights, directions and duration at the entrance of ADM simulated with the GENIVAR parametric wave model coupled with the wave propagation model STWAVE provide reliable estimates for all significant events measured in 2011. Comparison between in-situ wave measurements and predicted waves reveals that the Baie-Comeau wind data set provides a better adequacy when compared to the Mont-Joli station.

Based on results provided in Appendix 2, the Baie-Comeau wind data set was retained as the reference station to evaluate the near shore wave climate at the entrance of ADM.

### **5.2 ADM Wave Characteristics**

#### **5.2.1 Wave Rose and Seasonal Statistics**

The GENIVAR parametric wind-wave hindcast model was used to generate the offshore wave climate as described in section 3. The resulting wave climate was imported in the STWAVE model to transform the wave characteristics from the offshore location to the Hydro-1 location at the entrance of ADM. The STWAVE parameters outputs resulting of this transformation analysis are summarize in Table 4 (section 4.2).

Figure 8 and Table 6 show the near shore wave rose at the entrance of ADM and associated wave distribution for the observation period of 1970 to 2011.



**ALCOA**

Sediment Rehabilitation  
of Anse du Moulin, Baie des Anglais, Baie-Corneau  
Hydrodynamic and sediment Dynamics Modeling

**GENIVAR**

February 2012  
111-2/1002-00

---

**Map 3**

**2011 Wave Measurements  
ADCP Location**

Sources:  
Image, XEOS(SCHM), 21 septembre 2007  
Hydrometric stations, GENIVAR, 2011  
Mapping, GENIVAR, gég  
Fichier: 111\_2/1002\_RY\_geq\_c3\_ADCP\_120227\_AN.mxd

ADCP Stations

**Hydro1**

---

0 60 120 m

MTM, Zone 6, NAD83

Legend: ADCP Stations

**Hydro1**

68°7'40"



49°15'

68°7'40"

68°8'

68°8'

68°8'20"

68°8'40"

49°15'

Cargill

**ALCOA**

Anse  
du Moulin

Hydro1

Hydro2

ADCP Stations

**Hydro1**

**GENIVAR**

February 2012

111-2/1002-00

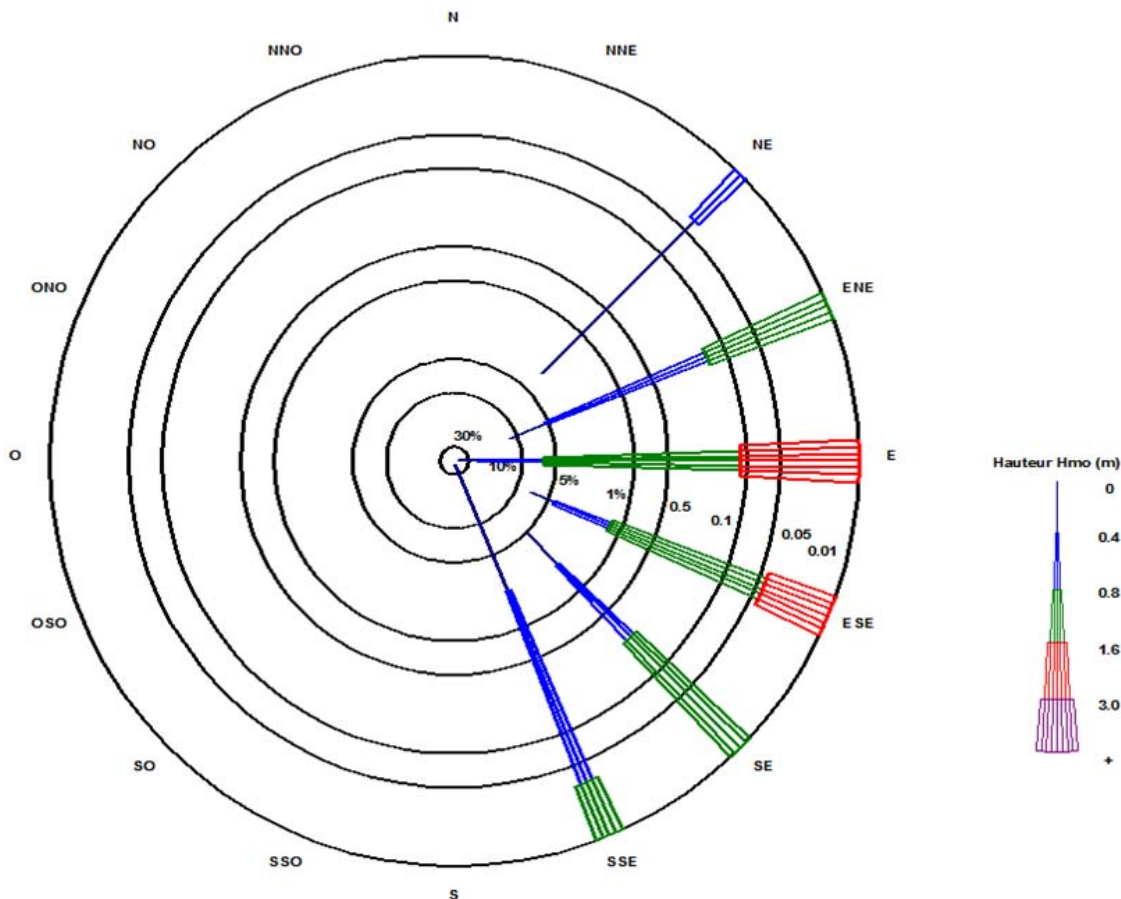


Figure 8 Near Shore Wave Rose at the Entrance of ADM from 1970 to 2011.

Table 6 indicates that “calm water” at the entrance of ADM is slightly lower than the offshore climate with 81.6% of wave hours less than 0.4 m compared to 85.2%. These results indicate that offshore wave climate compared to the entrance of ADM gives similar conditions with around 80 to 85% of the wave hours less than 0.4 m height.

To get a better understanding of the near shore wave climate at the entrance of ADM, monthly wave characteristics were computed to look at seasonal trends in terms of wave heights and frequencies. Highest wave heights are observed from October to April from the East (E) direction. During the same period, dominant wave frequency is associated to the East North East (ENE) and East (E). Near shore waves conditions during May to September are smoother.

Figure 9 shows the near shore monthly wave roses.

Table 6 Near Shore Wave Distribution at the Entrance of ADM from 1970 to 2011.

Wave Height H <sub>m0</sub> (m)	Direction From																TOTAL			
	N	NNE	NE	ENE	E	ESE	SE	SSE	S	SSW	SW	WSW	W	WNNW	NW	NNW	Total	%	%Cumul	%Exceed.
0 - 0.2	0	0	6030	12706	22860	5692	5832	68733	0	0	0	0	0	0	0	0	121853	61.87	61.87	100.00
0.2 - 0.4	0	0	74	7653	20803	3811	2500	3940	0	0	0	0	0	0	0	0	38781	19.69	81.56	38.13
0.4 - 0.6	0	0	0	2335	14407	2215	942	452	0	0	0	0	0	0	0	0	20351	10.33	91.89	18.45
0.6 - 0.8	0	0	0	221	7099	1224	292	60	0	0	0	0	0	0	0	0	8896	4.52	96.40	8.11
0.8 - 1.0	0	0	0	61	3633	678	138	4	0	0	0	0	0	0	0	0	4514	2.29	98.70	3.60
1.0 - 1.2	0	0	0	11	1303	320	36	0	0	0	0	0	0	0	0	0	1670	0.85	99.54	1.30
1.2 - 1.4	0	0	0	0	399	180	12	0	0	0	0	0	0	0	0	0	591	0.30	99.84	0.46
1.4 - 1.6	0	0	0	0	130	64	0	0	0	0	0	0	0	0	0	0	194	0.10	99.94	0.16
1.6 - 1.8	0	0	0	0	51	20	0	0	0	0	0	0	0	0	0	0	71	0.04	99.98	0.06
1.8 - 2.0	0	0	0	0	15	0	0	0	0	0	0	0	0	0	0	0	15	0.01	99.99	0.02
2.0 - 2.2	0	0	0	0	17	0	0	0	0	0	0	0	0	0	0	0	17	0.01	99.99	0.01
2.2 - 2.4	0	0	0	0	6	0	0	0	0	0	0	0	0	0	0	0	6	0.00	100.00	0.01
2.4 - 2.6	0	0	0	0	3	0	0	0	0	0	0	0	0	0	0	0	3	0.00	100.00	0.00
2.6 - 2.8	0	0	0	0	2	0	0	0	0	0	0	0	0	0	0	0	2	0.00	100.00	0.00
2.8 - 3.0	0	0	0	0	0	0	0	0	0	0	0	0	0	0	0	0	0	0.00	100.00	0.00
3.0 - 3.2	0	0	0	0	0	0	0	0	0	0	0	0	0	0	0	0	0	0.00	100.00	0.00
3.2 - 3.4	0	0	0	0	0	0	0	0	0	0	0	0	0	0	0	0	0	0.00	100.00	0.00
3.4 - 3.6	0	0	0	0	0	0	0	0	0	0	0	0	0	0	0	0	0	0.00	100.00	0.00
3.6 - 3.8	0	0	0	0	0	0	0	0	0	0	0	0	0	0	0	0	0	0.00	100.00	0.00
3.8 - 4.0	0	0	0	0	0	0	0	0	0	0	0	0	0	0	0	0	0	0.00	100.00	0.00
4.0 - 4.2	0	0	0	0	0	0	0	0	0	0	0	0	0	0	0	0	0	0.00	100.00	0.00
4.2 - 4.4	0	0	0	0	0	0	0	0	0	0	0	0	0	0	0	0	0	0.00	100.00	0.00
4.4 - 4.6	0	0	0	0	0	0	0	0	0	0	0	0	0	0	0	0	0	0.00	100.00	0.00
4.6 - 4.8	0	0	0	0	0	0	0	0	0	0	0	0	0	0	0	0	0	0.00	100.00	0.00
4.8 - 5.0	0	0	0	0	0	0	0	0	0	0	0	0	0	0	0	0	0	0.00	100.00	0.00
5.0 - 5.2	0	0	0	0	0	0	0	0	0	0	0	0	0	0	0	0	0	0.00	100.00	0.00
5.2 - 5.4	0	0	0	0	0	0	0	0	0	0	0	0	0	0	0	0	0	0.00	100.00	0.00
5.4 - 5.6	0	0	0	0	0	0	0	0	0	0	0	0	0	0	0	0	0	0.00	100.00	0.00
5.6 - 5.8	0	0	0	0	0	0	0	0	0	0	0	0	0	0	0	0	0	0.00	100.00	0.00
5.8 +	0	0	0	0	0	0	0	0	0	0	0	0	0	0	0	0	0	0.00	100.00	0.00
Total	0	0	6104	22987	70728	14204	9752	73189	0	0	0	0	0	0	0	0	196964			
Total (%)	0	0	3.10	11.67	35.91	7.21	4.95	37.16	0	0	0	0	0	0	0	0	100			

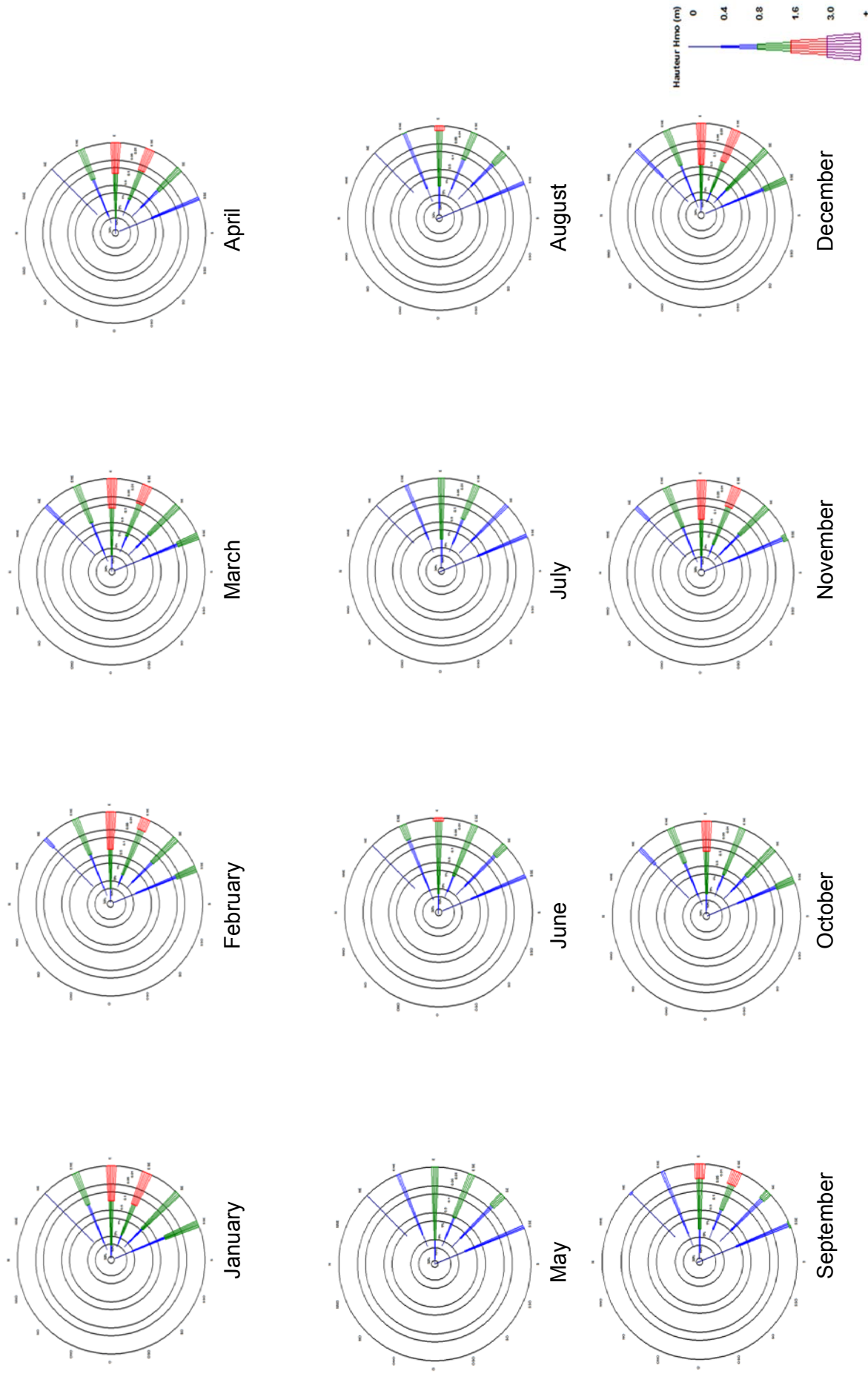


Figure 9 Monthly Near Shore Wave Roses from 1970 to 2011.

## 5.2.2 Storm Events and Extreme Wave Heights

Storm events observed in the Baie-Comeau region were previously analyzed by GENIVAR in 2006 for the Environmental Assessment of the Riprap protection of the “Parc des Pionniers”. The information provided in this report was collected from the Baie-Comeau Airport meteorological station from 1968 to 2006 by analyzing both wind and water levels characteristics. Using the GENIVAR wind-wave model, the corresponding wave parameters ( $H_{m0}$ ,  $T_p$  and direction) were extracted to fully describe each storm event including the storm event of December 2010.

Table 7 gives the storm events characteristics from 1968 to 2011 for the Baie-Comeau region.

Table 7 Storm Events Characteristics from 1968 to 2011 for the Baie Comeau Region.

Date	Time	Offshore Wave Height $H_{m0}$ (m)	Offshore Peak Period $T_p$ (s)	Direction From (°)	Water Level (CD, m)	Water Level (MWL, m)
06/12/2010	16:00	1.94	5.70	90	4.91	3.1 (estimated)
5/02/2006	3:00	0.94	3.98	70	3.34	1.53
17/02/2006	13:00	0.90	3.89	70	2.98	1.17
14/03/2006	22:00	1.71	5.36	80	3.71	1.90
5/04/2006	5:00	0.54	3.01	70	N/A	N/A
31/08/2005	23:00	0.46	2.76	60	3.48	1.67
1/09/2005	2:00	1.47	4.96	100	3.56	1.75
20/09/2005	18:00	0.61	3.21	70	3.95	2.14
2/12/2005	17:00	1.96	5.73	100	4.52	2.71
26/12/2005	15:00	0.40	2.58	50	2.80	0.99
9/10/1976	23:00	1.03	4.16	70	3.59	1.78
10/10/1976	5:00	3.15	7.27	80	3.97	2.16
21/10/1976	18:00	2.55	6.54	80	3.99	2.18
3/04/1975	0:00	2.76	6.81	80	2.44	0.63
4/04/1975	0:00	2.76	6.81	80	3.33	1.52
4/12/1968	23:00	0.18	1.76	180	N/A	N/A
5/12/1968	10:00	0.25	2.05	70	N/A	N/A

The 3 following storm events, considering as severe conditions for the Baie-Comeau region, were simulated using the STWAVE wave model:

- December 6th 2010
- December 2nd 2005
- October 10th 1976

Appendix 3 shows the STWAVE results for these 3 events. Maximum wave heights observed inside ADM range between 2.8 and 3.0 m and correspond to the 1976 storm event.



Return periods for extreme wave heights, according to best fits provided by the Log-Pearson Type III or Log-Normal statistical distribution, were estimated for each direction. Table 8 and Figure 10 show the results.

Table 8 Extreme Near Shore Wave Height ( $H_{m0}$ ) by Direction (Mean Water Level, 0.0m).

Direction From	Return Periods					
	2	5	10	25	50	100
NE	0.3	0.4	0.5	0.5	0.6	0.6
ENE	0.7	0.9	1.0	1.1	1.2	1.3
E	1.6	1.9	2.1	2.4	2.6	2.9
ESE	1.2	1.4	1.5	1.6	1.7	1.8
SE	0.9	1.1	1.2	1.4	1.5	1.5
SSE	0.5	0.7	0.8	0.9	1.0	1.2

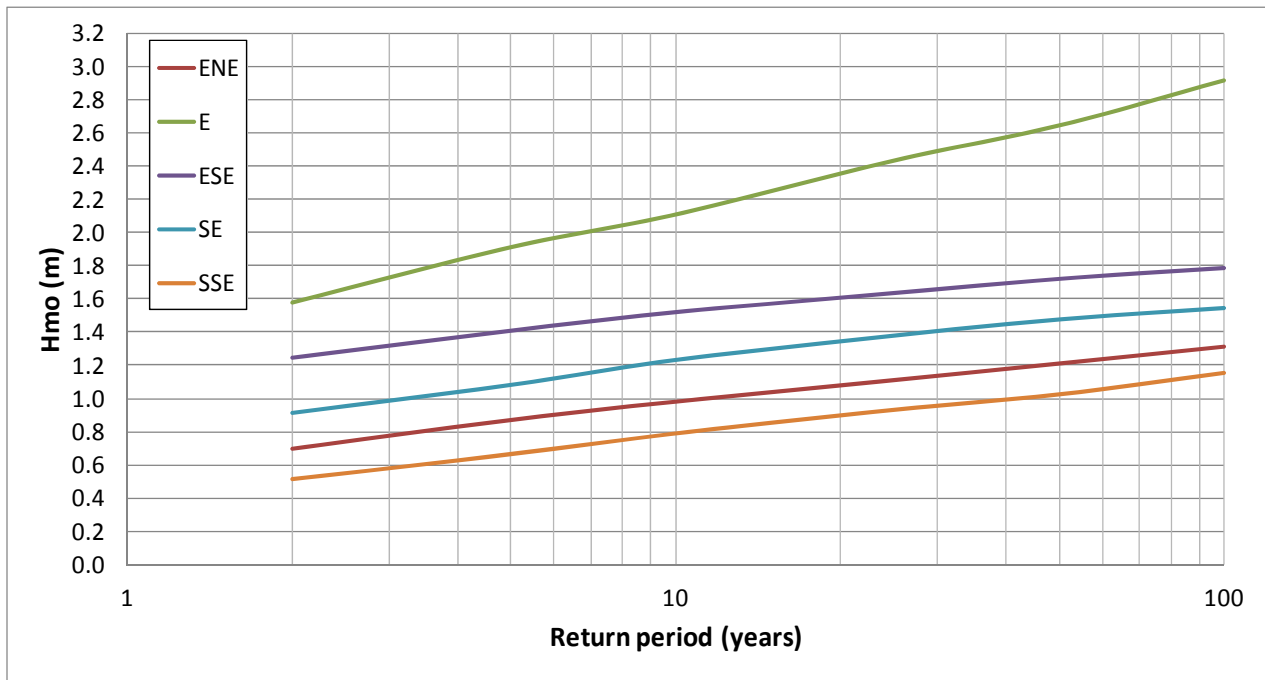


Figure 10 Extreme Near Shore Wave Height ( $H_{m0}$ ) by Direction (Mean Water Level, 0.0 m).

Finally, extreme wave conditions inside ADM were simulated using a wave height of 100 years return period from the East (E) and combined to an extreme water level at El.3.1 m. The following characteristics describe these extreme conditions:

- Offshore Wave height ( $H_{m0}$ ) = **3.64 m**
- Offshore Peak period ( $T_p$ ): **7.8 s**

- Direction From: **East**
- Extreme Water Level: **3.1 m (MWL)**

Figure 11 shows the STWAVE results. The maximum wave heights observed range from 3.2 m at the entrance of ADM to around 2.9 m in the north-central part of the harbour.

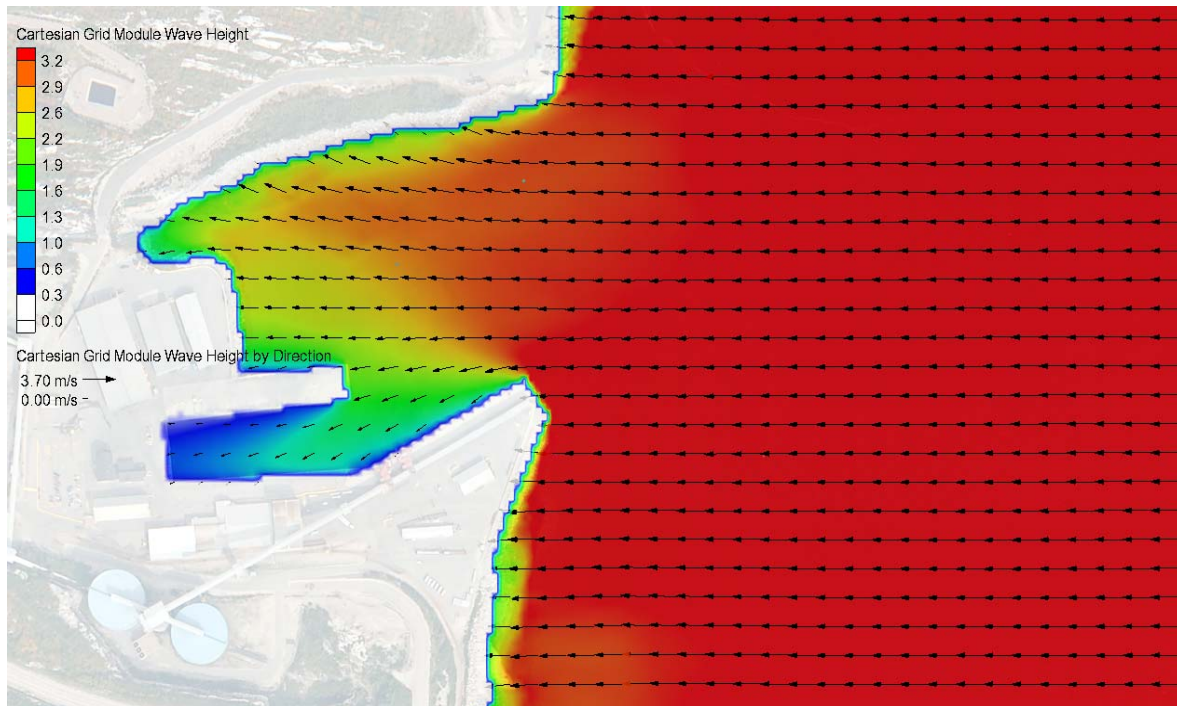


Figure 11 Extreme Wave Conditions in ADM. ( $H_{m0} = 3.64$  m;  $T_p = 7.8$ s; Direction From = East, Water Level = 3.1 m)

## 6. SEDIMENT STABILITY AND CIRCULATION PATTERNS IN ADM

---

### 6.1 Sediment Stability

This section of the report attempts to support the engineering feasibility study by providing sediment stability mapping to confirm or refine the design of the Monitoring Natural Recovery (MNR) and the Capping Zones.

#### 6.1.1 Theory and Approach

##### Theory

Motion of a sediment particle is the result of resulting forces that are sufficient in magnitude to dislodge the particle from its resting place.

Calculations and numerical modelling of erosion, transport and sediment deposition in estuaries and coastal environment rely heavily on expressions that contain the bed shear-stress, representing the frictional force exerted by the flow per unit area of the seabed. The initiation of sediment motion becomes possible when the waves and currents induced bed shear stress is greater than the critical bed shear-stress which is defined by the bed sediment characteristics. The resulting stress consists of a steady component due to the current-alone and an oscillatory component due to the waves.

The maximum bed shear-stress is calculated to determine the threshold of sediment motion and is given by a vector addition:

$$\tau_{max} = [(\tau_m + \tau_w |\cos\phi|)^2 + (\tau_w |\sin\phi|)^2]^{1/2}$$

[SOULSBY R.L. and CLARKE S. 2005]

In which  $\tau_m$  and  $\tau_w$  are respectively the cycle-mean bed shear-stress and the oscillatory wave-alone bed shear-stress.

##### Approach

The maximum bed shear-stress was calculated on a grid with a resolution of 2 x 2 m to provide the sediment stability mapping of the entire Anse du Moulin (ADM) under different hydrodynamic conditions. This analysis was performed by transferring the output wave data issued from the STWAVE model to a GENIVAR script (MATLAB) in order to obtain the maximum bed shear stress at each node of the grid. Appendix 4 describes in details the model setup, inputs and equations used to assess the sediment stability in Anse du Moulin (ADM) based on the bed shear-stress analysis.

A summary of the input data and main assumptions used to assess the sediment stability is described here:

- A depth average current velocity of 10 cm/s was used to calculate the wave cycle-mean bed shear-stress ( $\tau_m$ ). This value is based on the 2011 current measurements collected by both ADCP (Hydro-1 and Hydro-2);
- The water depths (based on 2011 bathymetric data), wave heights and wave periods were extracted from STWAVE at each node of the grid and for each simulated scenario;
- The critical bed shear-stress ( $\tau_{critical}$ ) was calculated using the median grain size (D50) issued from all the sample collected during the 2011 survey as well as some samples collected in 2006, 2007 and 2008 to complete the dataset;
- High quality videos taken in 2011 show no ripples on the seabed of ADM, thus a bed roughness equal to the median grain size (D50) was assumed;
- The angle between the current direction and direction of wave travel was considered equal to zero to calculate the maximum bed shear-stress (vector addition);
- As the oscillatory wave-alone bed shear-stress varies through a wave cycle, the maximum orbital velocity at the seabed was considered to calculate this component;

The next section described the hydrodynamic conditions selected to perform the sediment stability assessment.

### 6.1.2 Hydrodynamic conditions

Water levels and wave heights are both significant parameters to be considered to assess the sediment stability in ADM. The near shore wave characteristics (see section 5.2) and the tide levels were combined to define the hydrodynamic conditions to be simulated. The 24, 6 and 1 hour wave heights were selected to simulate a representative range of energetic wave conditions in ADM.

In theory, the occurrence of large waves and high water level may be correlated under certain weather conditions. In fact, under storm conditions, both large waves and storm surges tend to be associated. The CIRIA (2007) explains that the correlation between the water level and waves remains modest in areas where the astronomical component of the tides is much larger than the storm-surge component, which is the case in Baie-Comeau.

For the current analysis, since the hydrodynamic conditions were established by the combination of the astronomical component of the water level and the wave height, it remains appropriated to consider the independence between the water level (tides) and the wave height. Therefore, there is no correlation between them and the joint probability of this event is simply the product of the two marginal probabilities (CIRIA, 2010).

Table 9 shows the selected hydrodynamic conditions used to assess the sediment stability in ADM as well as the frequency associated to each event.

Table 9 Selected Hydrodynamic Conditions for the Sediment Stability Assessment in ADM.

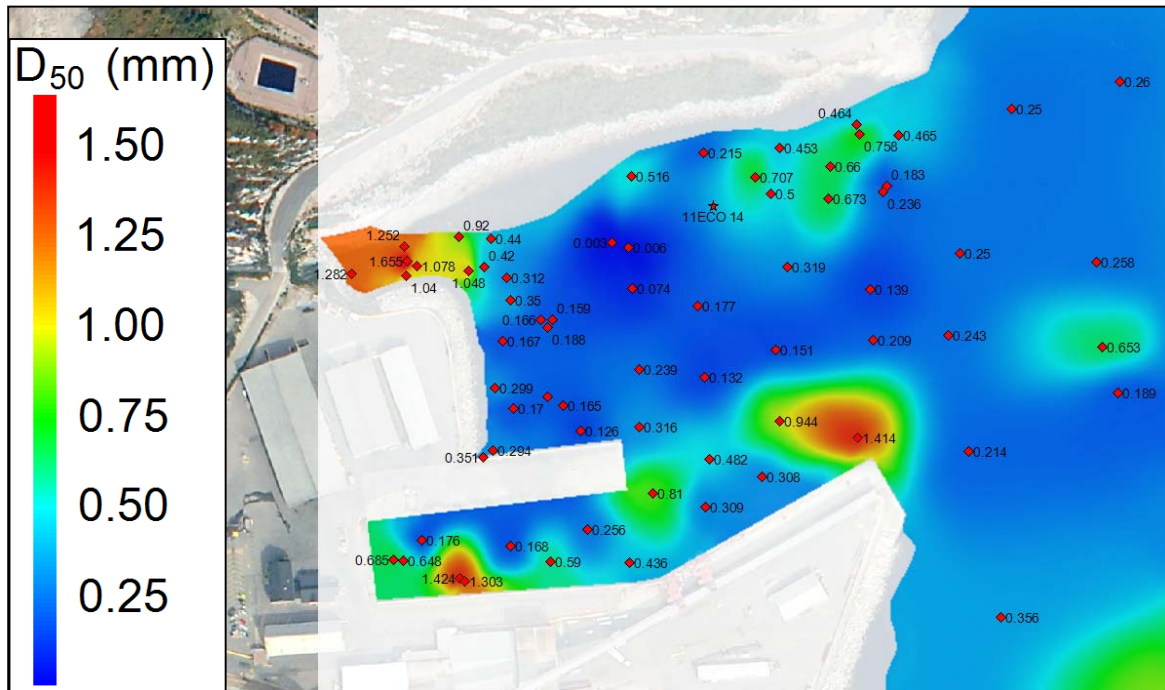
Scenario	Near Shore Wave Characteristics			Tide Level			Event Occurrence
	Hm0 (m)	Tp (s)	Frequency (hours/year)	Tide label	Water Elevation (MWL, m)	Frequency (hours/year)	Frequency (hours/year)
1	1.2	4.8	24	(MWL)	< 0.0	4380	12
2	1.4	5.3	6	(MWL)	< 0.0	4380	3
3	1.8	6.1	1	(MWL)	< 0.0	4380	0.5

### 6.1.3 Sediment Stability Mapping

#### Median Grain Size and Critical Bed-Shear Stress

Evaluation of the critical bed shear-stress required to initiate sediment motion under steady flow conditions is based on the Modified Shield diagram (see Appendix 4). As such, the assessment of the sediment stability in ADM relies on the sediment grain sizes that characterize the surface seabed at multiple locations in Anse du Moulin. During the 2011 field survey, 30 sediment samples were collected at the seabed surface (within the first 15 cm depth) and the median grain size ( $D_{50}$ ) was used as reference value to generate the associated critical bed-shear stress map. Few sediment samples collected in 2006, 2007, 2008 and 2009 were also used to complete the 2011 dataset in area where no information were available. Sediment samples from previous years were added with caution and compare with the 2011 sediment characteristics to avoid outliers. In fact, it is considered that after 2 to 5 years, the sediment characteristics, for a same location, could have been modified and therefore considered not anymore representative of the grain size observed in 2012.

Figures 12 and 13 show respectively the median grain size and the associated critical bed-shear stress maps.



**Note:** Sample 11ECO-14 with a  $D_{50}$  of 2.14 mm was removed from the dataset to avoid interpolation irregularities

Figure 12 Median Sediment Grain Size ( $D_{50}$ , mm) at the Seabed Surface of Anse du Moulin.

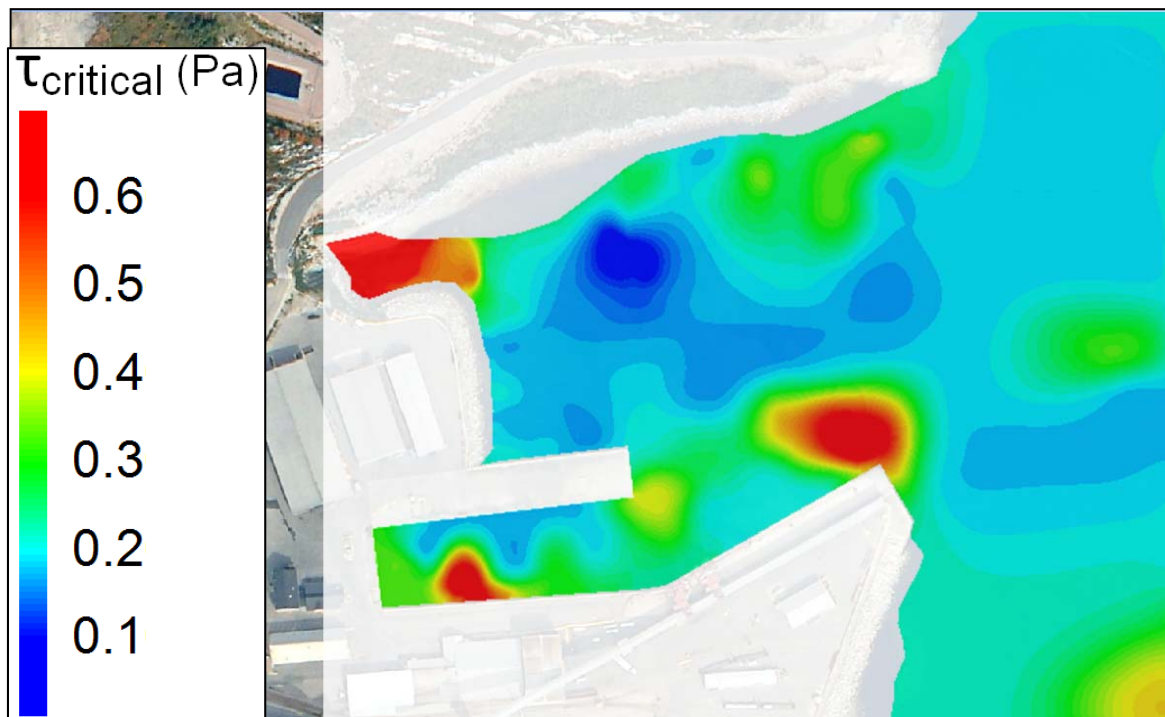


Figure 13 Critical Bed Shear-Stress (Pa) in Anse du Moulin.

## Sediment Stability in Anse du Moulin

Sediment stability mapping of Anse du Moulin was established by the comparison between the critical bed-shear stress and the maximum bed-shear stress (cycle-mean bed shear-stress combined to the oscillatory wave-alone bed shear-stress, see Appendix 4). Hydraulic conditions showed in Table 9 were used and waves were propagated offshore from the East since this sector remains the more frequent and the most representative of the wave conditions inside the bay. The 2011 bathymetric data collected in ADM was used to perform this analysis.

The following criteria were used to assess the sediment stability in ADM:

- If  $\frac{\tau_{max}}{\tau_{critical}} < 1$       **[Stable]**
- If  $\frac{\tau_{max}}{\tau_{critical}} > 1$       **[Unstable]**
- Hatched polygon      **[Unstable, Surf Zone]**

It is important to mention that in the surf zone, wave breaking injects a considerable amount of turbulence into the water column, which provides an additional mobilizing effect that may allow sediment motion at considerably lower velocities than predicted from the Shield curve. For this reason and because the theory confirms that wave breaking induced alongshore sediment transport, the surf zone is logically considered as an “unstable” zone. The shoreline riprap protection located in the North of Anse du Moulin was delimited using information provided by ALCOA and GENIVAR during the 2011 field survey as well as verifications with aerial photo taken at low tide. No stability results were provided within this area where bottom sediments are protected by rock armour.

Finally, it is important to mention here that “sediment stability” refers to potential for movement of sediment (re-suspension) and does not indicate or specify how far the sediment might be transported.

Figures 14 to 16 show the sediment stability results for each hydraulic condition provided in Table 9.

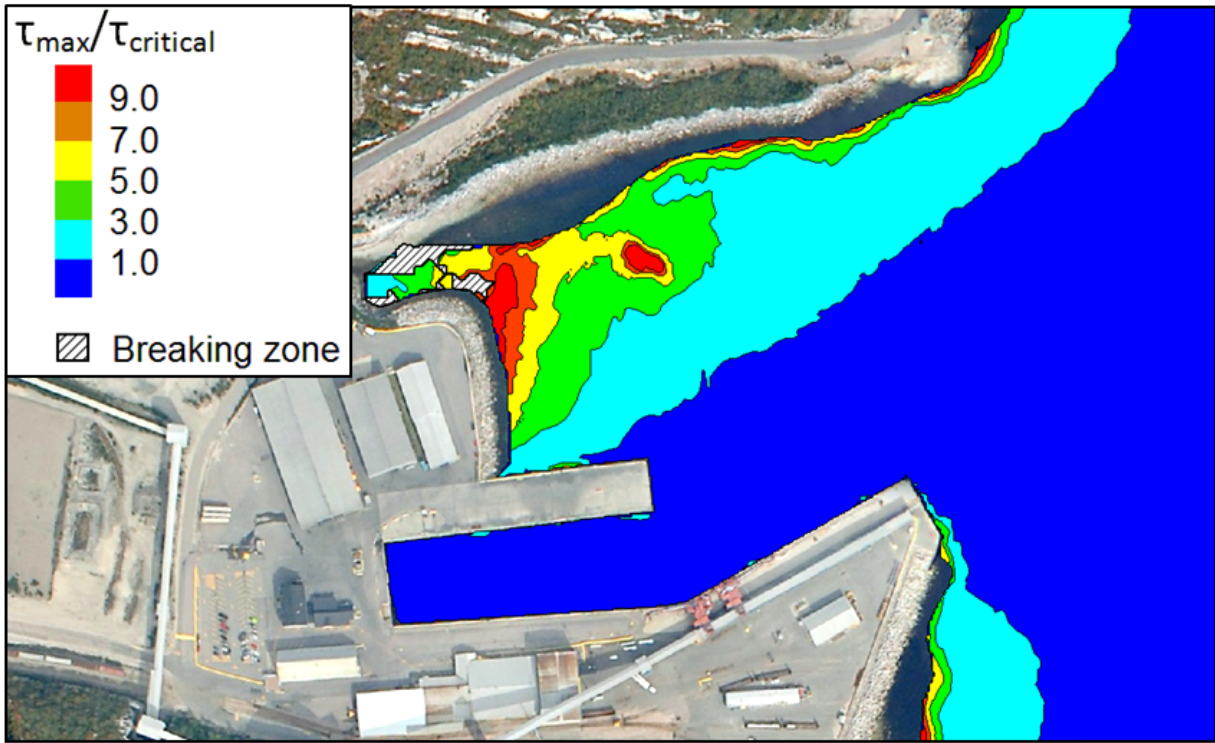


Figure 14 Sediment Stability under a Wave Height of 1.2 m (24 hrs/year) from the East combined with a Mean Water Level (MWL).

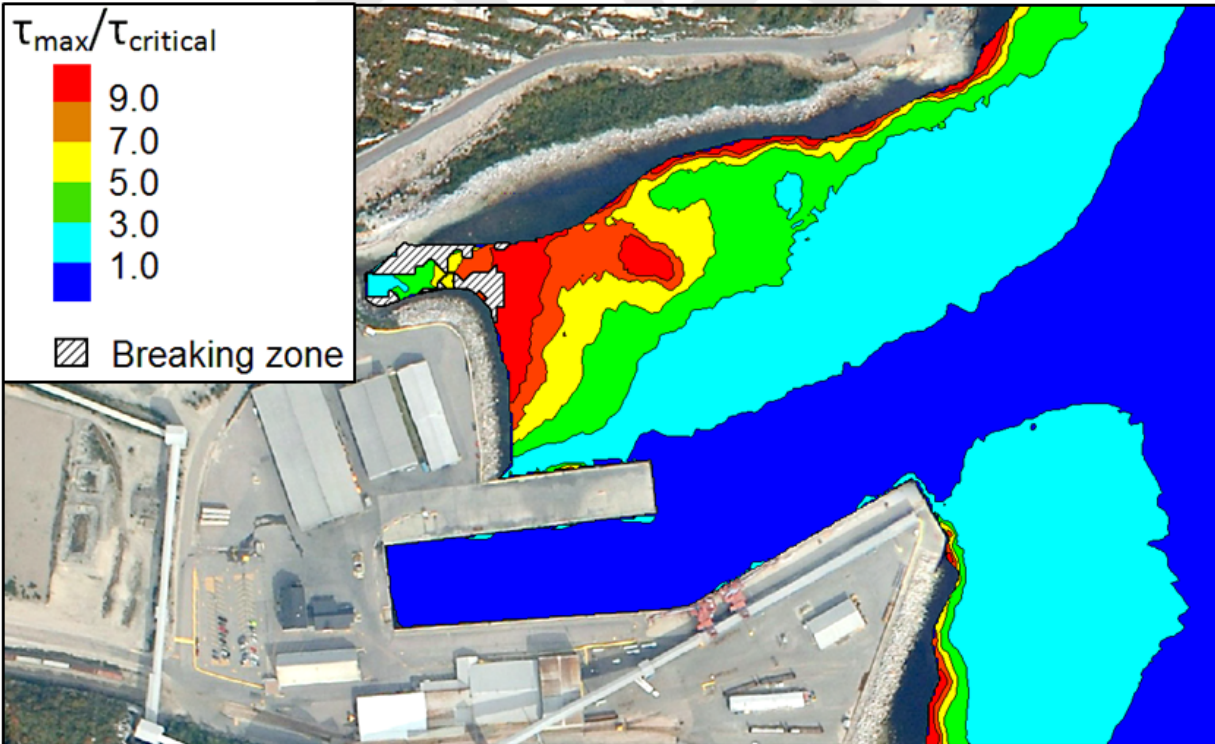


Figure 15 Sediment Stability under a Wave Height of 1.4 m (6 hrs/year) from the East combined with a Mean Water Level (MWL).



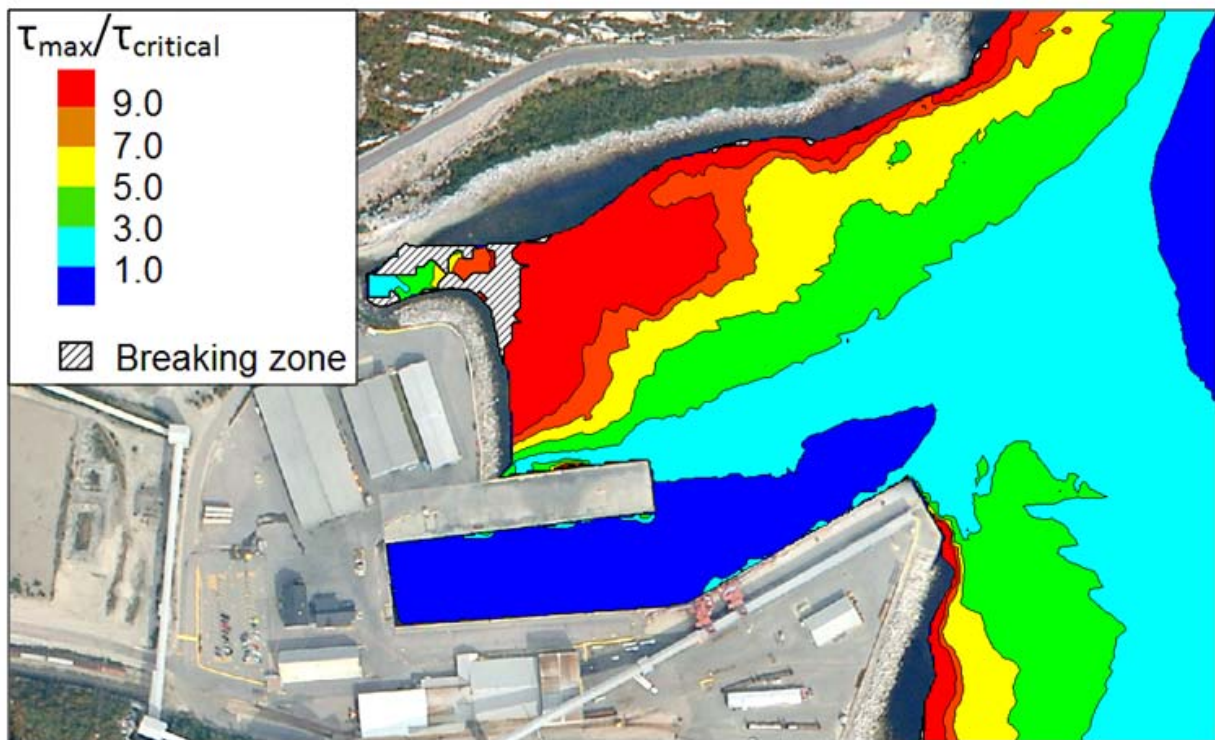


Figure 16 Sediment Stability under a Wave Height of 1.8 m (1 hrs/year) from the East combined with a Mean Water Level (MWL).

Results shown on Figures 14 to 16 indicate that the North-West part of the bay (preliminary capping zone) remains unstable under all simulated conditions with ratio ranging between 4 and 9. Within the preliminary MNR zone located in the North-East of ADM, ratio between 1 and 4 are mainly observed under a 24 hours/year wave height (1.2 m) to reach ratio ranging between 3 and 7 in shallow water (water depth of less than 2 m). Under the 6 and 1 hour/year wave height conditions, ratio between 3 and 9 cover this same preliminary MNR zone.

The waterway located at the entrance of ADM in the South remains stable under the 24 and 6 hours/year wave heights, which is slightly different under the 1 hour/year wave height with ratio between 1 and 3 at the entrance of the bay.

The sediment stability maps presented in this section remains an appropriated tool to assess the spatial variability under a representative range of hydraulic conditions. Theoretically, ratio above 1 would lead to instability, but in practice, ratio slightly above 1 can be also considered stable. Turbidity measurements in specific area of Anse du Moulin should be used to confirm the upper limit ratio value at which sufficient sediment movement would be observed. Finally, information provided by

the stability maps should be combined with results from the risk assessment study to identify contaminated zones that represent a potential environmental risk for the Anse du Moulin and Baie des Anglais ecosystem. The next section describes the main circulation patterns within ADM using measured and simulated current magnitudes and directions.

## 6.2 Current Velocities and Directions in the ADM

### 6.2.1 Instantaneous Current Measurements – ADCP Transects

During October 4<sup>th</sup>, 5<sup>th</sup> and 7<sup>th</sup> 2011, instantaneous currents measurements (magnitudes and directions) were collected using an Acoustic Doppler Current Profiler (ADCP) along 5 transects inside and outside of Anse du Moulin. Figure 17 shows the transect locations and ID (letters).

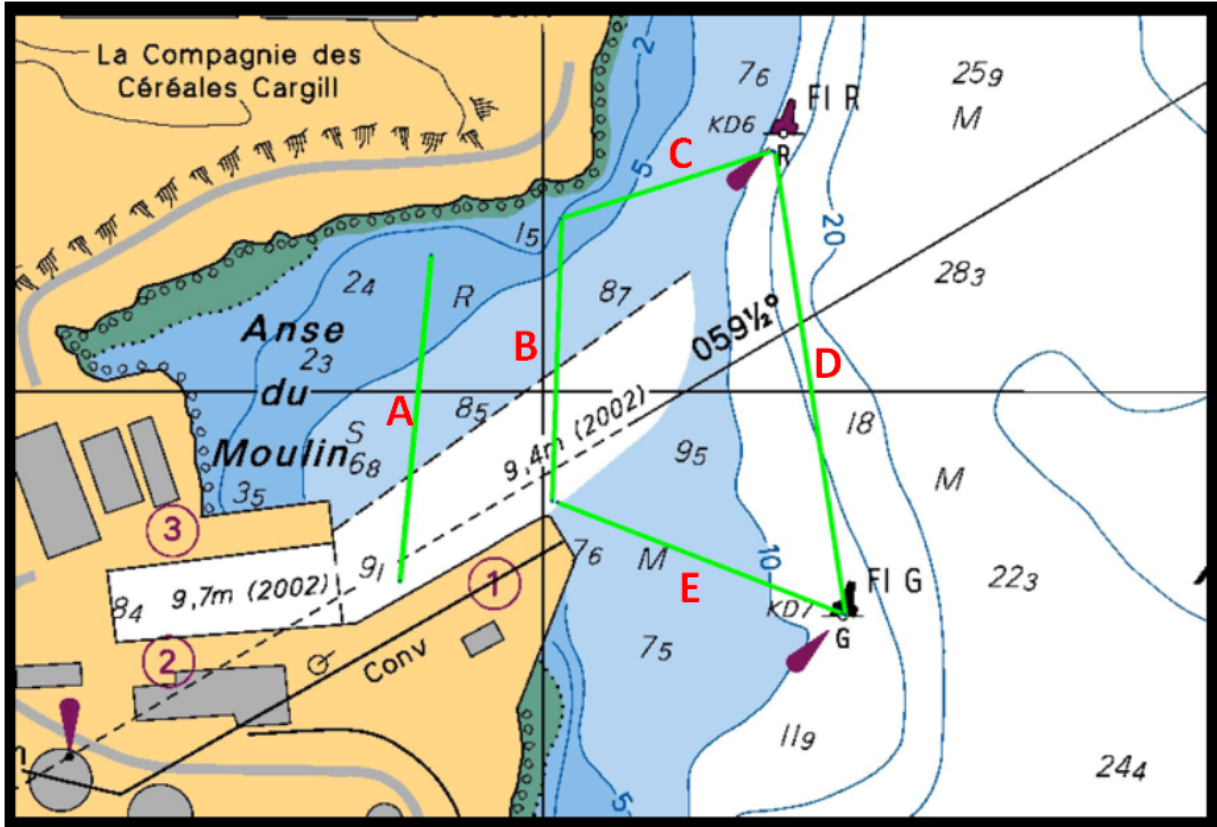


Figure 17 ADCP Transect Locations and ID (letters) Used to Measure Instantaneous Current Magnitudes and Directions on October 4<sup>th</sup>, 5<sup>th</sup> and 7<sup>th</sup> 2011.

A total of around 100 transects were collected during these 3 days with approximately 50 cross-sections collected inside Anse du Moulin along transect A and B (Figure 17). The meteorological and hydraulic conditions observed in ADM during these 3 days of measurement are summarized in Table 10.

Table 10 Meteorological and Hydraulic Conditions Observed in ADM on October 4<sup>th</sup>, 5<sup>th</sup> and 7<sup>th</sup> 2011.

Date	Measurement Period	Water Level Range (MWL, m)	Wind Direction (from)	Wind Speed (km/h)	Wave Direction (from)	Wave Height (Hm0, m)	Peak Period (Tp, s)
October 4th 2011	9:30 AM to 4:00 PM	from 2.4 m to 1.0 m	East	20 - 35	East	0.9	4
October 5th 2011	8:30 AM to 12:30 PM	from 2.0 m to 2.5 m	North	18 - 27	N/A	N/A	N/A
October 7th 2011	8:30 AM to 12:00 PM	from 1.2 m to 2.4 m	West	9 - 20	N/A	N/A	N/A

Note: N/A: Wave Height Non-Available.

The next sections describe the current magnitudes and directions for the ADCP profiles located inside Anse du Moulin along transects A and B during October 4<sup>th</sup>, 5<sup>th</sup> and 7<sup>th</sup> 2011 respectively. The current characteristics are given for selected ADCP profiles providing the most representative conditions of current magnitudes and directions.

#### October 4<sup>th</sup> 2011

Table 11 provides the ADCP profile characteristics collected on October 4<sup>th</sup> 2011, while Figure 18 shows the ADCP profiles along transect A and B respectively. The selected profiles are considered representative of the current conditions measured in ADM on October 4<sup>th</sup> under wave conditions incoming from the East (Table 10).

Table 11 Profile Characteristics Measured on October 4<sup>th</sup> 2011 with the ADCP.

Transect ID	Location (see Figure 17)	Time	Water Level (MWL, m)
A-1	Transect A	9:40	2.4 m, Ebb
A-2	Transect A	13:00	1.2 m, Ebb
A-3	Transect A	14:00	1.0 m, Flood
B-1	Transect B	10:40	1.9 m, Ebb
B-2	Transect B	10:55	1.8 m, Ebb
B-3	Transect B	15:00	1.2m, Flood

During the first day of measurement, wind speeds of 20 to 35 km/h from the East lead to significant wave heights of 0.9 m (Tp = 4s) during the entire day in ADM. Under these conditions, the ADCP profiles reveal that alongshore currents from the East (negative current magnitudes) are induced in the North part of the bay with magnitudes ranging between 15 to 30 cm/s, while this pattern is inversed in the

South beside the wharves with current magnitudes in the order of 10 to 30 cm/s toward the East (positive current magnitudes). All transects shown on Figure 18 confirm the presence of longshore currents induced by waves in the shallow part of the bay (North), mainly within the top surface layer of the 5 m water depth profile. Comparison between transect A and B indicates that alongshore currents from the East are observed within a smaller area along transect A (first 100 m from the shoreline), while currents from the East along transect B are observed relatively over the entire cross-section within the first 4 m water depth from the surface. Alongshore currents in the northern part of the bay are observed between 0 to 7.5 m water depth with maximum current magnitudes in the order of 30 cm/s.

Currents exiting the bay in the South part are stronger (15 to 30 cm/s) along transect B within the 4 to 12 m depth. In fact, the South part of transect A is relatively well protected by the wharf # 3 which seems to reduce the current magnitudes in this area with speeds in the order of 5 to 15 cm/s. The current magnitudes exiting the bay are higher during ebb conditions as observed by the comparison between transect B-1 and B-2 with transect B-3. The tidal influence likely explains this small magnitude difference based on the fact that wave heights were around 0.9 m during the entire day of October 4<sup>th</sup>.

Transect A-1 to A-3 indicate clearly that the resulting current direction is from East to West within the first 100 m from the North shore, while the South part of the bay shows resulting current directions from West to East. The same pattern is also observed along transect B with the difference that currents observed in the South area of the bay, near the wharves, are from both directions with surface currents entering the bay and exiting from the deeper zone.

Finally, the current magnitudes and directions measured with the ADCP on October 4<sup>th</sup> were compared with the simulated currents obtained from the model CMS-FLOW (USACE, 2006). This model uses the output wave data from STWAVE to simulate the wave-induced currents based on the resulting radiation stress.

Appendix 4 describes the CMS-FLOW model setup and input parameters.

The results provide depth-averaged current magnitudes and directions. Figure 19 shows the simulated currents on October 4<sup>th</sup> 2011.

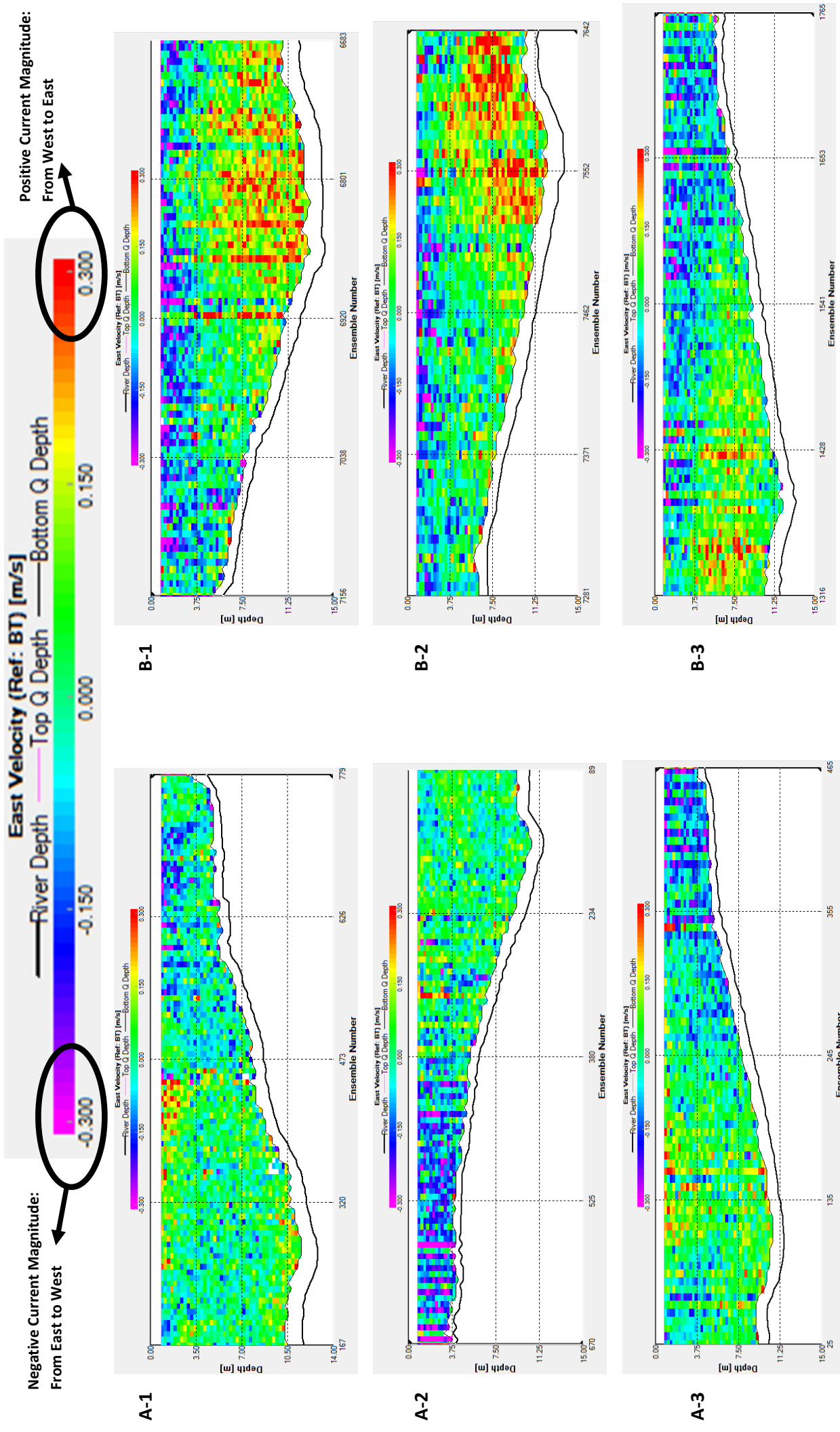


Figure 18 ADCP Profiles Measured October 4<sup>th</sup> 2011 Along Transect A and B in the Anse du Moulin.

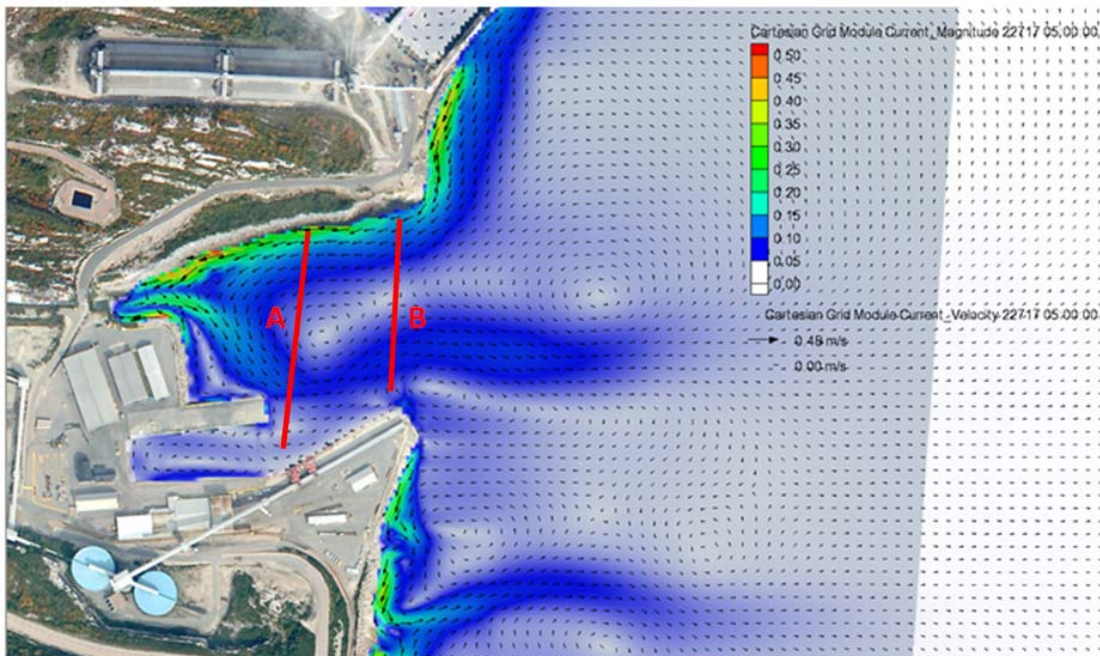


Figure 19 Wave-Induced Currents in ADM, October 4<sup>th</sup> 2011 ( $H_m0 = 0.9$  m;  $T_p = 4.0$ s).

The pattern shown on Figure 19 can be described as an anti-clockwise gyre with maximum speed currents of 30-35 cm/s in the vicinity of the breaking zone located near the shoreline in the northern and western part of ADM. In the South part of the bay, current magnitudes of 5 to 15 cm/s are observed along transect A compare to speeds ranging from 5 to 10 cm/s along transect B. The depth averaged currents simulated with CMS-FLOW indicate the main circulation pattern in ADM, but cannot reproduce the current inversion observed within the water column along transect B (see ADCP profiles B-1 to B-3, Figure 18). In fact, the CMS-FLOW model cannot reproduce the effect of wind blowing from the East that induces currents toward the West within the top surface layer of the water column.

Following these analyses, the results obtained from CMS-FLOW are considered realistic on a depth-averaged basis since the simulated currents are in the same direction and in the same order of magnitude than those measured with the ADCP along both transects.

Finally, it is important to mention that within the surf zone located in the northern and western part of the bay, wave breaking injects a considerable amount of turbulence into the water column, which mainly explains the maximum currents magnitudes in this area.

October 5<sup>th</sup> and 7<sup>th</sup> 2011

The current conditions observed in ADM during October 5<sup>th</sup> and 7<sup>th</sup> 2011 are mainly driven by tides since no waves were observed during this period with wind incoming from the North and the West respectively (Table 10). Figure 20 and Table 12 show the ADCP profile characteristics for the selected transects along cross-section A and B (Figure 17). These profiles are considered representative of the current conditions observed on October 5<sup>th</sup> and 7<sup>th</sup>.

Table 12 Profile Characteristics Measured on October 5<sup>th</sup> and 7<sup>th</sup> 2011 with the ADCP.

Transect ID	Date	Location (see Figure 17)	Time	Water Level (MWL, m)
A-4	October 5th	Trasect A	9:00	2.0 m, Flood
A-5	October 7th	Trasect A	10:15	2.0 m, Flood
A-6	October 5th	Trasect A	11:00	2.1 m, Ebb
B-4	October 7th	Trasect B	8:10	1.3 m, Flood
B-5	October 5th	Trasect B	10:50	2.2 m, Ebb
B-6	October 7th	Trasect B	11:40	2.3 m, Flood

ADCP profiles shown on Figure 20 indicate that under tide and wind influence with no wave in ADM, the maximum instantaneous current magnitudes range from -15 to 15 cm/s along both transects A and B. The 2 main patterns are given by comparing transects A-4 and B-4 measured during the flood as well as transects A-6 and B-5 measured during the ebb.

Both transects A-4 and B-4 were collected both during the flood tide (early in the morning, 8:00 – 9:00) show a current pattern entering in ADM mainly in the deeper part of the bay (South) with magnitudes in the order of 10 to 15 cm/s. The opposite pattern is observed during the ebb tide along transect A-6 and B-5 while magnitudes around 15 cm/s from West to East were collected once again in the deeper zone of the bay.

In general, based on the 6 profile characteristics shown on Figure 20, incoming and outgoing currents are observed in ADM under flood and ebb tide respectively with magnitudes oscillating between 0 to 15 cm/s. This pattern seems more defined in the navigation channel in the South part of ADM.

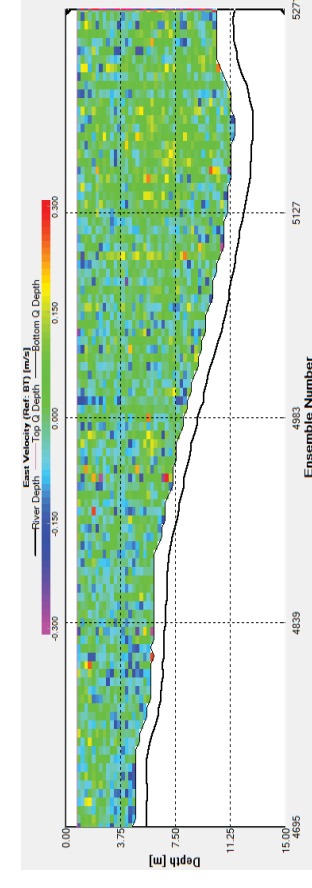
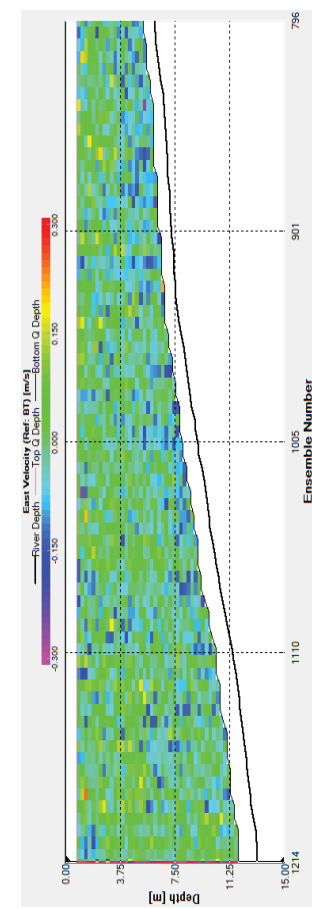
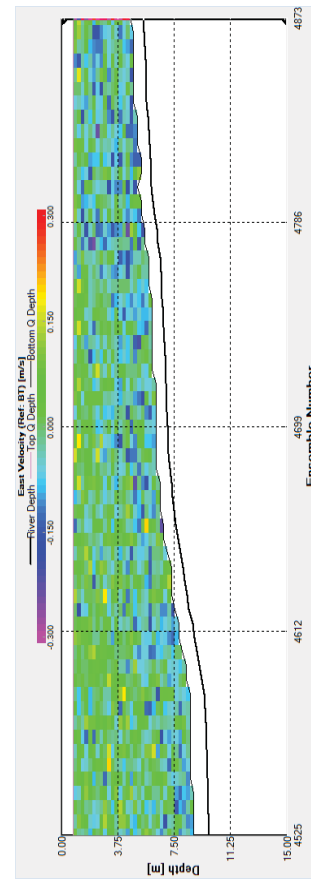
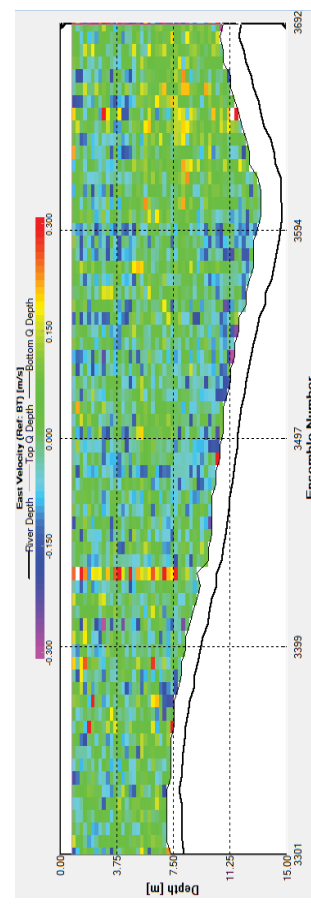
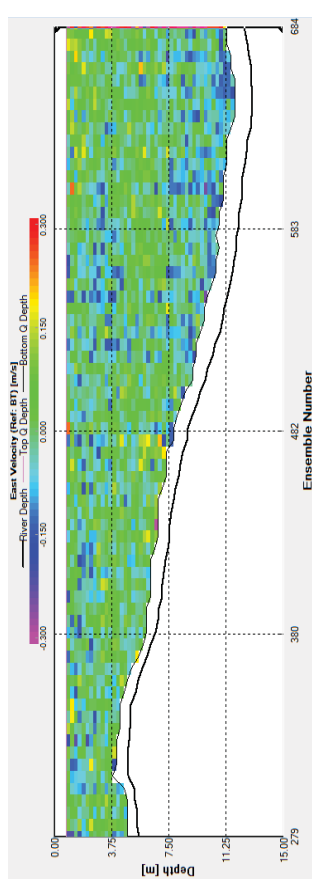
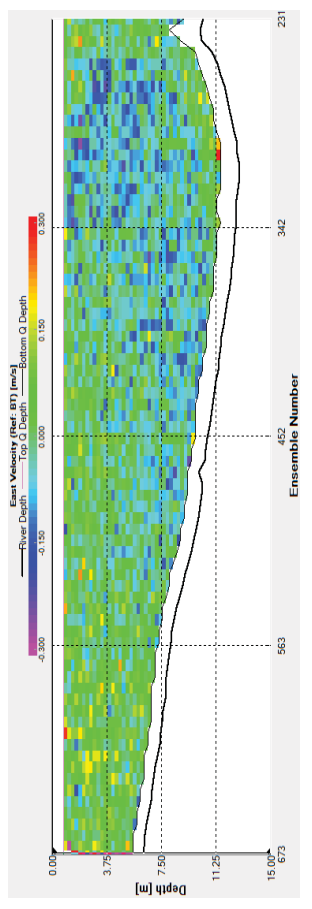


Figure 20 ADCP Profiles Measured October 5<sup>th</sup> and 7<sup>th</sup> 2011 Along Transect A and B in Anse du Moulin.



## 6.2.2 Surface Current Measurements – Drogue Tracks

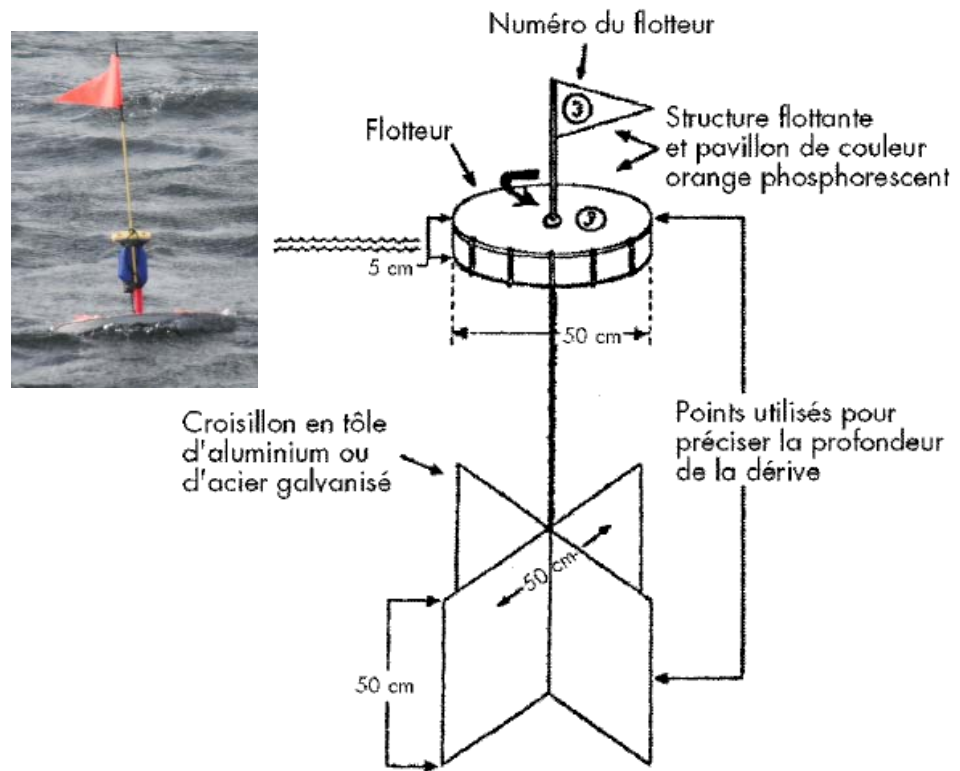
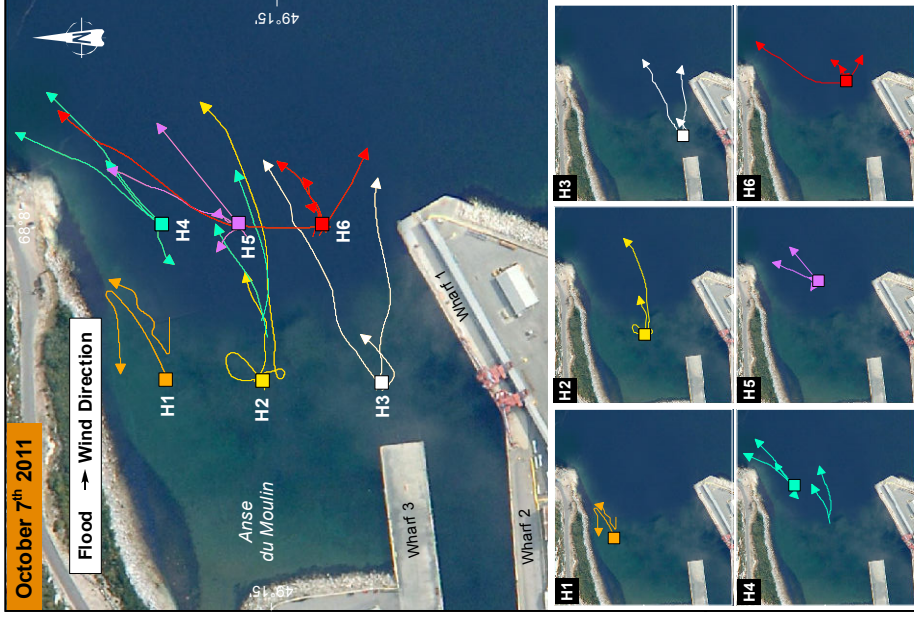
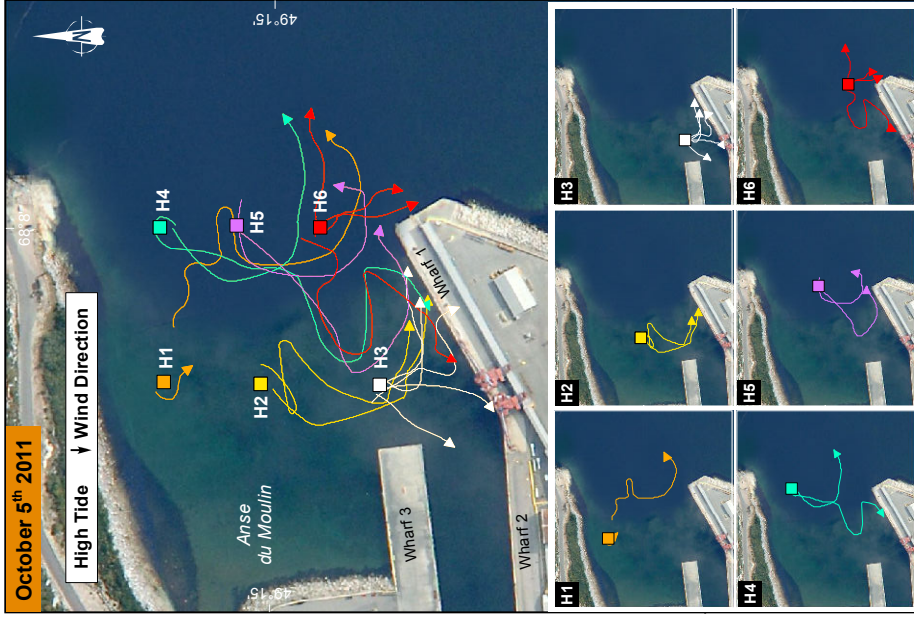
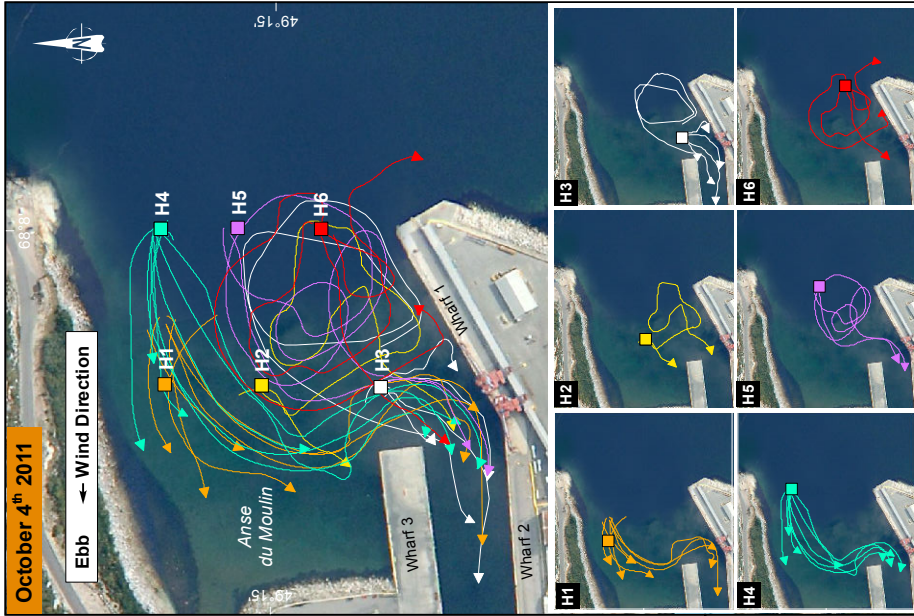


Figure 21 Drogue Model Used During the 2011 Field Work.

During the same 3 days of October 4<sup>th</sup>, 5<sup>th</sup> and 7<sup>th</sup> 2011, drogues were released in ADM to collect the surface currents pattern. Figure 22 summarizes all the drogue tracks observed during these 3 days and gives the associated hydraulic and meteorological conditions. Figure 21 shows the schematic of the drogue used during the survey work.

The drift patterns are primarily influenced by surface currents generated by winds that occurred during October 5<sup>th</sup> and 7<sup>th</sup> and, by the combined effect of wind and waves on October 4<sup>th</sup>. Under wave conditions from the East (October 4<sup>th</sup>), the drogues released in the North part of the bay followed a path from East to West before drifting to the South with a final path to the West to stop in the berthing area located between wharves # 2 and 3. This current pattern remains consistent with the results discussed previously (Figures 18 and 19) showing an anti clockwise gyre under wave conditions from the East in ADM. In the proximity of the wharves, the surface currents are driven by the winds and directed to the West which also remains consistent with the ADCP profiles showing surface currents incoming from the East (Figure 18) in this specific sector of the bay. In fact, the drogue paths were not influenced by the bottom currents exiting ADM near the wharves since they are only driven by currents within the layer defined by the first 3m of water from the surface. Drifters released near the wharves show the same pattern with resulting directions from East to West to finish their courses between wharves # 2 and 3.



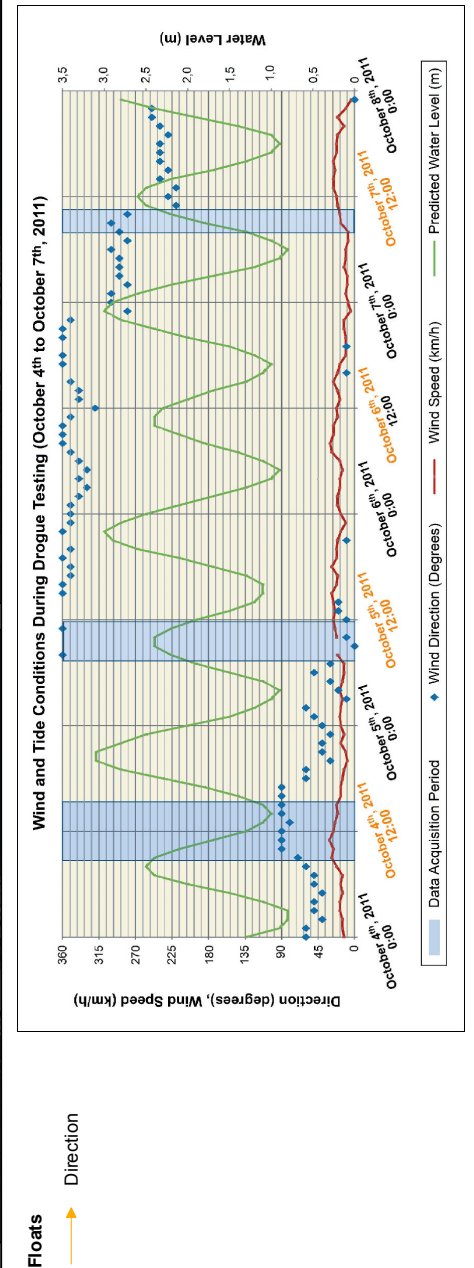
Sediment Rehabilitation  
of Anse du Moulin, Baie des Anglais, Baie-Comeau  
Hydrodynamic and Sediment Dynamics Modeling Study -  
Anse du Moulin



Figure 22  
**Drogue Tracks Released October 4<sup>th</sup>, 5<sup>th</sup> and 7<sup>th</sup>, 2011 and Overview of Hydrodynamic Conditions**

Sources :  
Image : XEOS(SCHM), 21 septembre 2007  
Floates, GENIVAR, 2011  
Tables, Marc Pellerin, 2011 (figure\_pour carte denivour\_feuille\_vent.xlsx)  
Mapping: GENIVAR, geq  
File: 111\_21002\_RY\_geq\_122\_Derive\_120620\_AN.mxd

0 55 110 m  
MTM, fuseau 6, NAD83



Floates  
Direction

Under winds from the North (October 5<sup>th</sup>) and from the West (October 7<sup>th</sup>), the drogue were driven in the same direction than wind with a path resulting outside the bay and in the South respectively. These results confirm that wind induce currents in the first 3 m water depth which is also observed on the ADCP profiles shown on Figure 20.

### 6.2.3 Average Current Measurements – ADCP Moorings

From October 8<sup>th</sup> to November 23<sup>rd</sup> 2011, two ADCP were moored in the Anse du Moulin. Map 3 (see section 5.1) indicates the location of both ADCP (Hydro-1 and Hydro-2). During this period, the current magnitudes were measured continuously and averaged over periods of 20 minutes. The current magnitudes were averaged on cells (bin) of 35 cm height constituting the water column above the ADCPs. Figure 23 shows the averaged current magnitudes measured in surface and near the bottom by Hydro 1 from October 8<sup>th</sup> to November 23<sup>rd</sup> 2011. The comparison between current magnitudes measured by Hydro 1 and 2 did not reveal significant differences and for this reason, data from Hydro-1 were selected to describe the current conditions.

Figure 23 reveals that averaged current magnitudes are most of the time lower than 10cm/s with no significant difference between surface and bottom patterns. No significant correlation was found between the current magnitudes and the significant wave events measured in ADM over the observation period (see Appendix 2). The main reason that likely explains these results remains the location of both ADCP relative to the shoreline where stronger currents were measured. Figure 24 shows the locations of both ADCPs with associated currents induced by waves under storm conditions measured on April 23<sup>rd</sup> 2012 (Hm0 = 2.04 m).

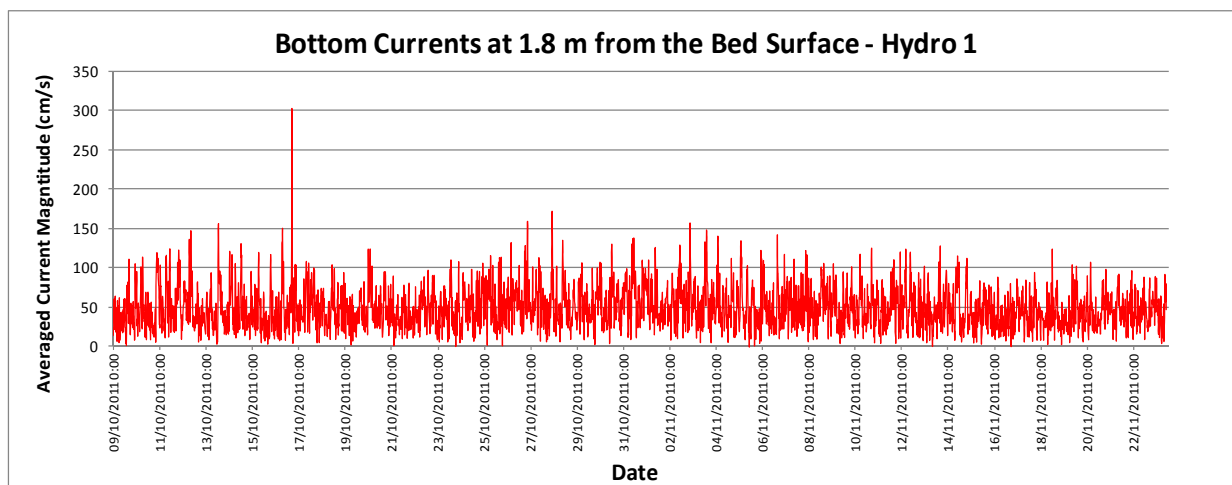
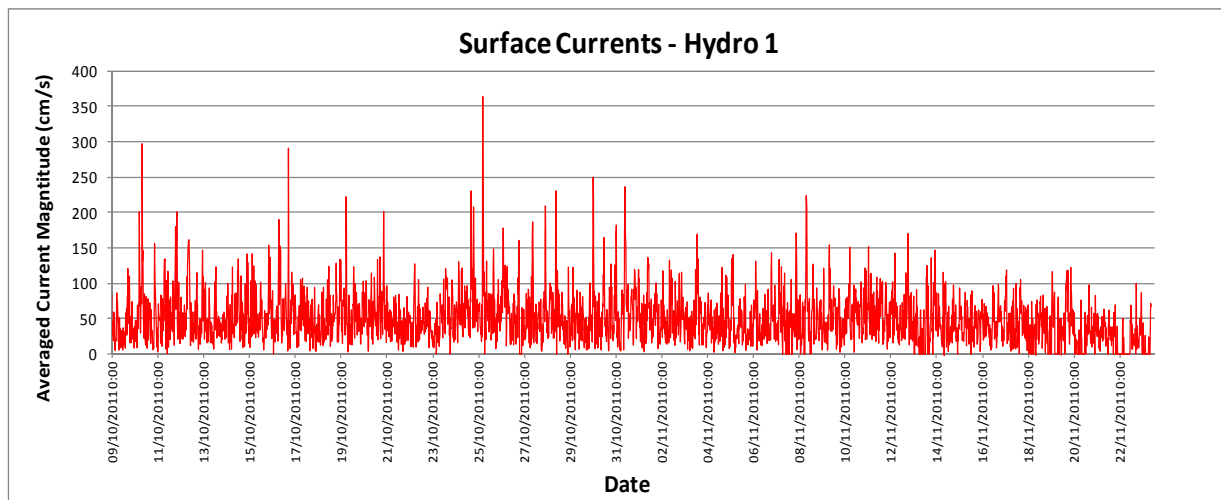


Figure 23 Averaged Surface and Bottom Current Magnitudes Measured by Hydro-1 from October 8<sup>th</sup> to November 23<sup>rd</sup> 2011.

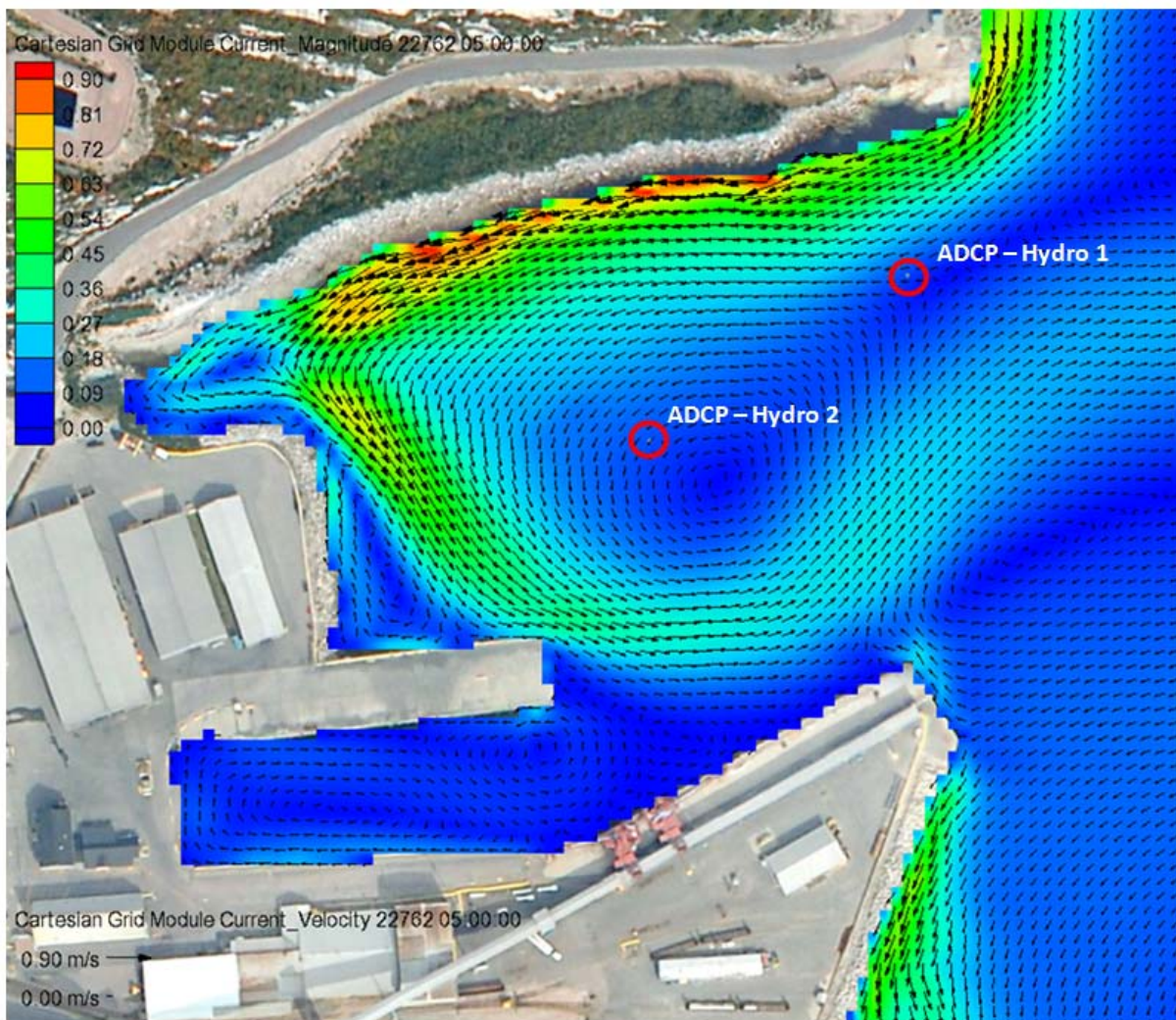


Figure 24 Location of ADCPs and currents induced by waves on April 23<sup>rd</sup> 2012 (Hm0 = 2.04m; Tp = 5.8s; Direction from East).

Current magnitudes induced by tides and by winds at the surface remain most of the time smaller than 10 cm/s. These findings are in agreement with the current velocities shown on Figure 20.

#### 6.2.4 Bathymetry Comparison 2007-2011

Bathymetric data measured during the Fall 2007 and during the Fall 2011 were compared to identify potential zone of erosion and accumulation in Anse du Moulin. Figure 25 shows the difference in elevation obtained by comparing the 2011 and 2007 dataset. Since, the shoreline north of ADM as well as part of the seabed is protected with a riprap (rock armoured), no bathymetric comparison was conducted

in this sector of the bay. It is important to note here that the submerged limit armoured by rocks north of ADM was surveyed during the fall 2011. The elevation accuracy of this bathymetry comparison is evaluated at  $\pm 20$  cm.

Two zones show a larger variation in elevation in Anse du Moulin since 2007. The first area is located along the North shore and shows some significant sign of erosion over the 4 years with difference in ranging between 75 to 100 cm. This is in agreement with results shown in previous sections, showing stronger measured and simulated currents within the surf zone which is the most dynamic sector of the bay including the north-west part. Currents induced by wave under storm events remain the principal cause of that erosion. Results should be taken with caution along the north shore limit where riprap protection and non protected sea-bed meet together.

The western part of the bay shows sign of accumulation with maximum difference in elevation in the order of 50 cm. The sediment accumulation in this sector can be explained by the sediment discharge from the “Ruisseau du Moulin” stream, mainly during the spring flood or during intense summer rainfalls. This stream partially drains the ALCOA industrial site located directly upstream. Long shore currents incoming from East as well cross-shore transport induced by waves incoming from the East sectors remain also 2 plausible explanations that contribute to sediment deposition in this area over 4 years.

Finally, the erosion spot on the nose of wharf # 3 is probably a consequence of the construction works in this area before October 2011. Local scour could be also plausible at the nose of wharf # 3, but the slope observed in this sector remains relatively steep which reduce the chance of having natural scour induced by waves in this sector. Navigation activities could also explain this difference in elevation.

#### 6.2.5 Bathymetry Comparison 2011-2012

Bathymetric data measured during fall 2011 and during spring 2012 were compared to identify potential zones of erosion and accumulation following the significant storm of April 23<sup>rd</sup> 2012. The estimated wave conditions observed at the entrance of ADM under this storm event are the following:

- Maximum Wind Speed: **50km/h**
- Hm0 = **2.04 m**
- Tp = **5.8 s**
- Direction from: **East**

Figure 25-B shows the difference in elevation obtained by comparing the 2012 and 2011 dataset. As mentioned previously, since the shoreline north of ADM as well as part of the seabed is protected with a riprap (rock armoured), no bathymetric comparison was conducted in this sector of the bay. It is important to note here that the submerged limit armoured by rocks north of ADM was surveyed during the fall 2011. The elevation accuracy of this bathymetry comparison is evaluated at  $\pm 20$  cm.

The bathymetric comparison shows on Figure 25-B indicates that non-significant differences in depth is observed in ADM with the exception of one erosion spot observed in the north-west part where the sea bed is mainly made up of sand and differences in elevation range between 40 to 100 cm. These results remain consistent with the high current velocities simulated in this sector (Figure 24) with values ranging between 0.5 to 0.75 m/s. The influence of waves incoming from East during a severe storm that hit the riprap protection in this sector of the bay could also explain the bathymetric changes observed in this shallow area.

In the area North of Wharf # 3, with the exception of this local erosion spot, the sector remains mainly unchanged. No sediment accumulation is observed north of wharf # 3 under the 7 months interval (October 2011 to June 2012) which could be explained by the fact that eroded sediments incoming from this specific spot located north are spread into the water column and result in a non-significant sediment accumulation over a large area of ADM.

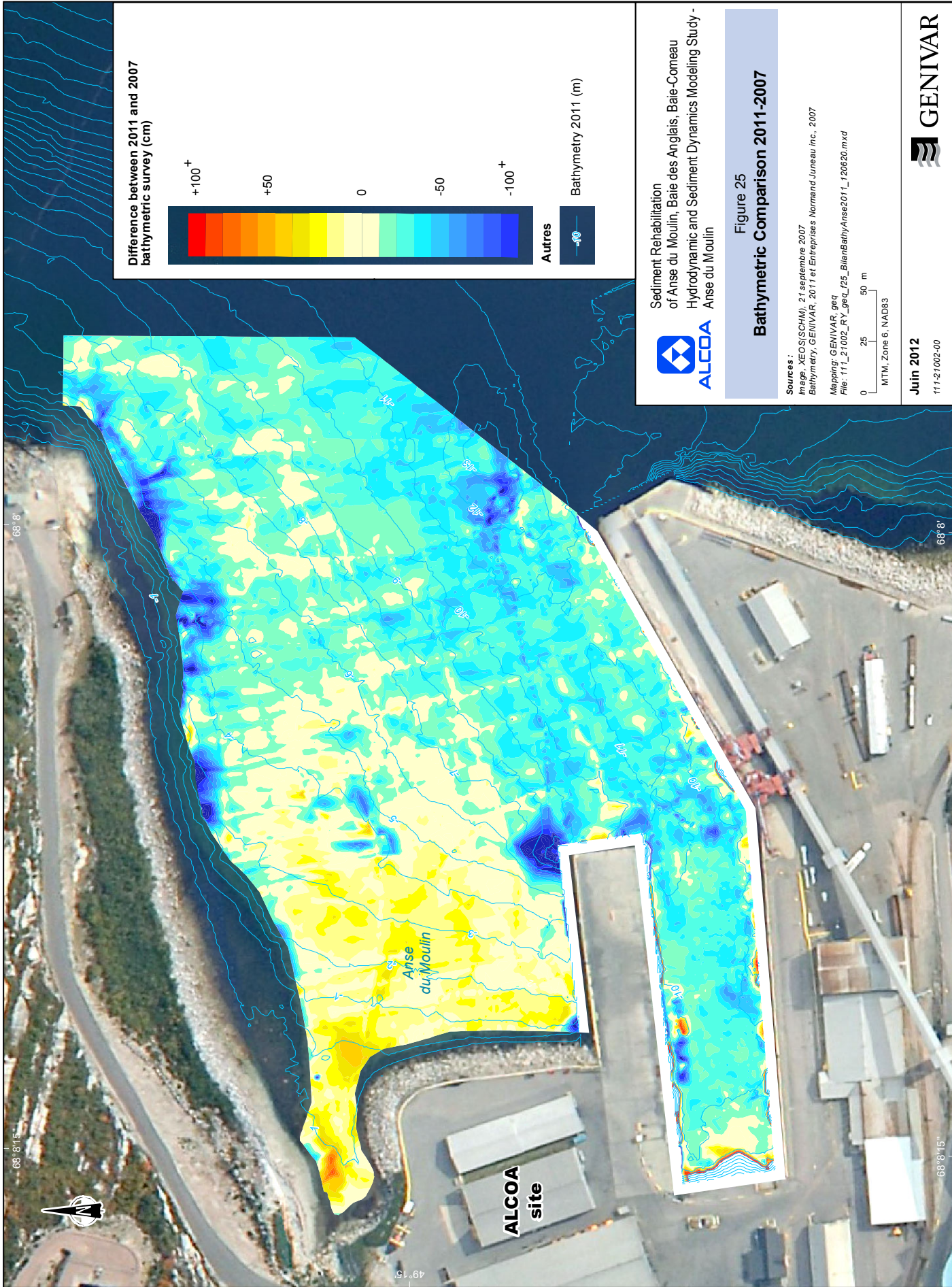
The accumulation sector identified as Zone 1 is explained by material added during the construction works between the 2 bathymetric surveys carried out in October 2011 and June 2012 respectively. Finally, no significant bathymetric changes are observed in ADM for water depths ranging between -2 and -12 m.

#### 6.2.6 General Discussion

The 2012-2011 comparison (Figure 25-B) tends to indicate a potential risk of local erosion in the shallow area located north west of ADM under severe storm conditions (short term) while a longer term period of 4 years seems to generate sediment deposition in the same sector of the bay. The sediment dynamic comparison over a short term period remains highly dependent of the intensity and the number of storms incoming from the East sectors while the analysis of long term sediment budget should take into account the storm events, the effect of constructive waves (seasonal trend) that build the beach as well as all other sources of sediment such as the Ruisseau du Moulin. Strictly based on these 2 comparison maps, it is not possible to fully interpret and predict the short-term and long-term sediment budget in ADM.

Finally, we consider that bathymetric comparisons shown on Figures 25 and 25-B remain a complementary analysis to understand the sediment dynamic in ADM, however because it is highly dependent of the time-scale, the instrument accuracy as well as the density of points used for interpolation, results should be taken with caution. Additional measurements in ADM such as magnitude and direction of currents induced by waves and tides as well as turbidity measurements combined to sediment transport modeling remain one of the option to go deeper with the assessment of the short term (storms) and long term (yearly +) sediment budget in ADM.



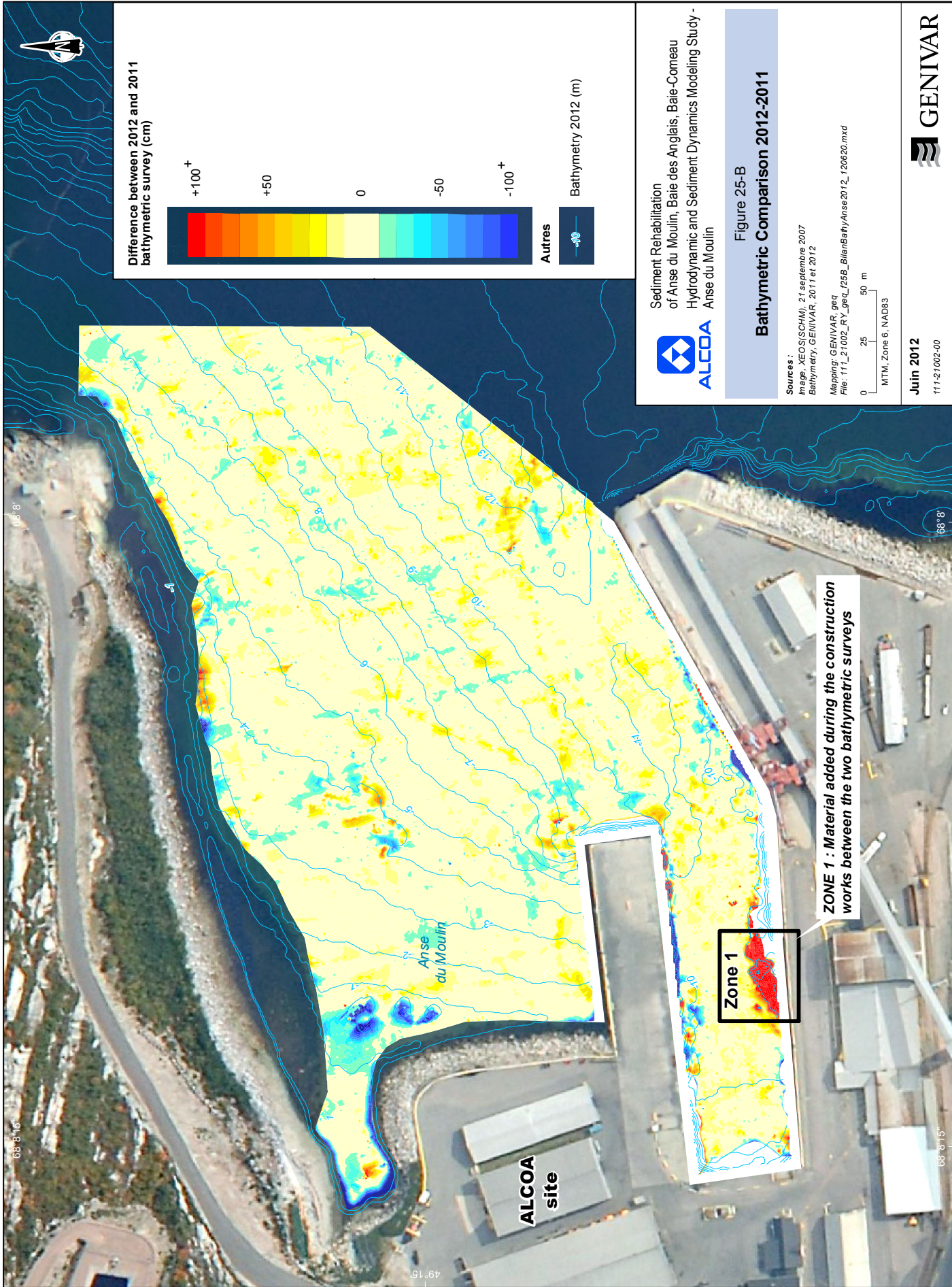


**ALCOA**

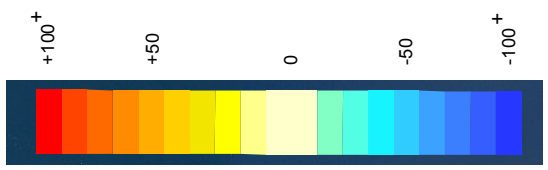
Sediment Rehabilitation  
of Anse du Moulin, Baie des Anglais, Baie-Corneau  
Hydrodynamic and Sediment Dynamics Modeling Study -  
Anse du Moulin

**Figure 25**  
**Bathymetric Comparison 2011-2007**

**Sources :**  
Image: XEOS(SCHM), 21 septembre 2007  
Bathymetry: GENIVAR, 2011 et Entreprises Normand Juneau inc, 2007  
Mapping: GENIVAR, geq  
Fig. 111\_21002\_FY\_ges\_L25\_BlanBathyAnse2011\_120620.mxd



Difference between 2012 and 2011 bathymetric survey (cm)



Autres

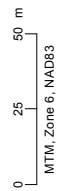
Bathymetry 2012 (m)



Sediment Rehabilitation of Anse du Moulin, Baie des Anglais, Baie-Corneau Hydrodynamic and Sediment Dynamics Modeling Study - Anse du Moulin

Figure 25-B  
Bathymetric Comparison 2012-2011

Sources :  
Image: XEOS(SCHM), 21 septembre 2007  
Bathymetry: GENIVAR, 2011 et 2012  
Mapping: GENIVAR, geq  
File: 111\_21002\_FY\_ges\_L255\_BillenBathyAnse2012\_120620.mxd



Jun 2012  
111-21002-00



Zone 1

ZONE 1 : Material added during the construction works between the two bathymetric surveys

ALCOA site

49°15'

68°3'

68°3'15"

68°3'

68°3'15"

## **7. MODELING OF DREDGING ACTIVITIES WITH DREDGE**

---

The project of contaminated sediments rehabilitation within the Anse-du-Moulin is expected to require different rehabilitation approaches for each area under study. One of these approaches consists in dredging the contaminated sediments in an area near the wharf # 1. The dredged sediment will be transported and disposed in a confined disposal facility (CDF) located between wharves 2 and 3.

The dredging activities could impact the water quality with re-suspension of bottom sediment and the potential of contaminant release and transport outside Anse-du-Moulin. In order, to evaluate the impact of the dredging works, the DREDGE module of Automated Dredging and Disposal Alternatives Modeling System (ADDAMS) is used to calculate the plume concentrations at different distances from the dredge and evaluate the potential sediment transport outside Anse-du-Moulin.

### **7.1 Model Description and Approach**

#### **7.1.1 General Description and Model Limitations**

DREDGE was developed to assist users in making a priori assessment of environmental impacts from proposed dredging operations. DREDGE estimates the mass rate at which bottom sediments become suspended into the water column as the result of hydraulic and mechanical dredging operations and the resulting suspended sediment concentrations.

DREDGE uses empirical and analytical models to estimate the re-suspension and transport of sediments and associated contaminants during dredging operations. DREDGE combines an empirical sediment re-suspension (near-field) approach with a simple suspended sediment transport (far-field) approach to estimate suspended sediment concentrations at specific locations within the water column. DREDGE uses a linear equilibrium partitioning approach to translate water column suspended sediment concentrations to particulate and dissolved contaminant concentrations. All calculations made by DREDGE assume steady-state (non-time varying) conditions.

Observed sediment re-suspension rates and contaminant concentrations during dredging operations show that concentrations are generally less than historically thought. While these raw data provide valuable general information, it is difficult to extrapolate these data to other dredging sites considering different conditions or dredging equipment. DREDGE provides a predictive methodology to estimate re-suspended sediment and contaminant concentrations based on sediment characteristics and dredging conditions.

### 7.1.2 Detailed Model Approach

DREDGE calculates the suspended sediment concentrations within the water column resulting from a static and continuous source of sediment. The geometry and strength of the source depends upon the operating characteristics of the dredge as well as bottom sediment characteristics. DREDGE assumes that dredge movement and temporal variations in re-suspension are small compared to downstream suspended sediment transport.

#### Source Strength

DREDGE uses empirical formulations developed from field studies to estimate the rate of sediment re-suspension that results from a dredging operation (near-field source strength). The model allows the user to estimate this value using Nakai's TGU method or the dredge specific Correlation Models. Additionally, DREDGE allows users to select the source strength values to be entered for any dredge type. Nakai's TGU method can be used for most of the dredge types. Correlation models are available for cutterhead and bucket dredges. The model also calculates the amount of sediment loss resulting from sediment re-suspension during the dredging operation.

The TGU Method is based upon a paper entitled "Turbidity Generated by Dredging Projects" written by Osamu Nakai (1978). The general form of the TGU equation is:

$$m_R = q_s G / (R_o / R_{74})$$

This general equation is applicable to any dredge type for which the variables can be defined. The volume rate of re-suspended sediment ( $q_s$ ) can be defined for most of the dredge types. The turbidity generation unit (G) value depends on dredge operations and bottom sediment characteristics (see Nakai for G values).

Determining the fraction of sediment with a critical re-suspension velocity less than the ambient current velocity,  $R_o$ , requires determining and estimating the sediment particle size with a critical re-suspension velocity assumed as the ambient current velocity. Nakai (1978) suggests that particles around 0.005 mm in size (clay-size) have a critical re-suspension velocity of 0.03 cm/sec and critical re-suspension velocities of silt size particles (0.005 mm to 0.074 mm) range from 0.03 cm/sec to 7 cm/sec. Nakai referred the equations for calculating the critical re-suspension velocities to a report issued by Ingersol and McLaughlin (1960). This report appears to be the main reference, but only contains an equation for the critical re-suspension velocity of sand-sized particles. Since an alternative method for calculating  $R_o$  cannot be found, values for  $R_o$  or  $R_o/R_{74}$  can only be estimated.

## Far-field Transport

Analytic equations regarding the sediment transport approach for plume geometry characteristics of cutterhead and bucket dredges are used to estimate downstream (far-field) transport of suspended sediments under steady-state conditions. Considerable simplifications are needed to solve the fundamental transport equation. Since these simplifications limit the applicability of the model, the analytical solutions allow for rapid calculation of suspended sediment concentrations with accuracy compatible with the source strength models.

### **7.2 Application of DREDGE in ADM**

#### **7.2.1 Assumptions and Model Limits**

The model is applied to the dredging area shown on Figure 26. This area covers the approach and the berthing area of wharf # 1 as well as the area between wharves #2 and 3 outside the CDF footprint (between wharf #2 and3). All on-site condition characteristics are valid for this study area (blue line) since conditions could change abruptly outside the ADM limits (bathymetry, currents, gran-size).

For the current evaluation, only the mechanical dredging was considered. To account for spatial variability, two (2) water depths (10 and 13m) and two (2) median grain size diameters (150 and 400 $\mu\text{m}$ ) were used as input to the model and defined as scenarios ALCOA 1 to ALCOA 4. Table 13 shows these values for each scenario under study.

Table 13 Water Depth and Median Grain Size for each scenario under study.

<b>Scenarios</b>	<b>Water depth (m)</b>	<b>D<sub>50</sub> (<math>\mu\text{m}</math>)</b>
ALCOA 1	10	150
ALCOA 2	10	400
ALCOA 3	13	400
ALCOA 4	13	150

To quantify the sediment re-suspension in the near field area, TGU method was used. This method is mostly conceptual and relies on a value called the “turbidity generation unit” (TGU) to distinguish between the re-suspension rates of various dredge types. Nakai’s method converts TGU values to a source generation rate. TGU value selected for the model was 17,6 kg/m<sup>3</sup> which was the most representative case of our conditions (bucket of 3m<sup>3</sup> dredging in sand with 10,2% finer than 74 $\mu\text{m}$  and 1,5% finer than 5 $\mu\text{m}$ ).

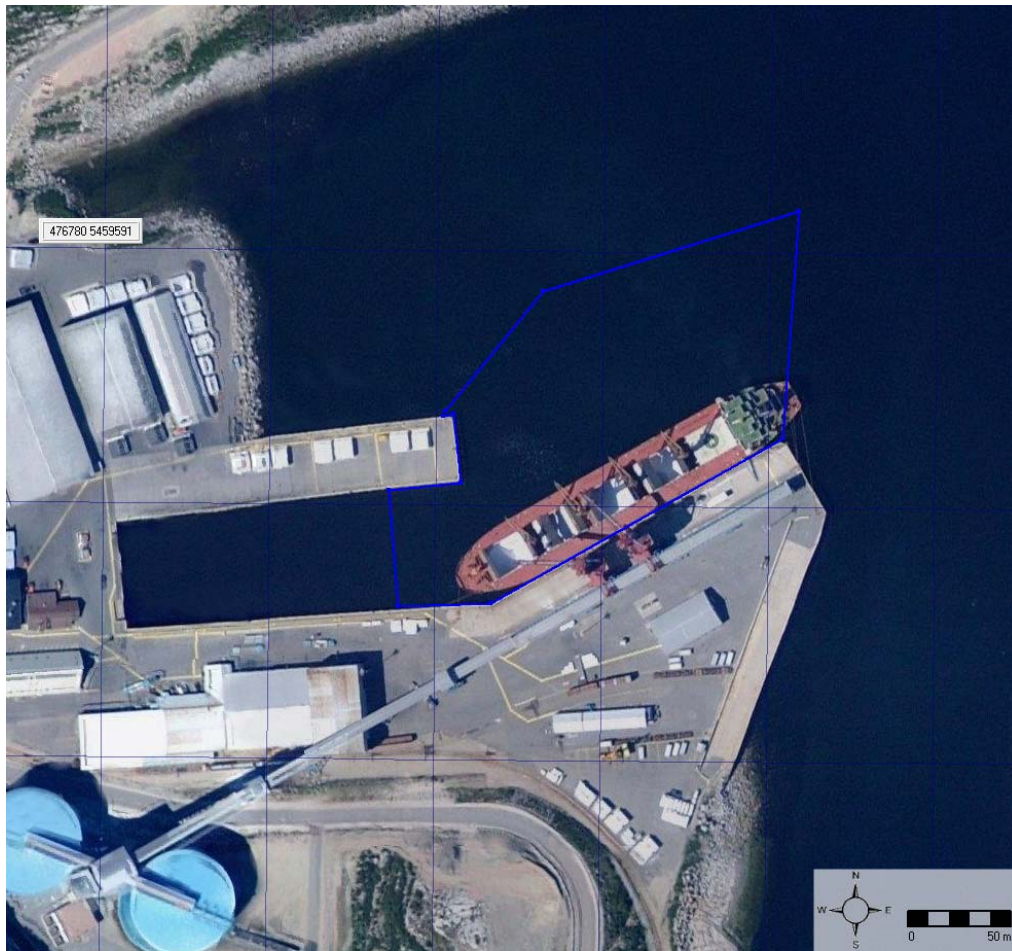


Figure 26 Dredging Area Considered for the Modeling.

The current velocity used is the depth-averaged current velocity measured during the 2011 surveys which has been rounded off to 5cm/s. Larger velocities are generally associated with strong wind and waves from the East (see section 6.2) but these conditions will likely lead to an interruption of the dredging activities.

Table 14 shows the input data used to run the DREDGE model.

Table 14 Input Data used for the DREDGE model

<b>Case</b>		ALCOA_1	ALCOA_2	ALCOA_3	ALCOA_4
(D50, water depth)		150µm,10m	400µm,10m	150µm,13m	400µm,13m
<b>Dredging characteristics</b>					
	Unit				
Dredge Type		Open clamshell	Open clamshell	Open clamshell	Open clamshell
Bucket size	v <sup>3</sup> (m <sup>3</sup> )	5.5 (4,21)	5.5 (4,21)	5.5 (4,21)	5.5 (4,21)
Cycle time	sec	60	60	60	60
Settling velocity of dredged material	m/s	0.012	0.087	0.087	0.012
<b>Site characteristics</b>					
Water depth	m/s	10	10	13	13
Ambient water velocity	m/s	0.05	0.05	0.05	0.05
Mean particle size	µm	150	400	400	150
Specific Gravity		2.5	2.5	2.5	2.5
In-situ dry density	kg/m <sup>3</sup>	700	700	700	700
Fraction of particles < 74 mm	%	1.5%	1.5%	1.5%	1.5%
Fraction of particles < particles with critical settling velocity	%	40	40	40	40
Latéral diffusion coefficient	cm <sup>2</sup> /s	2000	2000	2000	2000
Vertical diffusion coefficient	cm <sup>2</sup> /s	14	14	14	14
<b>Near-field model characteristics</b>					
TGU method (for sand) =	kg/m <sup>3</sup>	17.6	17.6	17.6	17.6
Correlation method =	m/s	0.05	0.05	0.05	0.05

### 7.3 Results

The Result values show in this section are expressed as increase in total suspended matter (TSS) (in mg/L) downstream from the point source (dredge) in the main current axis (East). The Downstream distance is expressed in meters from the point source (dredge) and lateral distance is expressed in meters from the main current axis. The criteria used by the federal and provincial departments propose an increase limit of 25mg/L over a background concentration of less than 250mg/L and an increase of less than 10% over of background concentration greater than 250mg/L. These criteria were used for the current study.

Table 15 gives the main result associated with each scenario. It shows the estimated source strength in terms of kg/s and percentage of loss. It gives also the total increase of suspended matter (TSS) at various distances downstream from the dredge in the main axis of current assuming steady-state (non-time varying) conditions. In this particular case, the main axis of current within the dredging area is assumed as the East direction. The detailed results are gathered in Appendix 5. The results respectively presented in Appendix 5 are the following:

- Downstream concentration versus distance from dredge- line graph (**ALCOA 1 to ALCOA 4**)
- Downstream concentration versus distance from dredge-plan view (**ALCOA 1 to ALCOA 4**)
- Numerical results (**ALCOA 1 to ALCOA 4**).

The results show that the increase of total suspended matter (TSS) is always lower than 10 mg/l at 25m downstream from the dredging activity considering a  $D_{50}$  of 150mm and also lower than 10 mg/l at 10m downstream from the dredge for a  $D_{50}$ = 400mm. This relatively short and low concentration plume of re-suspended sediment is explained by the relatively high particle diameters (grain size) which settle quite rapidly as well as a slow current velocity which reduces the advection.

In the worst case ( $D_{50}$ = 150mm and a water depth of 10m), the TSS increase remains lower than 1mg/l at 80m downstream from the dredge. The detailed results are showed in Table 15.



Table 15 Dredge Results obtained for each scenario under study.

<b>Results</b>					
Case		ALCOA_1	ALCOA_2	ALCOA_3	ALCOA_4
(D50, depth)		150µm,10m	400µm,10m	150µm,13m	400µm,13m
Estimated source strength	kg/s	0.41	0.41	0.41	0.41
Estimated source strength	% loss	0.84	0.84	0.84	0.84
Downstream distance from dredge (m)	Far field increase in TSS in mg/l				
5		44.010	16.400	16.400	35.140
10		26.480	3.700	4.800	21.940
15		18.390	0.950	1.600	15.820
20		13.550	0.260	0.580	12.100
25		10.310	0.070	0.210	9.560
30		8.010	0.020	0.080	7.700
35		6.310	0.010	0.031	6.300
40		5.020	0.002	0.012	5.200
45		4.030	0.001	0.005	4.330
50		3.250		0.002	3.630
55		2.630		0.001	3.060
60		2.150			2.580
65		1.750			2.190
70		1.440			1.868
75		1.180			1.590
80		0.970			1.360
85		0.810			1.168
90		0.670			1.002
95		0.550			0.862
100		0.460			0.742
105		0.380			0.639
110		0.310			0.552
115		0.260			0.476
120		0.220			0.412
125		0.180			0.356
130		0.150			0.309
135		0.120			0.268
140		0.100			0.232
145		0.089			0.201
150		0.074			0.175
155		0.062			0.152
160		0.052			0.132
165		0.044			0.115
170		0.037			0.100
175		0.031			0.087
180		0.026			0.076
185		0.022			0.066
190		0.018			0.058
195		0.015			0.050
200		0.013			0.044



## 8. DISCUSSIONS AND RECOMMENDATIONS

---

### 8.1 Hydrodynamic and Sediment Stability

The sediment stability assessment (Figures 14 to 16) reveals that ratios  $\left(\frac{\tau_{max}}{\tau_{critical}}\right)$  greater than one are observed within a significant area under storm conditions given by the 1 hour per year wave height (1.8m). Under a 24 hours per year wave height (1.2 m), almost half of ADM remains stable, mainly in the southern part where water depth range between 8 and 12 m. For each scenario simulated, the area located in the western part of ADM, North of wharf # 3, remains largely unstable because of the wave breaking observed in this shallow part of the bay. As mention previously, ratios above one (1) would lead to instability in theory, but in practice, ratio slightly or more significantly higher than one (1) may be considered stable. Turbidity measurements in specific area of Anse du Moulin could be used to confirm the upper limit bed shear stress ratio value at which significant sediment movement would be observed under wave conditions. Finally, more information related to the effect of boat and ship propeller jets could be taken to assess the impact on sediment stability in the vicinity of wharf # 1, 2 and 3.

The comparison analysis of measured (ADCPs) and simulated currents indicates that an anti-clockwise gyre is observed in ADM under significant wave heights (> 0.9 m) from the East. Wave induced currents from East to West with maximum magnitudes (depth-average) ranging from 30 to 50 cm/s (Figure 19) were simulated along the North shore and west part of the bay on October 4<sup>th</sup> 2011. The comparison of the simulated currents with the measurements collected the same day by an ADCP (Figure 18) reveals maximum velocities in the order of 30 cm/s (depth average) under a wave height (Hm0) of 0.9 m from the East. The slight difference between measured and simulated currents on October 4<sup>th</sup> 2011 is likely explain by the limitation of the boat to access and measure at the proximity of the shoreline in the shallow and more turbulent area of ADM where alongshore current velocities are higher. Under moderate storm conditions such as the event of April 23<sup>rd</sup> 2012 (Hm0 = 2.04 m, Tp = 5.8s), the simulated wave induced-currents indicate velocities in the order of 50 to 110 cm/s in the north and west part of ADM as shown on Figure 24. Under no-wave conditions in ADM such as October 5<sup>th</sup> and 6<sup>th</sup>, current velocities induced by tides are most of the time smaller than 10 cm/s as indicated on Figure 20. These measurements confirm that maximum current velocities are mainly driven by waves in ADM. Based on results shown on Figure 23 for Hydro 1, the ADCP mooring during the Fall 2011 reveals that average currents in the order of 5 to 10 cm/s were measured at 1.8 m from the sea bottom and maximum velocities in the order of 20 to 30 cm/s at proximity of the surface. In fact, the ADCP-Hydro 1

location as shown of Figure 24 remains outside the area where higher current velocities were simulated and likely explains why lower current velocities were measured by Hydro-1 during the Fall 2011 compared to the simulated values, especially during wave events.

The sediment stability results shown on Figures 14 to 16 combined to maximum wave-induced currents ranging from 30 to 100 cm/s under wave conditions from East can lead to a potential risk of sediment drifting outside of ADM. In fact, contaminated areas within the breaking zone where transport may be more significant should be considered as a potential risk because sediments can be mobilized in deeper zone by wave orbital currents, creating sediment pulses in the water column. Combined to wave-induced currents generating an anti-clockwise circulation in ADM, contaminated sediment could be transport along a certain distance before being deposited on the bottom. Results from the Risk Assessment Study should be analyzed and combined to the sediment stability and current velocity analysis to indentify zones and limits where potential risk of re-suspension of contaminated sediments remain higher. The depth within the sediment layer at which contaminated sediments are found remains an important parameter to identify zones at potential risk of having re-suspension of contaminated sediments.

In fact, to validate if the wave-induced currents are sufficient (magnitude and duration) to transport suspended sediments outside ADM, additional current velocities and directions could be measured under significant wave conditions by installing one or two ADCP just North of wharf # 1 and 3, within the coastal jet toward the West observed in this sector of the bay. Turbidity measurements could also be collected in this sector as well as underwater pictures and videos to visualize and confirm the presence of sediment in suspension as well as potential transport under wave conditions in ADM. Finally, further analysis could also be performed based on sediment transport modeling to allow a broader range of wave conditions (duration and intensity) to be simulated in unsteady state using a circulation model that include wave, wind and tide parameters. The results of these modeling simulations could be used to interpret with more confidence the short and long term sediment dynamic and budget within ADM and confirm with more confidence the risk of having sediment drifting outside of ADM.

Finally, we consider that bathymetric comparisons shown on Figures 25 and 25-B remain a complementary analysis to understand the sediment dynamic in ADM, however because it is highly dependent of the time-scale, the instrument accuracy as well as the density of points used for interpolation, results should be taken with caution. As discussed, additional measurements in ADM such as magnitude and direction of currents induced by waves and tides as well as turbidity measurements combined to sediment transport modeling remain the best alternative to better understand and quantify the short term (storms) and long term (yearly +) sediment budget in ADM.

## 8.2 Dredging Operations

Based on the results of DREDGE model simulations, the dredging impacts on water quality with an increase higher than 1mg/l is estimated to be concentrated in a small plume limited to 80 m around the dredging activities considering the worst case ( $D_{50}$ = 150mm and water depth of 10m). The most concentrated plume with an increase of TSS over 10mg/l is restricted to an envelope of 25m around the dredge.

There are a number of limitations associated to the model DREDGE. The sediment re-suspension approach is only applicable to dredging operations similar to those used in the development of the empirical equations. As example, the far-field transport equations assume a dominant and uni-directional current with a sufficient period of time to assume that suspended sediment concentrations would reach a steady-state. In the case of ADM, this assumption is a rough simplification as the current may vary significantly under tide and wave conditions. The model also assumes a steady source from a specific location (identified in the models as 0,0,0).

In terms of accuracy, the model used for near-field processes remains empirical. However, some input data were taken directly from field measurements which increase the confidence in model results. The model generally produce reasonable estimates for normal operating characteristics, but unusual operating parameters may yield to unreasonable results.

Finally, as the wave climate could induced an acceleration of current velocity and therefore a potential increase in the dredging plume towards the Baie-des-Anglais, we recommend to stop the dredging activities and operations when forecast indicate wind speed over 25-30 km/h incoming from the direction range define between North-East (NNE) to South-South-East (SSE). In these conditions, we assumed that currents velocities can reach 30 cm/s or more. Wind speeds of more than 25-30 km/h incoming from the West will not generated waves and high turbulence in ADM but should also take into consideration during the dredging activities since currents induced by winds are generated toward the Baie-des-Anglais under these conditions, especially in the first 3m water depth from the surface.



## 9. REFERENCES

---

- BASCO D.R. 2012. *Lecture Notes: Coastal Hydrodynamics and Sediment Transport Processes (CEE 788)*, Old Dominion University, Virginia.
- CANADIAN HYDROGRAPHIC SERVICE (CHS). 2011. <http://www.waterlevels.gc.ca/eng>. Environment Canada.
- CANADIAN ICE SERVICE (CIS). 2005. *MANICE*, Manual of Standard Procedures for Observing and Reporting Ice Conditions, Revised ninth edition, June 2005.
- CANADIAN ICE SERVICE (CIS). 2011. <http://www.ec.gc.ca/glaces-ice/default.asp?lang=En&n=D32C361E-1> . Environment Canada.
- CIRIA (2010). *Beach management manual (second edition)*, C685, CIRIA, London.
- CIRIA, CUR, CETMEF (2007). *The Rock Manual*. The use of rock in hydraulic engineering. (2<sup>nd</sup> edition). C683, CIRIA, London.
- DEAN R.G. and DALRYMPLE R.A. 2002. *Coastal Processes with Engineering Applications*. Cambridge University Press.
- GENIVAR. 2006. *Réfection en urgence de la digue de retenue en enrochement du Parc des Pionniers à Baie-Comeau*, Évaluation Environnementale Sommaire, présentée au MDDEP pou le compte d'Abitibi-Consolidated (division Baie-Comeau).
- HAYES D.F. AND JE C.-H. 2000. *DREDGE module user's guide*. Draft report. Dept of Civil and Environmental Engineering, 27 p.
- INGERSOLL, A. C. AND MC LAUGHLIN R. T. 1960. *The resuspension of flocculents solids in sedimentation basins*. Technical Report. Sedimentation Laboratory. California Institute of Technology, May.
- KAMPHUIS J.W. 2010. *Introduction to Coastal Engineering and Management*, World Scientific – Advanced Series on Ocean Engineering, 2<sup>nd</sup> Edition.
- KUOA., C. WELCH, AND R. LUKENS. 1985. *Dredge Induced Turbidity Plume Model*, ASCE Journal of Waterway, Port, Coastal, and Ocean Engineering, Vol. 111, No. 3.
- MASSELINK G and HUGHES M. G. 2003. *Introduction to Coastal Processes & Geomorphology*, Hodder Education, Hachette UK Company, Great Britain. 354 p.
- NAKAI, O. 1978. *Turbidity Generated by Dredging Projects*, Proceedings of the 3<sup>rd</sup> U.S./Japan Experts Meeting, US Army Engineer Water Resources Support Center, Ft. Belvoir, VA.

- SMITH J.M., SHERLOCK A.R., RESIO D.T. 2001. *STWAVE: Steady-state spectral wave model user's manual for STWAVE*, Version 3.0. ERDC/CHL SR-01-1. Vicksburg, MS: U.S. Army Engineer Research and Development Center.
- SOULSBY R.L. and CLARKE S. 2005. *Bed Shear-Stresses Under Combined Waves and Currents on Smooth and Rough Beds*, HR Wallingford, Report TR 137.
- U.S. ARMY CORPS OF ENGINEERS (USACE). 2006. Two-dimensional Depth-Averaged Circulation Model CMS-M2D: Version 3.0, Report 2, Sediment Transport and Morphology Change. 212 p.



## **APPENDIX 1 – HISTORICAL HIGH WIND SPEEDS RECORDED AT THE BAIE-COMEAU STATION DURING WINTER**

---

This Appendix provides the information related to the ice concentration and distribution in the Baie-Comeau area associated with the 3 specific events described below:

- February 2<sup>nd</sup> 1976, wind speed of 103 km/h
- January 26<sup>th</sup> 1978, wind speed of 81 km/h
- January 23<sup>th</sup> 1987, wind speed of 84 km/h

The historical ice charts issued by the Canadian Ice Service (CIS, 2011) for the St-Lawrence River and Gulf are available from the Environment Canada web site:

<http://www.ec.gc.ca/glaces-ice/default.asp?lang=Fr&n=D32C361E-1>

Information received from Mr. André Cyr from Environment Canada as well as additional data collected from the *Manual of Standard Procedures for Observing and Reporting Ice Conditions* issued by the CIS (2005) were used to characterize the ice cover in the Baie-Comeau area.

The following section is an information summary used to interpret the ice charts issued between 1967 and 1981. This ratio code described below was used to characterize the 1976 and 1978 events.

## Interpreting Canadian Ice Charts (1967-1981) Ratio Code

A unique ice observing and reporting system has been developed in Canada which conveys information concerning ice amount and age (thickness) simultaneously in digital form. The basis of the system is that the amount of ice in each of 6 age categories is reported in an invariable order:

- Multi Year Ice
  - Second Year Ice
    - First Year Ice
      - Grey-White Ice
      - Grey Ice
      - Nilas and New Ice.

The older (thicker) forms are omitted if they are not present but the amount of the thinner types or a zero if there is none is always required. This means that nilas and new ice are always in the units column of the digital report, grey ice in the tens column, first year ice in the thousands column, etc.

Examples:

42	Indicates 4 tenths grey ice and 2 tenths of nilas or new ice.
402	Indicates 4 tenths of grey-white ice and the same 2 tenths of nilas or new ice. There is no grey ice.
4200	Indicates 4 tenths of first year ice with 2 tenths of greywhite ice. There is no grey, nilas or new ice

This simple system is used in southern waters during the winter but in the Arctic, when the older forms of ice are present the number of digits can become unwieldy, particularly when only zeros to denote the absence of an ice type are used. For this reason a second reference mark is introduced - a decimal point - always between second and first year ice. It is considered as part of the second year ice report.

Thus 3.4000 would indicate 3 tenths of second year ice with 4 tenths of first year ice; there is no grey-white, grey, nilas or new ice. With the decimal reference point, there is no need to report the zeros for their function is merely to put the 4 into the proper column. The report 3.40 conveys the same information, the single zero being added by convention as a reminder.

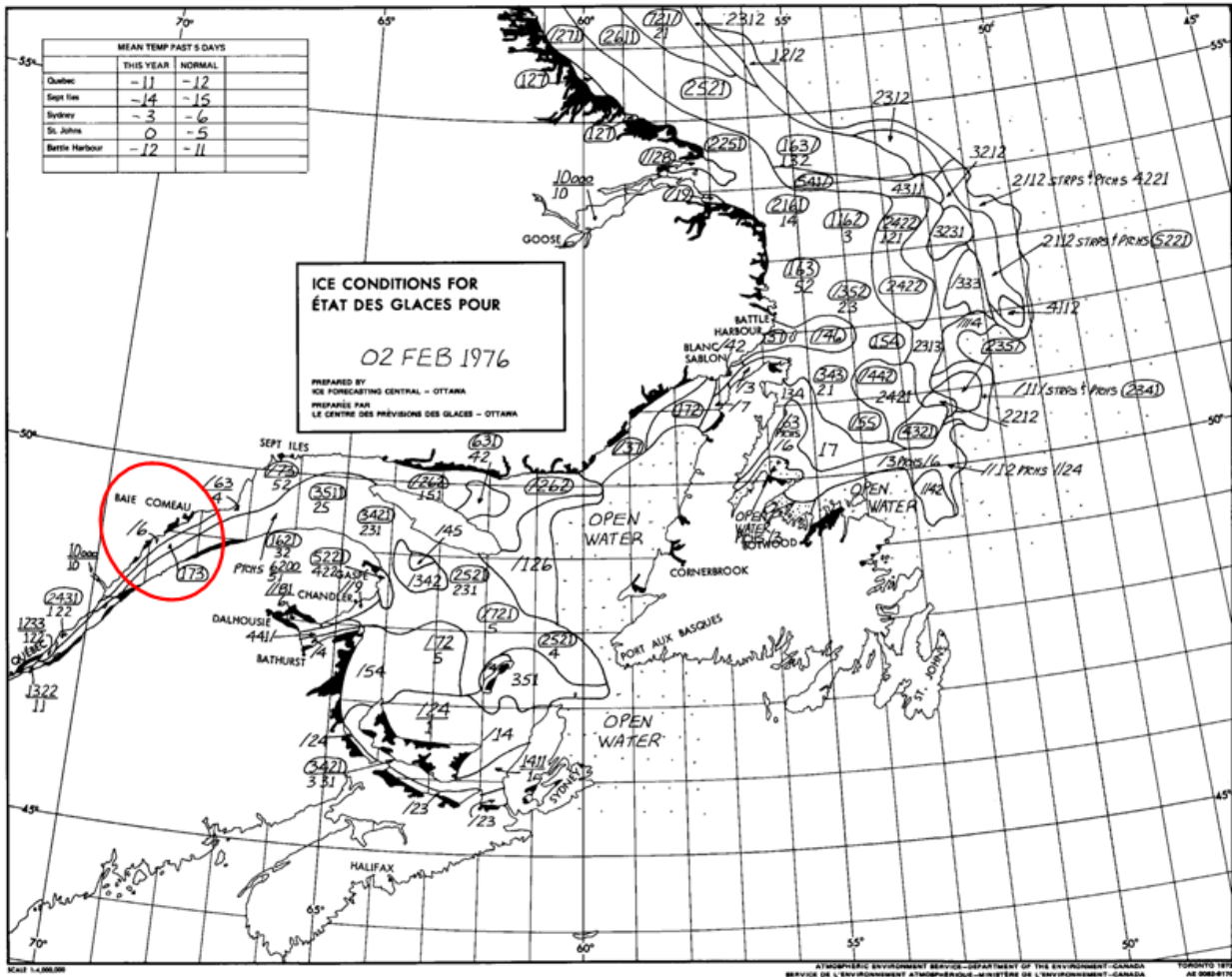
## Event 1 - February 2<sup>nd</sup> 1976 - Wind speed of 103 km/h

Ratio codes related to the Baie-Comeau area are:

**16:** 1 tenth of grey ice and 6 tenths of nilas or new ice.

**073:** 0 tenths of grey-white ice, 7 tenths of grey ice and 3 tenths of nilas or new ice.

**Conclusion:** Based on ice concentration and distribution observed in the Baie-Comeau area during February 2<sup>nd</sup> 1976, the wind speed of 103 km/h must be removed from the wind dataset.

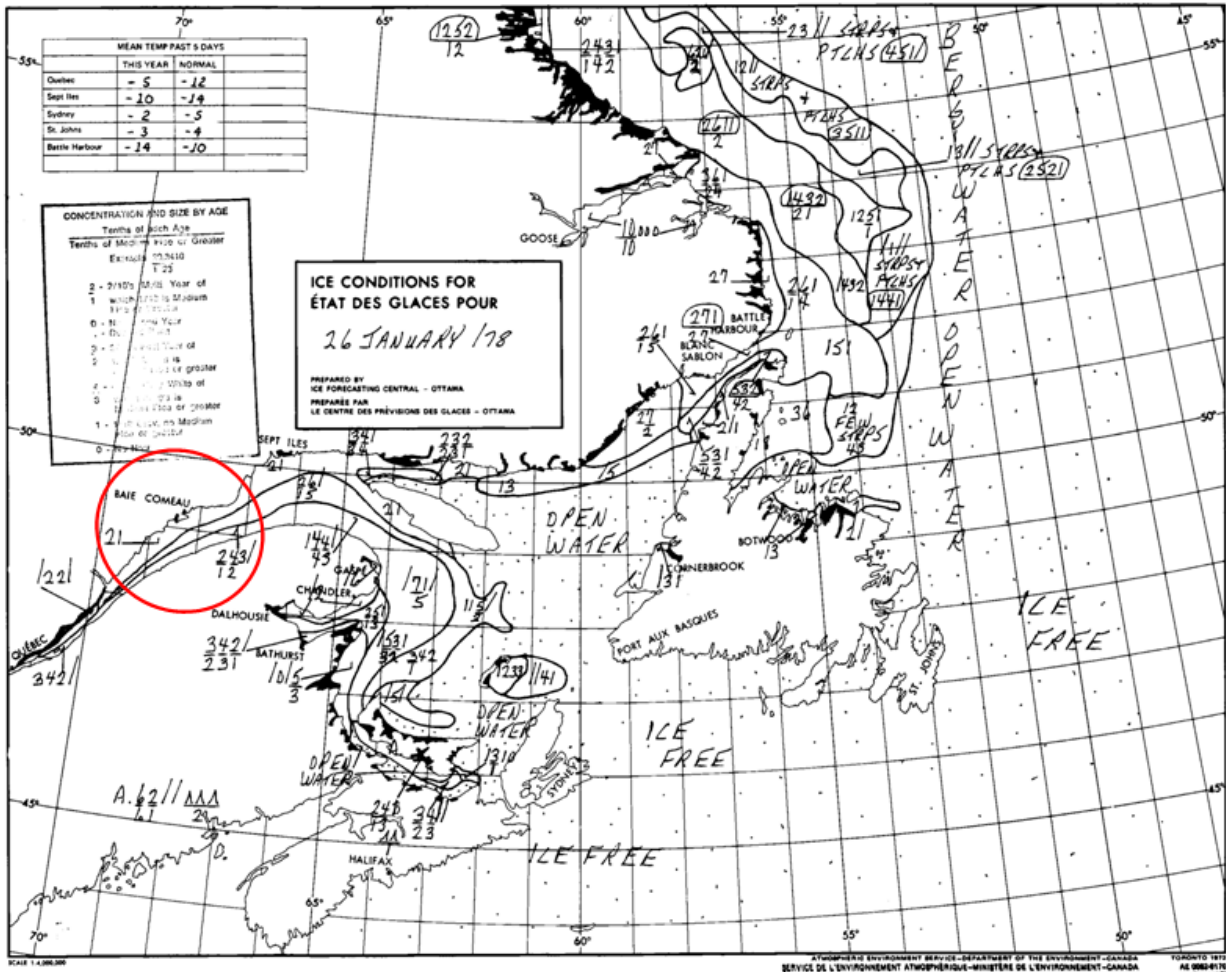


**Event 2 - January 26<sup>th</sup> 1978 - Wind speed of 81 km/h**

Ratio codes related to the Baie-Comeau area are:

- 21:** 2 tenths of grey ice and 1 tenths of nilas or new ice.
- 243/12:** 2 tenths of grey-white ice which 1 tenth is in floes medium size or greater, 4 tenths of grey ice which 2 tenths of medium floe or larger and 3 tenths of nilas or new ice with all small floe or less in size.

**Conclusion:** Based on ice concentration and distribution observed in the Baie-Comeau area during January 26<sup>th</sup> 1978, the wind speed of 81 km/h must be removed from the wind dataset.



**Event 3 - January 23<sup>th</sup> 1987 – Wind speed of 84km/h**

The following is a summary diagram of the Egg Code which is used to interpret ice charts issued after 1981. This code conforms to international convention and shall be used in coding all visual sea ice and lake ice observations without exception. Three examples of charts interpretation using the egg code are given below.

For this specific event, ice charts of January 21<sup>st</sup> and January 25<sup>th</sup> 1987 were analyzed.

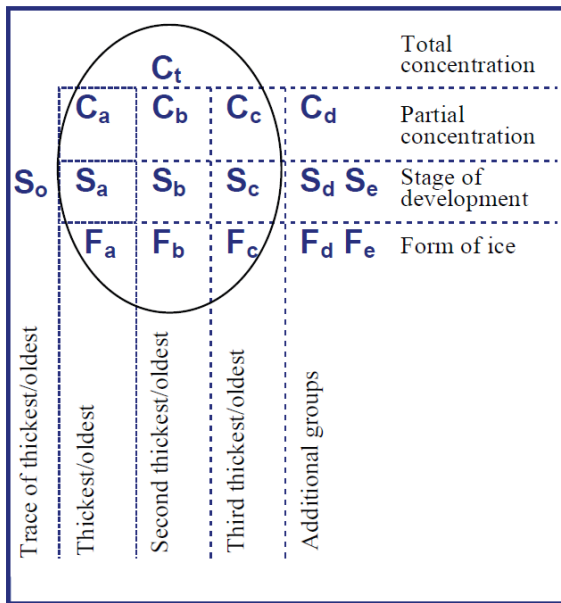
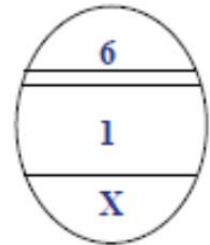


Figure 3.1: The Egg Code

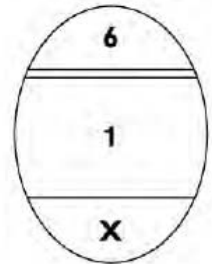
**Example 1**

6/10 of new ice with no form. Note that there is no partial concentration when only one ice type is represented in the egg.



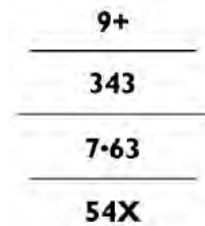
**Example 4**

6/10 of new ice with no floe form.



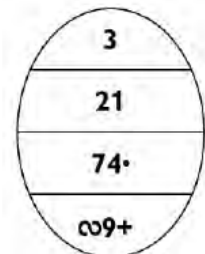
**Example 8**

9+/10 total ice concentration. 3/10 old ice in big floes, 4/10 first-year ice in medium floes and 3/10 young ice with floes undetermined. Horizontal lines with no egg shell indicates that data has been interpreted from radar.



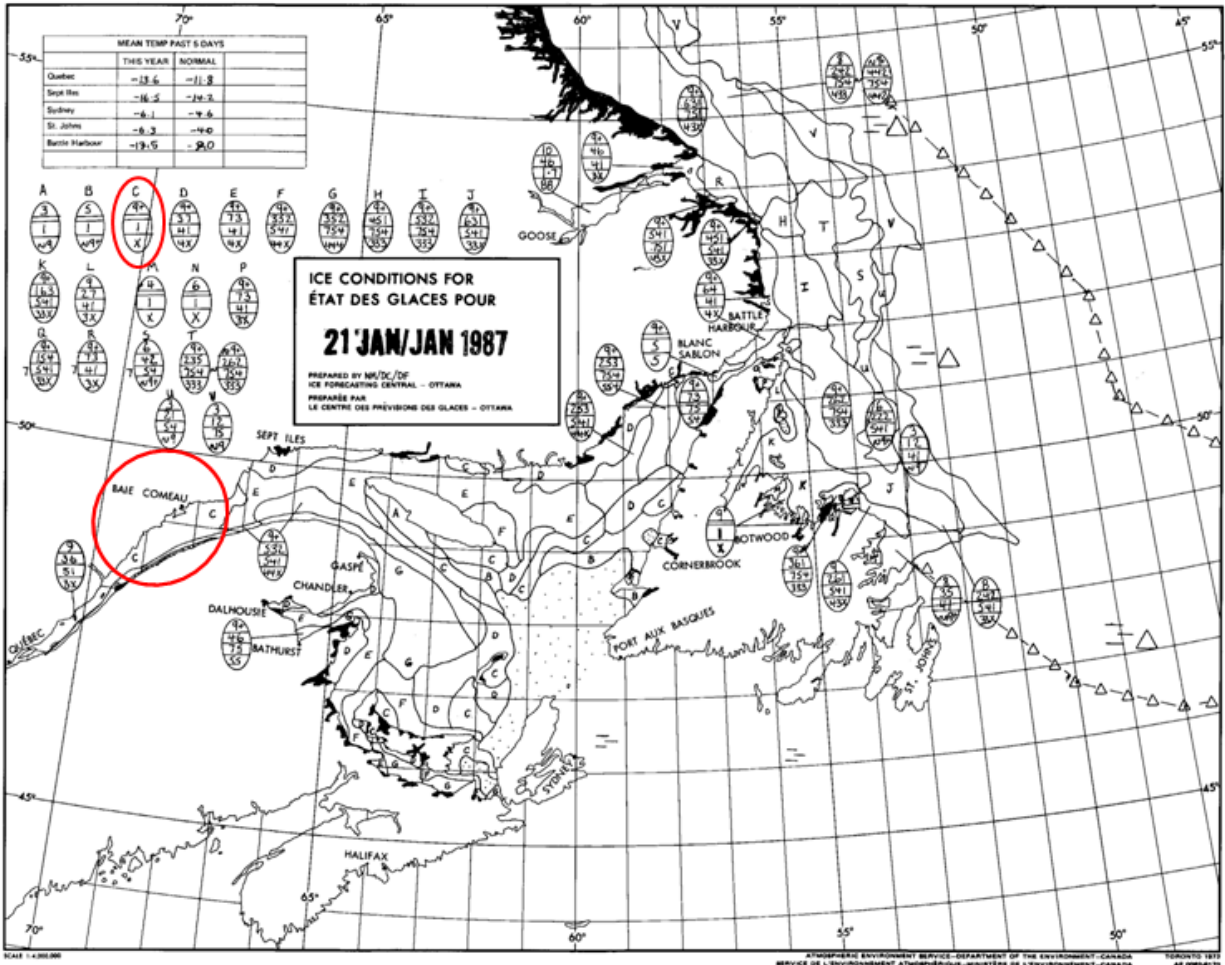
**Example 11**

3/10 total ice concentration. 2/10 old ice and 1/10 thick first-year ice. All ice is concentrated in strips and patches of 9+/10.



# January 21<sup>st</sup> 1987

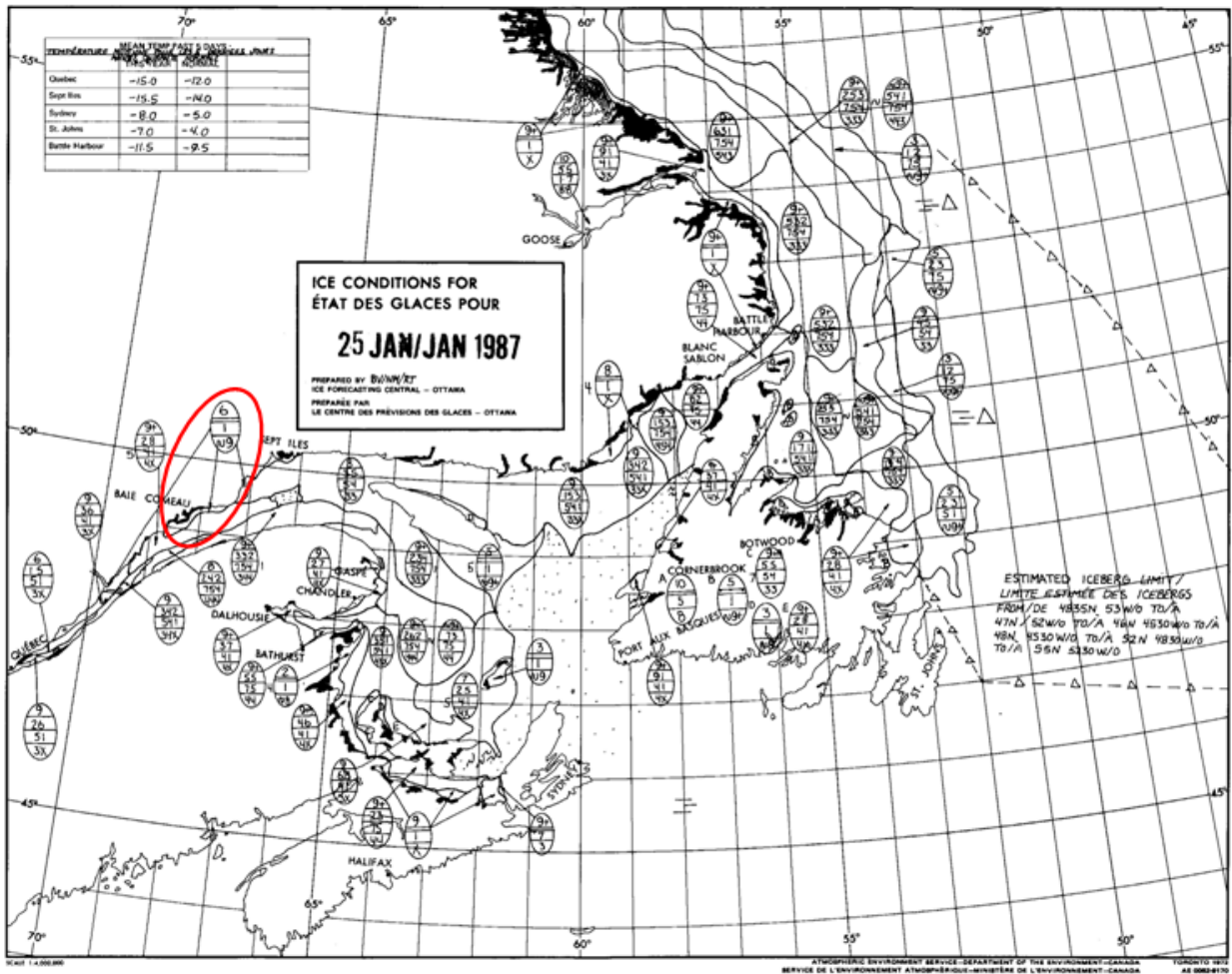
- 9+: 9+/10 of total ice concentration
- 1: no floe form
- X: no information



## January 25<sup>th</sup> 1987

- 6: 6/10 of total ice concentration
- 1: no floe form
- ∞9: All ice is concentrated in strips and patches of 9/10

**Conclusions:** Based on ice concentration and distribution observed in the Baie-Comeau area during January 21<sup>st</sup> and 25<sup>th</sup> 1987, the wind speed of 84 km/h must be removed from the wind dataset.



## **REFERENCES**

CANADIAN ICE SERVICE (CIS). 2005. *MANICE*, Manual of Standard Procedures for Observing and Reporting Ice Conditions, Revised ninth edition, June 2005.

CANADIAN ICE SERVICE (CIS). 2011. <http://www.ec.gc.ca/glaces-ice/default.asp?lang=En&n=D32C361E-1>. Environment Canada.



## APPENDIX 2 – VALIDATION OF THE WIND-WAVE MODEL

### 2011 Wave Measurements

Figure A-1 shows the wave heights measured by both Acoustic Doppler Current Profiler (ADCP, Hydro1 and Hydro 2) deployed in the Anse du Moulin (ADM) from October 7<sup>th</sup> to November 21<sup>st</sup> 2011. Both data sets provide a very similar wave pattern in terms of magnitude and phase which confirms the consistency of the data collected. Based on these results, HYDRO-1 was retained as the measurement reference station for the present analysis.

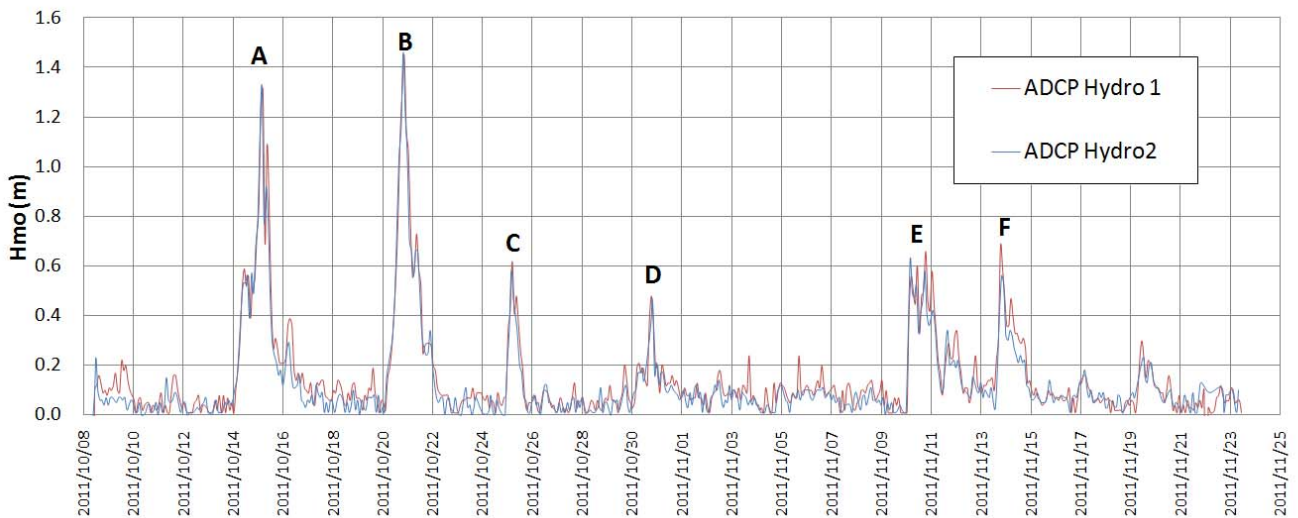


Figure A-1 Wave Height ( $H_{m0}$ ) Measured by ADCP's from October 7<sup>th</sup> to November 21<sup>st</sup> 2011 and significant wave events.

Over this specific measurement period, 6 main events were identified based on the following criteria:

- $H_{m0}$  threshold > 0.3 m
- Duration above  $H_{m0}$  threshold > 3 hours

Table A-1 shows the wave characteristics of these specific events, identified by a letter for ease of identification (Figure 1).

Table A-1 Wave Event Characteristics Measured from October 7<sup>th</sup> to November 21<sup>st</sup> 2011.

Wave Event Characteristics - ADCP - Hydro 1					
ID	Starting Date	End Date	Maximum Wave Height (m)	Direction From	Hours > 0.3 m
A	14/10/2011 6:20	15/10/2011 16:20	1.31	ESE	34
B	20/10/2011 10:20	21/10/2011 12:20	1.45	ESE	27
C	25/10/2011 0:20	25/10/2011 10:20	0.62	ESE	11
D	30/10/2011 16:20	30/10/2011 20:20	0.48	ESE	4
E	10/11/2011 2:20	11/11/2011 4:20	0.66	ESE	26
F	13/11/2011 16:20	14/11/2011 12:20	0.68	ESE	24
<b>Total</b>					<b>126</b>

#### Comparison between Measured and Simulated Wave Characteristics

As described in section 3 of the main report, the GENIVAR parametric wind-wave hindcast model was used to generate the offshore (deep water) wave climate. The focal point for which the offshore wave climate was generated is shown on Map 2. (see main report, section 3.2). The resulting wave climate was then imported in the STWAVE model to transform from the deep water location to the entrance of Anse du Moulin. By coupling these 2 wave models, the near shore wave climate was predicted using both Baie-Comeau and Mont-Joli wind data sets. No amplification factor was applied on wind speeds for both stations. Figure A-2 shows the location of the Baie-Comeau and Mont-Joli meteorological stations.

The resulting wave characteristics for the “simulated waves” were extracted at the ADCP location known as Hydro 1 (see Map 3, section 5.1) and then compared to the corresponding 2011 wave measurements.

Figures A-3 and A-4 illustrate the comparison between measured and simulated waves using both Baie-Comeau and Mont-Joli wind stations. Table A-2 and A-3 shows the comparison wave characteristics.

Figure A-3 - Measured vs Simulated Wave Heights - Baie-Comeau Wind Station

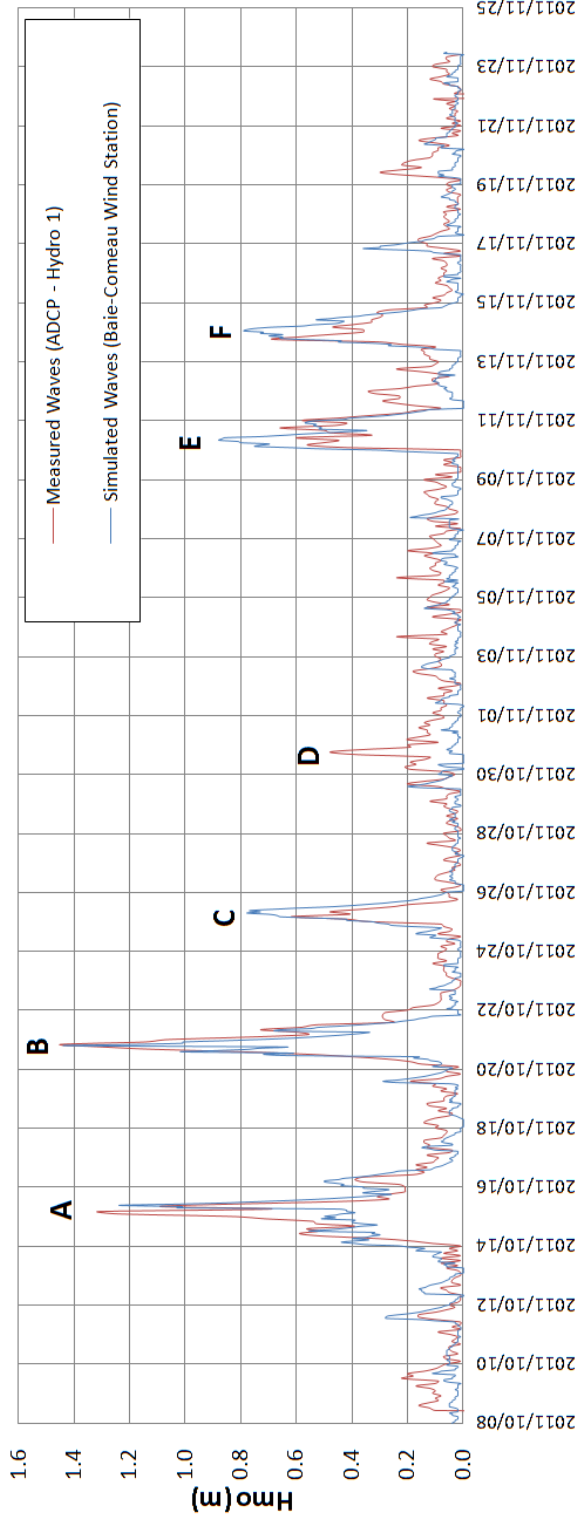
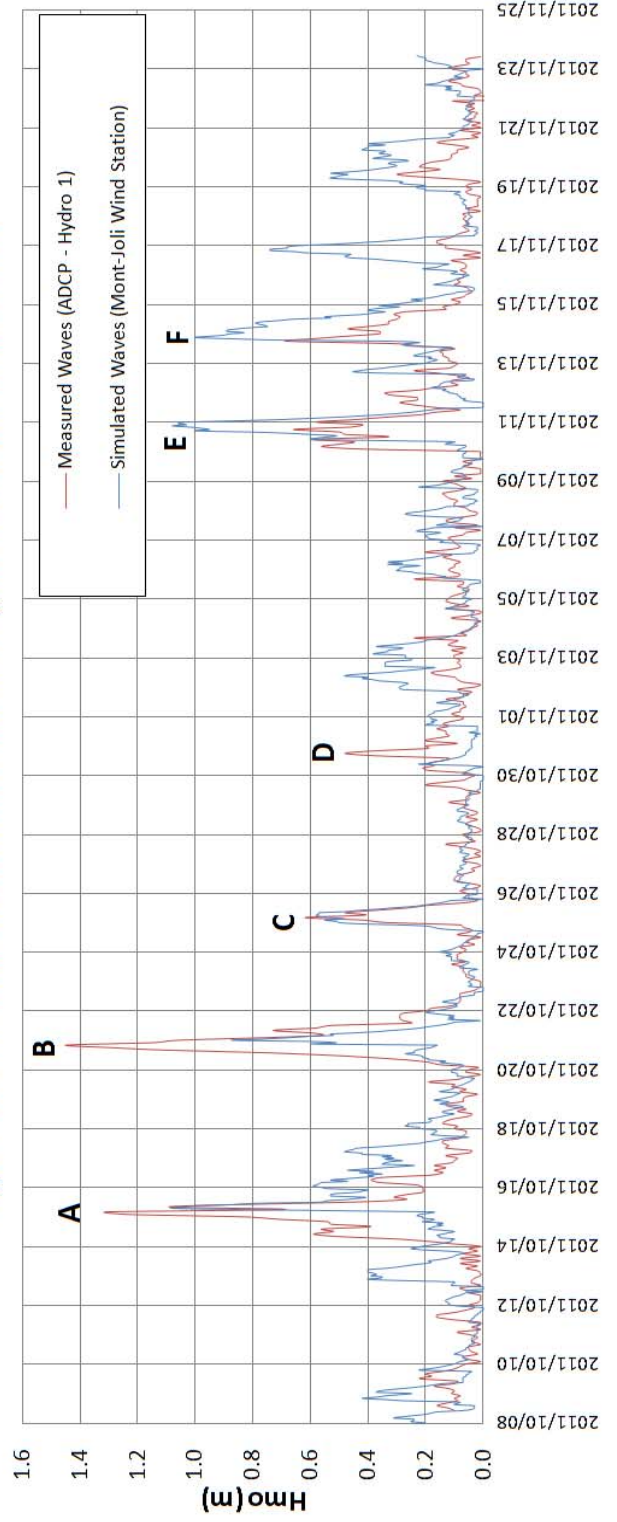


Figure A-4 - Measured vs Simulated Wave Heights - Mont-Joli Wind Station



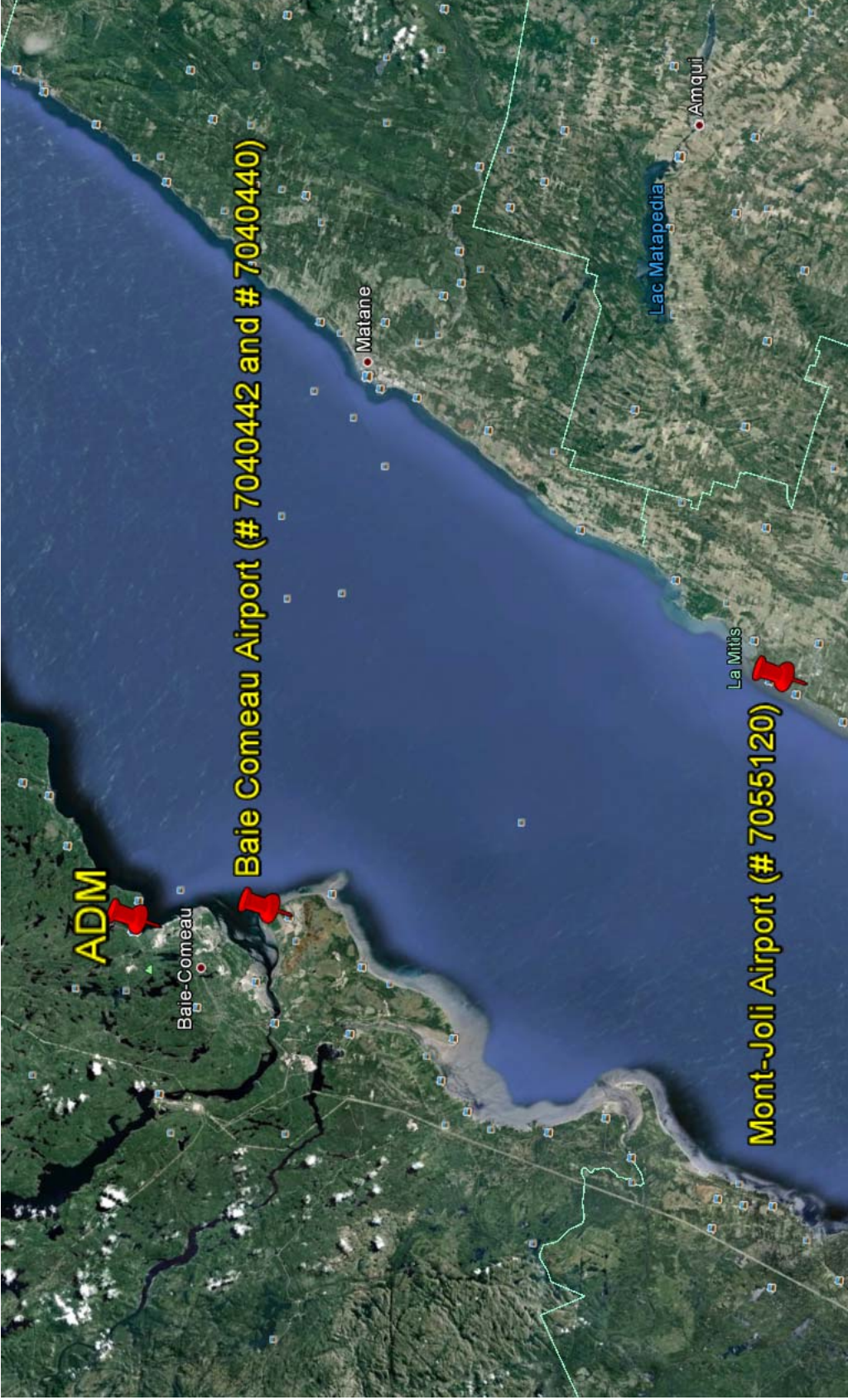


Figure A-2 Location of the Baie-Comeau and Mont-Joli Meteorological Stations.

Table A-2 Comparison of Wave Characteristics – Measured and Simulated Waves – Baie-Comeau Station.

Wave Event Characteristics - ADCP - Hydro 1						Simulated Waves - Baie-Comeau A		
ID	Starting Date	End Date	Maximum Wave Height (m)	Direction From	Hours > 0.3 m	Maximum Wave Height (m)	Direction From	Hours > 0.3 m
A	14/10/2011 6:20	15/10/2011 16:20	1.31	ESE	34	1.24	E	41
B	20/10/2011 10:20	21/10/2011 12:20	1.45	ESE	27	1.42	E	27
C	25/10/2011 0:20	25/10/2011 10:20	0.62	ESE	11	0.78	E	16
D	30/10/2011 16:20	30/10/2011 20:20	0.48	ESE	4	-	N	0
E	10/11/2011 2:20	11/11/2011 4:20	0.66	ESE	26	0.88	E	28
F	13/11/2011 16:20	14/11/2011 12:20	0.68	ESE	24	0.79	E	24
Total					126	136		

Table A-3 Comparison of Wave Characteristics – Measured and Simulated Waves – Mont-Joli Station.

Wave Event Characteristics - ADCP - Hydro 1						Simulated Waves - Mont-Joli A		
ID	Starting Date	End Date	Maximum Wave Height (m)	Direction From	Hours > 0.3 m	Maximum Wave Height (m)	Direction From	Hours > 0.3 m
A	14/10/2011 6:20	15/10/2011 16:20	1.31	ESE	34	1.08	SE	18
B	20/10/2011 10:20	21/10/2011 12:20	1.45	ESE	27	0.87	ESE	12
C	25/10/2011 0:20	25/10/2011 10:20	0.62	ESE	11	0.58	SE	14
D	30/10/2011 16:20	30/10/2011 20:20	0.48	ESE	4	-	NNW	0
E	10/11/2011 2:20	11/11/2011 4:20	0.66	ESE	26	1.08	SE	22
F	13/11/2011 16:20	14/11/2011 12:20	0.68	ESE	24	1.00	SE	31
Total					126	97		

## Model Adequacy

Based on results shown in Figures A-3, A-4 and Tables A-2, A-3, the model adequacy was assessed based on 3 specific criteria, defined as follow:

- Wave height peak values and phase signal (timing)
- Wave direction
- Period of exceedance above threshold

### **Wave Height Peak and Phase Signal**

The maximum wave heights for each event estimated using the Baie-Comeau station have a high level of accuracy, while the corresponding estimates from the Mont-Joli station have more gaps compared to the Hydro-1 measurements. A mean wave height difference of 0.12 m for Baie-Comeau compared to 0.32 m for Mont-Joli indicates the level of accuracy for both stations. The Mont-Joli station significantly underestimates event A and B and it overestimates events E and F. On the other hand, the Baie-Comeau wave height estimates remain relatively accurate for all events with the exception of event D, for which both stations have underestimated.

Estimates based on phase signal for the Baie-Comeau station have a good accuracy for both starting and ending times. However, the Mont-Joli station phase signal is less accurate especially for events A, B and E. These considerations are consistent with the number of hours over a 0.3 m wave height threshold for each main event.

### **Wave Directions**

All wave events measured during the fall 2011 were incoming from the East-South-East (ESE) as predominant wave direction. The GENIVAR wave model predicted near shore wave directions at the entrance of ADM from East (E) to South East (SE) for almost all events considering Baie-Comeau and Mont-Joli stations respectively. The difference in wave directions between measured and simulated values for both stations can be explained by the fact that incoming wind directions are near the boundaries of the East South East (ESE) sector (E and SE). In other words, only few degrees can change the direction from SE to ESE or from E to ESE which represents in fact, the accuracy of the model to predict the near shore direction. Based on these results, it is considered that an inaccuracy in the order of 10 degrees represents the difference observed between the measured and the simulated directions. These results are considered satisfactory and confirm the reliability of the wind-wave model coupled with the wave transformation model STWAVE in simulating the appropriate wave directions from offshore to the entrance of ADM.

## **Period of Exceedance**

Again, the number of hours over a 0.3 m wave height characterized in Table A-2 indicates a better match using the Baie-Comeau station compared to Mont-Joli. In fact, the Mont-Joli station does not adequately represent the phase signal: there are significant wave height gaps compared to the measured values. These two aspects are reflected for each station with a total number of hours above the 0.3 m threshold of 136 and 97 respectively for the Baie-Comeau and Mont-Joli station compared to the 126 hours measured with ADCP Hydro 1.

### Discussion and Recommendations

The adequacy of the model was verified in terms of the maximum wave height, direction and phase lag as well as wave duration periods for each main event characterized from October 7<sup>th</sup> to November 21<sup>st</sup> 2011.

The location and wind exposure of the Mont-Joli station (see Figure A-1) are the main reasons to explain the more significant differences observed in wave estimates compared to the Baie-Comeau station. The station is located on the South shore of the St-Lawrence River more than 70 km from ADM, compared to 14 km for the Baie-Comeau station. The significant distance of Mont-Joli compared to Baie-Comeau station makes more probable a wind field that differs from the one observed at ADM. In fact, a greater distance between the wind station and the site under study leads, in most of the case, to less accuracy between measured and predicted wave parameters. Moreover, with the Baie-comeau station being located on the North shore, it was expected to record more accurately the overwater water wind coming from the East, which is not the case with the Mont-Joli location. Results using the Mont-Joli station were thus expected to be less accurate.

In fact, compared to the Baie-Comeau station, six additional events ( $H > 0.3$  m) were predicted by the Mont-Joli station during the fall 2011. The wind data collected at the nearby Baie-Comeau station is more representative of the wind climate to estimate wave parameters in ADM. Results presented in Tables A-2, A-3 as well as Figures A-3 and A-4 reflect this reality and remain consistent with wave measurements collected from Hydro-1.

Uncertainties in the measurement of wave heights under 0.3 m can be explained by the following considerations:

- Wave agitation in ADM coming from wave reflection on wharves
- Construction works in ADM during the measurement period

- Ship displacements (arrival, departure and mooring) and other navigation activities

The degree of accuracy coming from the ADCP measurements, particularly for small wave height, may also explain some differences between measured and simulated wave parameters.

Event D, measured by Hydro-1 on October 30<sup>th</sup>, is not predicted by the wind-wave model because corresponding wind was measured from North. One of the above considerations likely explains this inconsistency in the measurements.

Based on the results summarized in this Appendix, the GENIVAR approach using a wind-wave hindcast model coupled to the near shore wave propagation model STWAVE provide reliable estimates of wave height, direction and duration at ADM using the Baie-Comeau wind data set. The wind-wave model and the methodology used to compute the near shore wave climate is deemed appropriated to estimate wave parameters in ADM. It is recommended to use wind speeds and directions from the Baie-Comeau station as wind data set for wave hindcast.

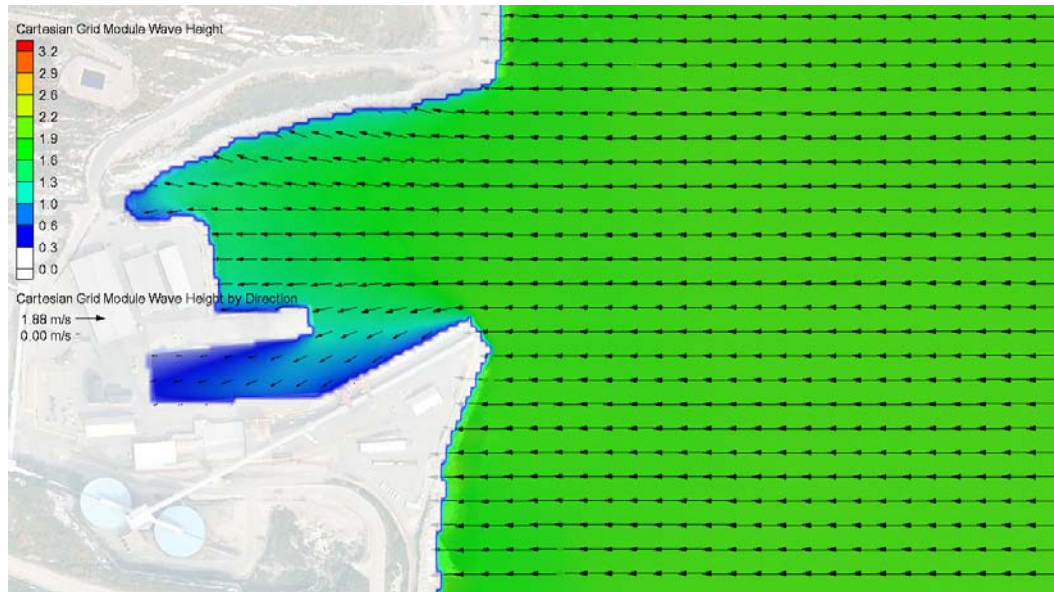


## APPENDIX 3 – HISTORICAL STORM EVENTS

---

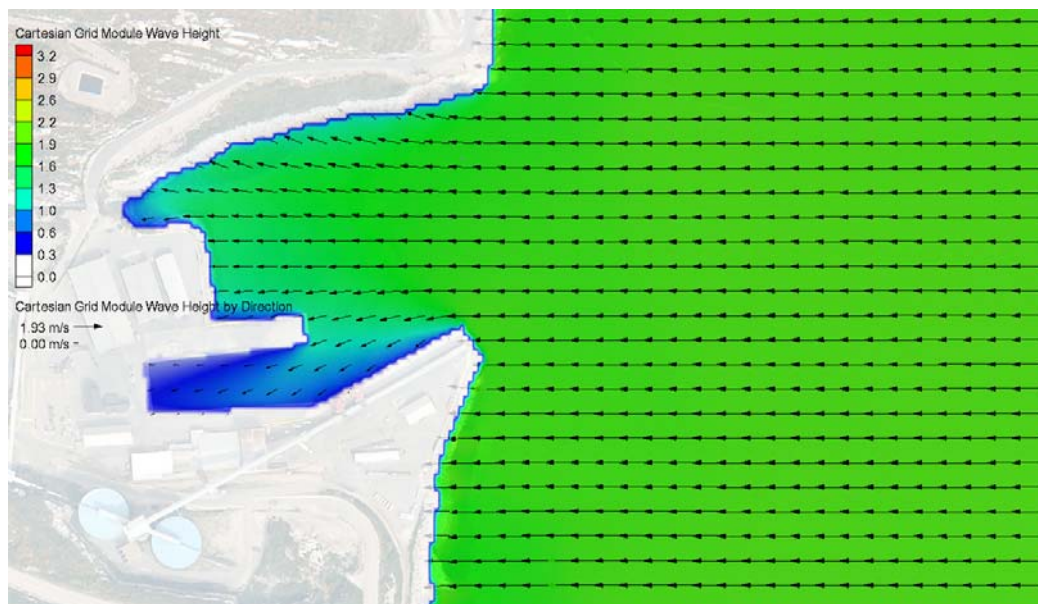
December 6<sup>th</sup> 2010

Hm0 = 1.94 m; Tp = 5.7 s; Direction = East; **Estimated Water Level = 3.1 m (MWL)**



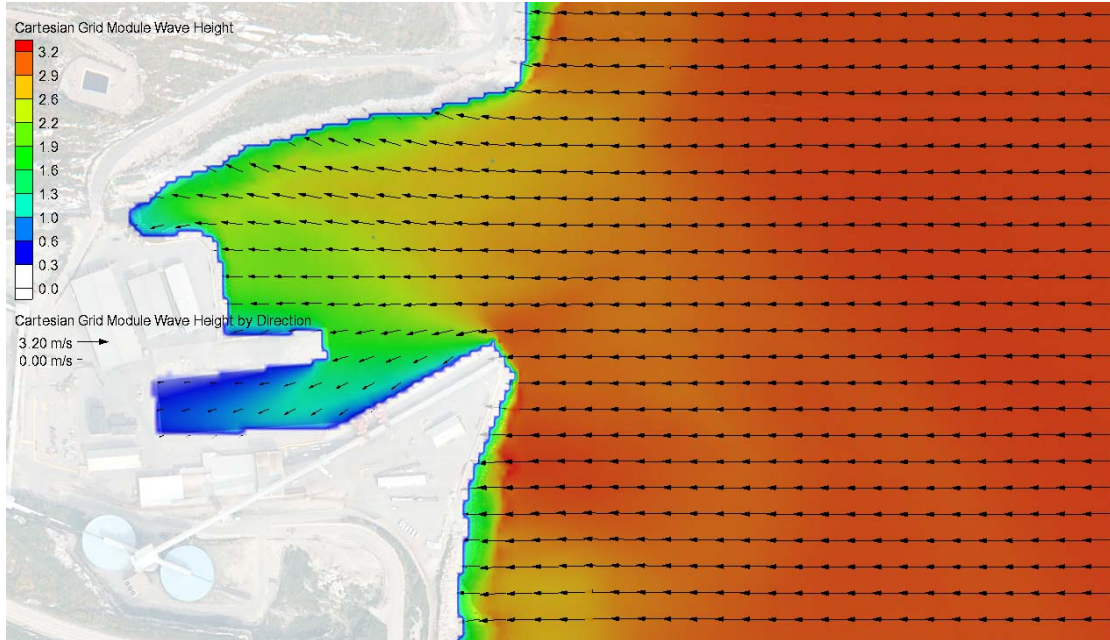
December 2<sup>nd</sup> 2005

Hm0 = 1.96 m; Tp = 5.73 s; Direction = East; Water Level = 2.71 m (MWL)



October 10<sup>th</sup> 1976

Hm<sub>0</sub> = 3.15 m; T<sub>p</sub> = 7.27 s; Direction = East; Water Level = 2.16 m (MWL)



## **APPENDIX 4 - MODELING APPROACH – MODEL SETUP & INPUT PARAMETERS**

---

This appendix summarizes the modeling approach (model setup and input parameters) used to perform the following modeling tasks:

1. Evaluate the wave refraction coefficients with STWAVE (**see section 4.2 in the main report**).
2. Sediment Stability Assessment using STWAVE and MATLAB (**see section 6.1 in the main report**).
3. Predict wave-induced currents with CMS-FLOW (**see section 6.2 in the main report**).

### **1. STWAVE - Wave Refraction Coefficients**

To evaluate the near shore wave transformation and determine the wave parameters (height and direction) in ADM, the steady-state spectral wave model STWAVE (Smith et al. 2001) was used. STWAVE simulates the wave refraction and shoaling, the wave diffraction and the depth and steepness-induced wave breaking. The wave reflection on structures and shorelines is not simulated with this model. The assumptions made in STWAVE are:

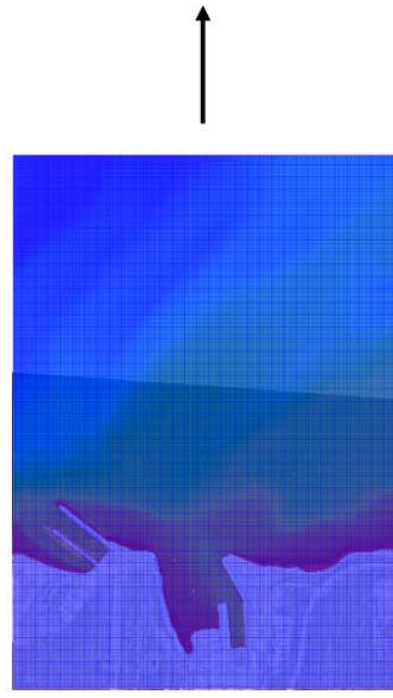
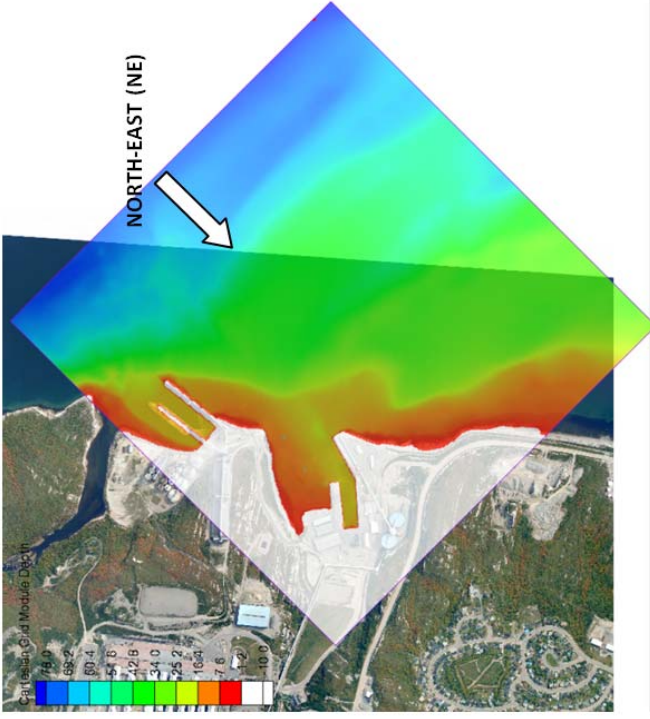
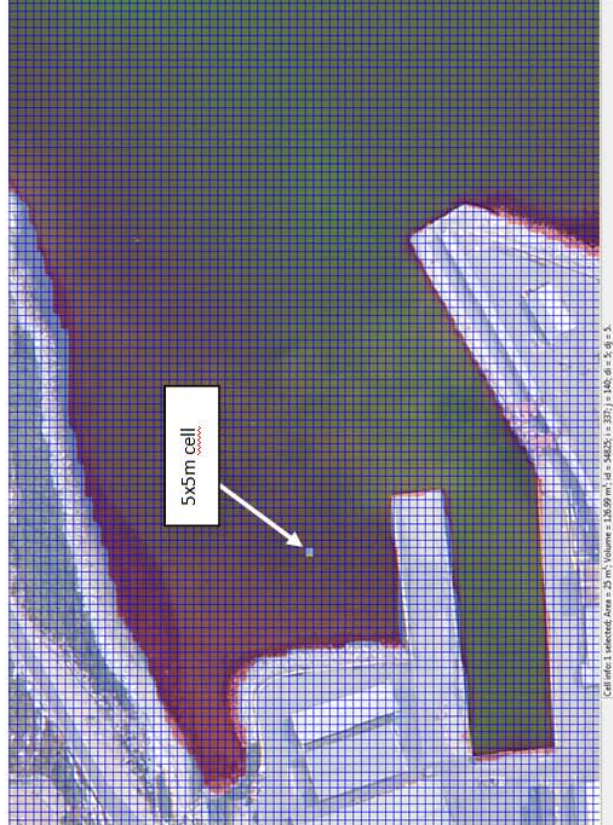
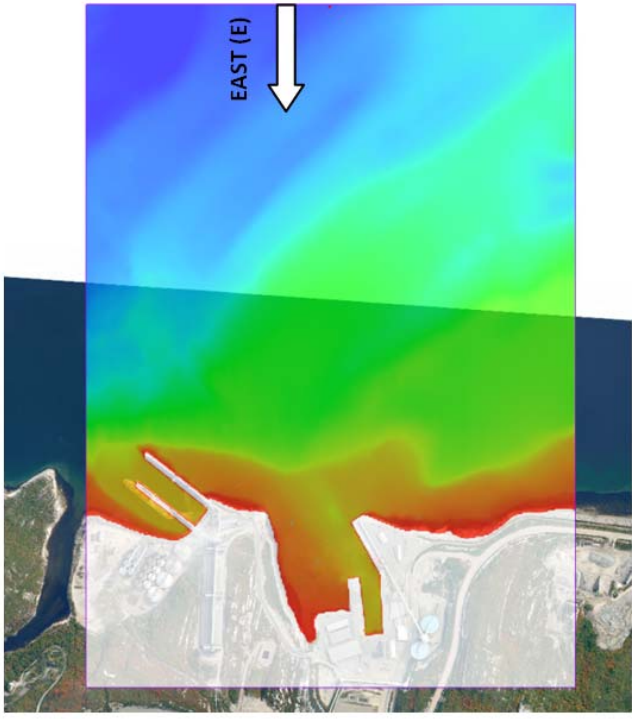
- Mild bottom slope
- Spatially homogenous offshore wave conditions
- Steady-state waves
- Linear wave refraction and shoaling
- Bottom friction neglected

STWAVE is a spectral wave model that solves the averaged wave energy over the phase. Thus for applications where near-field reflection on coastal structures is required, a phase-resolving model should be applied. The approximations and assumptions described herein are deemed acceptable to assess the near-shore wave climate at the entrance of ADM

STWAVE model setup includes the following parameters:

- The 2011 bathymetric measurements were used to generate the water depth grid;
- The grid size is 392 by 280 cells of 5m x 5m (area of 25m<sup>2</sup>);
- No grid nesting was used, uniform grid described above;
- A constant water level at 0.0 m (MWL) was used to establish the refraction coefficient. Observed water level were used for specific wave events (including storms);
- The domain extends out to deep water location in Baie des Anglais at a water depth of approximately 70 to 80 m (see Figure A-3 below);
- The offshore boundary condition is located in the same area than the point used to generate the deep water wave climate (see Map 2, section 2.2 in the main report);
- Multiple orientations were used depending on wave directions (see examples for East and North East on Figure A-3 below);
- Inputs parameters ( $H_{m0}$  et  $Tp$ ) were derived from GENIVAR wind-wave model hindcast (see Table 5, section 4.2 in the main report);
- JONSWAP wave spectrum was used by specifying  $H_{m0}$  and  $Tp$ ;
- Wave height, wave direction, wave period, wave breaking as well as radiation stresses were set as outputs.

The STWAVE model was calibrated as part of the GENIVAR wind-wave model calibration using the wave measurements collected with two ADCPs during the Fall 2011 at the entrance of Anse du Moulin. Appendix 2 of this report shows the calibration results and confirms the adequacy of the wind-wave hindcast model coupled to the near shore wave propagation model STWAVE to provide reliable estimates of wave height, direction and duration at ADM using the Baie-Comeau wind data set.



## 2. STWAVE-MATLAB - Sediment Stability Assessment

In order to assess the sediment stability in Anse du Moulin, a Matlab script was implemented using the STWAVE outputs to calculate the wave-current induced bed shear stress as well as the critical bed shear stress based on the Median Grain Size ( $D_{50}$ ).

The following section gives all the references, equations and input parameters implemented in the Matlab script to assess the sediment stability in Anse Du Moulin.

The references used to achieve this task are:

- [1] BASCO D.R. 2012. Lecture Notes: Coastal Hydrodynamics and Sediment Transport Processes (CEE 788), Old Dominion University, Virginia.
- [2] SOULSBY R.L. and CLARKE S. 2005. *Bed Shear-Stresses Under Combined Waves and Currents on Smooth and Rough Beds*, HR Wallingford, Report TR 137.
- [3] KAMPHUIS J.W. 2010. *Introduction to Coastal Engineering and Management*, World Scientific – Advanced Series on Ocean Engineering, 2<sup>nd</sup> Edition.
- [4] DEAN R.G. and DALRYMPLE R.A. 2002. *Coastal Processes with Engineering Applications*. Cambridge University Press.
- [5] MASSELINK G and HUGHES M. G. 2003. *Introduction to Coastal Processes & Geomorphology*, Hodder Education, Hachette UK Company, Great Britain. 354 p.

### 2.1 CRITICAL BED SHEAR-STRESS

The critical bed shear-stress required to initiate grain motion under steady flow conditions is defined by the following equation:

$$\tau_{critical} = \theta_c g D (\rho_s - \rho)$$

Where,

- $\tau_{critical}$  = Critical bed shear-stress required to initiate grain motion ( $N/m^2$ )
- $\theta_c$  = Shields Parameter (non-dimensional)
- $g$  = Gravitational acceleration ( $m/s^2$ )
- $D$  = Median Grain Size ( $D_{50}$ ) (m)
- $\rho_s$  = Sediment density ( $kg/m^3$ )
- $\rho$  = Sea water density ( $kg/m^3$ )

The proposed equation given by Soulsby (1997), which is the Modified Shield diagram, is used to predict the critical shear stress (dimensionless) parameter necessary to initiate sediment motion:

$$\theta_c = \frac{0.3}{1 + 1.2D_*} + 0.055[1 - \exp(-0.02D_*)]$$

Where the non-dimensional grain diameter is defined as:

$$D_* = D \left[ \frac{\rho^2 g (s-1)}{\mu^2} \right]^{1/3}$$

With

- $\mu$  = Water viscosity (Ns/m<sup>2</sup>)

## 2.2 WAVE-CURRENT INDUCED BED SHEAR-STRESS

In many cases both currents and waves make significant contributions to the bed shear-stress. The resulting bed shear-stress consists of a steady component due to the current together with an oscillatory component due to the waves. This results to a simple linear addition of the steady current-alone stress ( $\tau_c$ ) and the oscillatory wave-alone stress ( $\tau_w$ ).

Based on the theory for rough beds as would be found for sand and gravel, the maximum bed shear-stress used to determine the threshold of sediment motion is defined as:

$$\tau_{max} = [(\tau_m + \tau_w |\cos\phi|)^2 + (\tau_w |\sin\phi|)^2]^{1/2}$$

Where

$$\tau_m = \tau_c \left[ 1 + 1.2 \left( \frac{\tau_w}{\tau_c + \tau_w} \right)^{3.2} \right]$$

With

$$\tau_c = \rho C_{Dr} \bar{U}^2$$

$$C_{Dr} = \left[ \frac{0.4}{\ln\left(\frac{h}{z_0}\right) - 1} \right]$$

- $\phi$  = angle between current direction and direction of wave travel
- $\tau_{max}$  = Maximum bed shear-stress during a wave cycle under combined waves and currents (N/m<sup>2</sup>)
- $\tau_m$  = Mean bed shear-stress during a wave cycle under combined waves and currents (N/m<sup>2</sup>)
- $\tau_w$  = Oscillatory wave-alone stress (N/m<sup>2</sup>)
- $\tau_c$  = Steady current-alone stress (N/m<sup>2</sup>)
- $\rho$  = Sea water density (kg/m<sup>3</sup>)
- $\bar{U}$  = Depth-averaged velocity (m/s)
- $C_{Dr}$  = Drag coefficient during wave cycle;
- $h$  = Water depth (m)
- $z_0$  = Bed roughness (m)

And,

$$\tau_w = \frac{1}{2} \rho f_w u_o^2$$

$$f_w = \exp \left[ 5.5 \left( \frac{k_s}{d_0} \right)^{0.2} - 6.3 \right]$$

$$u_o = \frac{\pi H \cosh k(z+h)}{T \sinh kh} \cos(kx - wt)$$

With,

$$k = \frac{2\pi}{L}$$

$$w = \frac{2\pi}{T}$$

$$L = \frac{gT^2}{2\pi} \tanh kh$$

$$k_s = k' + k''$$

$$k' = D$$

$$k'' = \frac{8\eta^2}{\lambda}$$

$$d_0 = H \frac{\cosh k(z+h)}{\sinh kh}$$



- $\rho$  = Sea water density ( $\text{kg/m}^3$ )
- $f_w$  = Bed friction factor
- $u_0$  = orbital velocity (m/s)
- $H$  = Wave height (m)
- $g$  = Gravitational acceleration ( $\text{m/s}^2$ )
- $h$  = Water depth (m)
- $z$  = Vertical distance (m)
- $x$  = Horizontal distance (m)
- $t$  = Time (sec)
- $L$  = Wave length (m)
- $D$  = Median Grain Size (m)
- $T$  = Wave period (s)
- $\eta$  = Ripple height (m)
- $\lambda$  = Ripple length (m)

## 2.3 STABILITY ASSESSMENT

The Matlab script, based on these previous equations, was implemented using the following assumptions and input parameters:

- A depth average current velocity of 10 cm/s was used to calculate the wave cycle-mean bed shear-stress ( $\tau_m$ ). This value is based on the 2011 current measurements collected by both ADCP (Hydro-1 and Hydro-2);
- The water depths (based on 2011 bathymetric data), wave heights and wave periods were extracted from STWAVE at each node of the grid and for each simulated scenario;
- The critical bed shear-stress ( $\tau_{critical}$ ) was calculated using the median grain size ( $D_{50}$ ) issued from all the sample collected during the 2011 survey as well as some samples collected in 2006, 2007 and 2008 to complete the dataset;
- High quality videos taken in 2011 show no ripples on the seabed of ADM, thus a bed roughness equal to the median grain size ( $D_{50}$ ) was assumed;
- The angle between the current direction and direction of wave travel was considered equal to zero to calculate the maximum bed shear-stress (vector addition);

- As the oscillatory wave-alone bed shear-stress varies through a wave cycle, the maximum orbital velocity at the seabed was considered to calculate this component.

The Matlab outputs (maximum wave-current bed shear stress and critical bed shear stress) were calculated on a grid with a resolution of 2 x 2 m to provide the sediment stability mapping of the entire Anse du Moulin (ADM) under different hydrodynamic conditions. The selected hydrodynamic conditions are the following:

Scenario	Near Shore Wave Characteristics			Tide Level			Event Occurrence
	Hm0 (m)	Tp (s)	Frequency (hours/year)	Tide label	Water Elevation (MWL, m)	Frequency (hours/year)	Frequency (hours/year)
1	1.2	4.8	24	(MWL)	< 0.0	4380	12
2	1.4	5.3	6	(MWL)	< 0.0	4380	3
3	1.8	6.1	1	(MWL)	< 0.0	4380	0.5

Finally, the following criteria were used to assess the sediment stability and complete the final mapping:

- If  $\frac{\tau_{max}}{\tau_{critical}} < 1$             **[Stable]**
- If  $\frac{\tau_{max}}{\tau_{critical}} > 1$             **[Unstable]**
- Hatched polygon                **[Unstable, Surf Zone]**

It is important to mention that in the surf zone, wave breaking injects a considerable amount of turbulence into the water column, which provides an additional mobilizing effect that may allow sediment motion at considerably lower velocities than predicted from the Shield curve. For this reason and because the theory confirms that wave breaking induces alongshore sediment transport, the surf zone is logically considered as an “unstable” zone.

### 3. CMS-FLOW - WAVE INDUCED CURRENTS

CMS-Flow is a finite-volume numerical engine (USACE, 2006) which includes the capabilities to compute both hydrodynamics (water levels and current flow values under any combination of tide, wind, surge, waves and river flow) and sediment transport including morphology change.

In the current study, CMS-Flow was simply used in “steady state” mode to compute the wave induced currents using the radiation stress outputs from STWAVE.

CMS-FLOW model setup includes the following parameters:

- The 2011 bathymetric measurements were used to generate the water depth grid;
- The grid size is 392 by 280 cells of 5m x 5m (area of 25m<sup>2</sup>) [Exactly the same than STWAVE];
- No grid nesting was used, only the uniform grid described above;
- The domain extends out to deep water location in Baie des Anglais at a water depth of approximately 70 to 80 m (see Figure A-3 above);
- The offshore boundary condition is located in the same area than the point used to generate the deep water wave climate (see Map 2, section 2.2 in the main report);
- The East orientation was selected as a representative direction to simulate the wave-induced currents;
- A constant water level over time (steady-state, no tide influence) was used as boundary condition and values were selected based on the daily/hourly conditions observed. No wind effect was included as boundary condition to the model;
- The CMS-FLOW Input parameters on each cell of the grid are the STWAVE outputs which are: Radiation Stresses, Wave Heights, Wave Periods, Wave Directions, Energy Dissipation;
- No model steering was used which means that all boundary conditions and input parameters are constant over time (steady-state);
- The CMS-FLOW outputs are the wave-Induced currents.

The CMS-FLOW model was partially validated using the current measurement profiles collected by the ADCP during the wave event of October 4<sup>th</sup>. It remains relatively difficult to collect additional and precise current profiles with an ADCP under larger wave conditions in ADM, especially within the surf zone. However, we recommend to measure additional current information by mooring ADCPs at specific locations into the coastal jet (anti-clockwise gyre) to validate and get more confidence with the simulated currents velocities obtained with the CMS-FLOW model. The best time window to measure additional wave parameters and associated longshore currents would be Fall 2012. Finally, these current measurements should be combined to turbidity measurements in ADM to confirm sediment suspension and concentration.

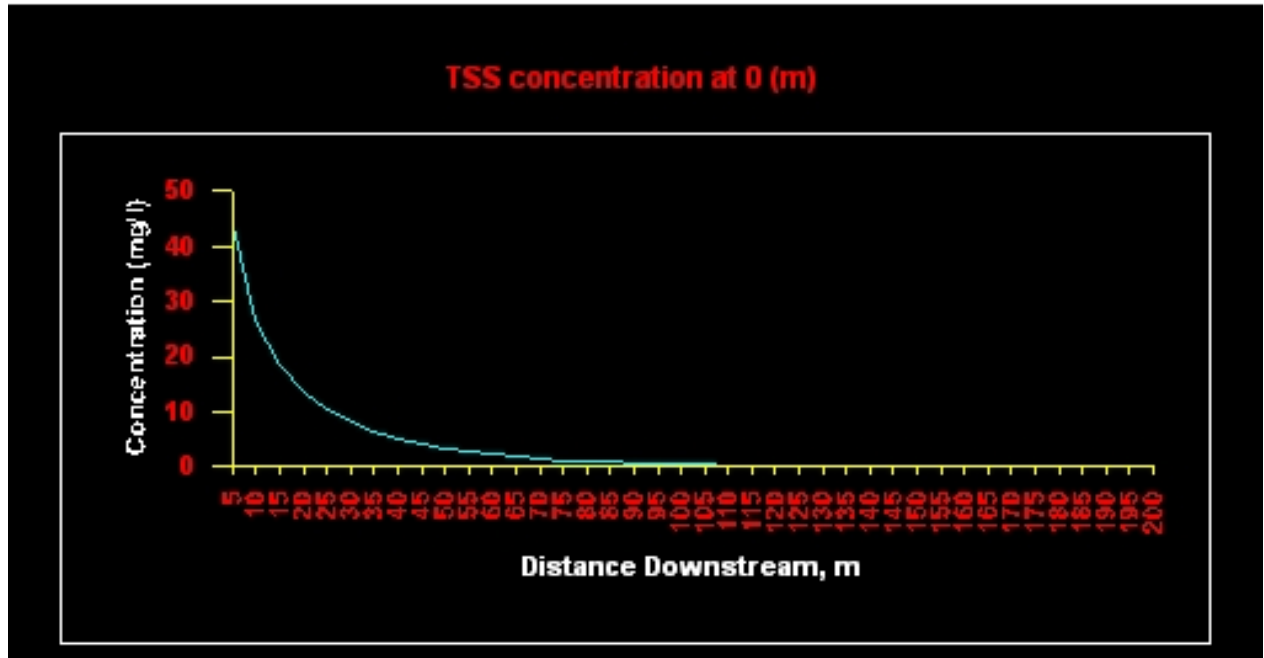


## APPENDIX 5 – DREDGE MODELING RESULTS

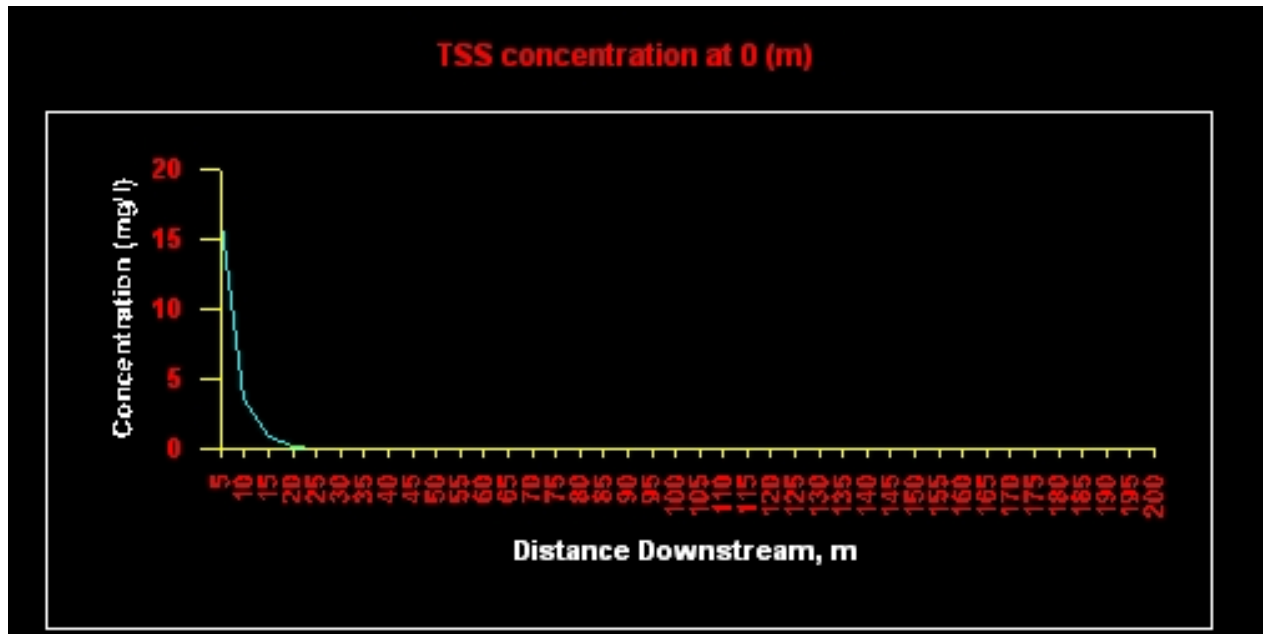
---

Downstream concentration versus distance from dredge - current axis

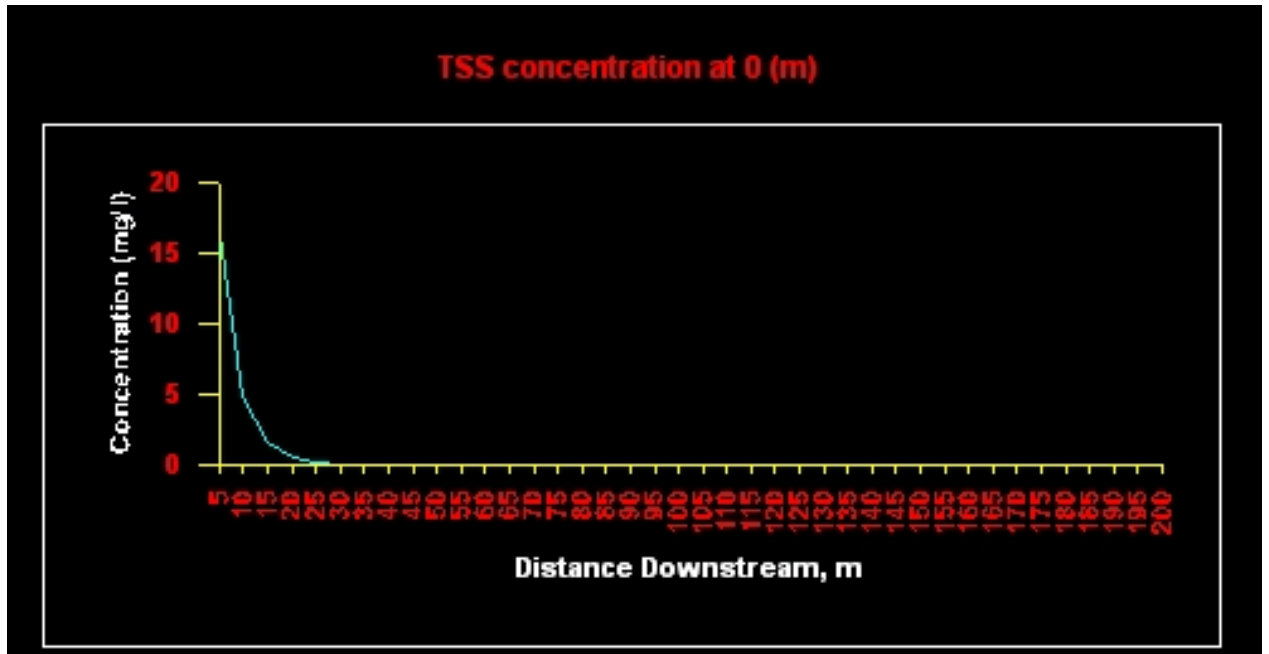
ALCOA 1



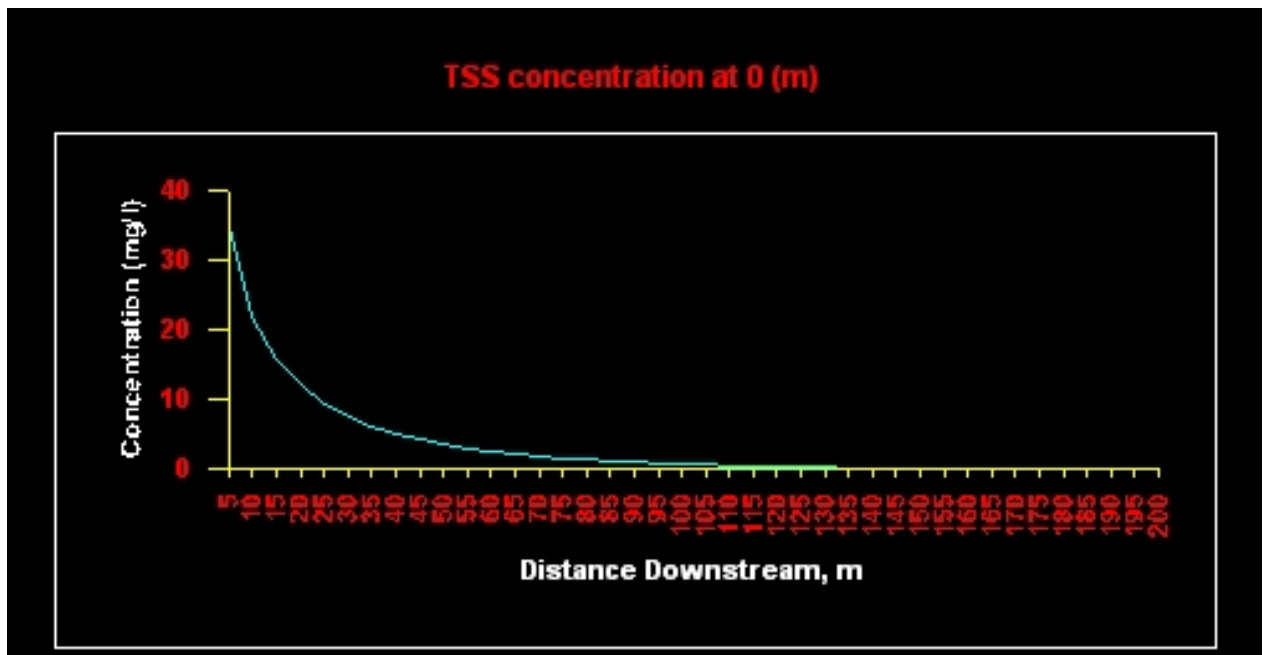
ALCOA 2



ALCOA 3

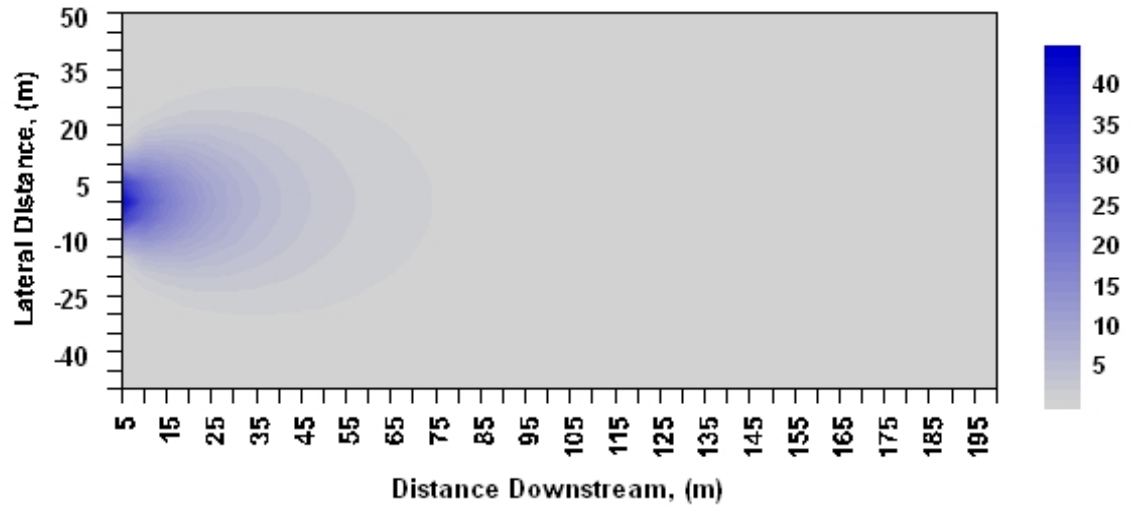


ALCOA 4

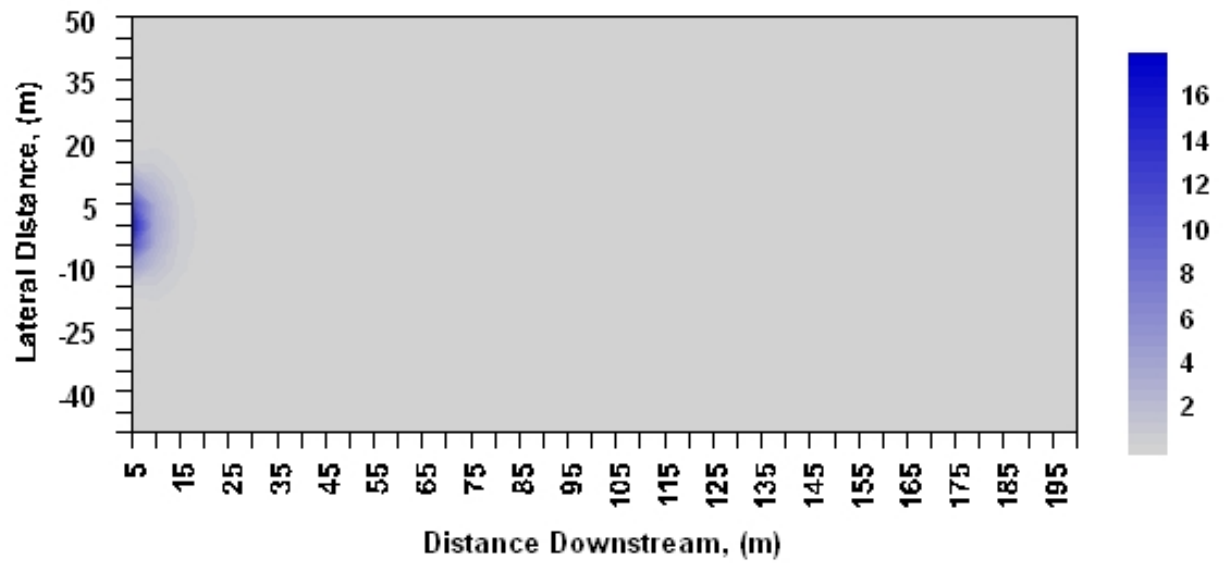


Downstream concentration versus distance from dredge – plan view (lateral distance)

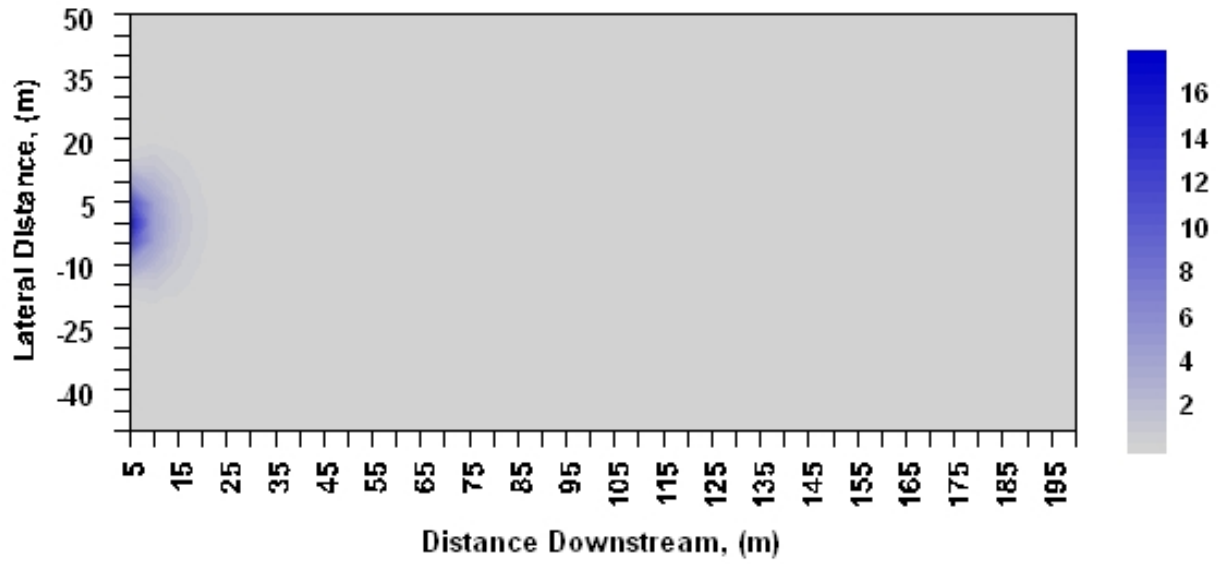
ALCOA 1



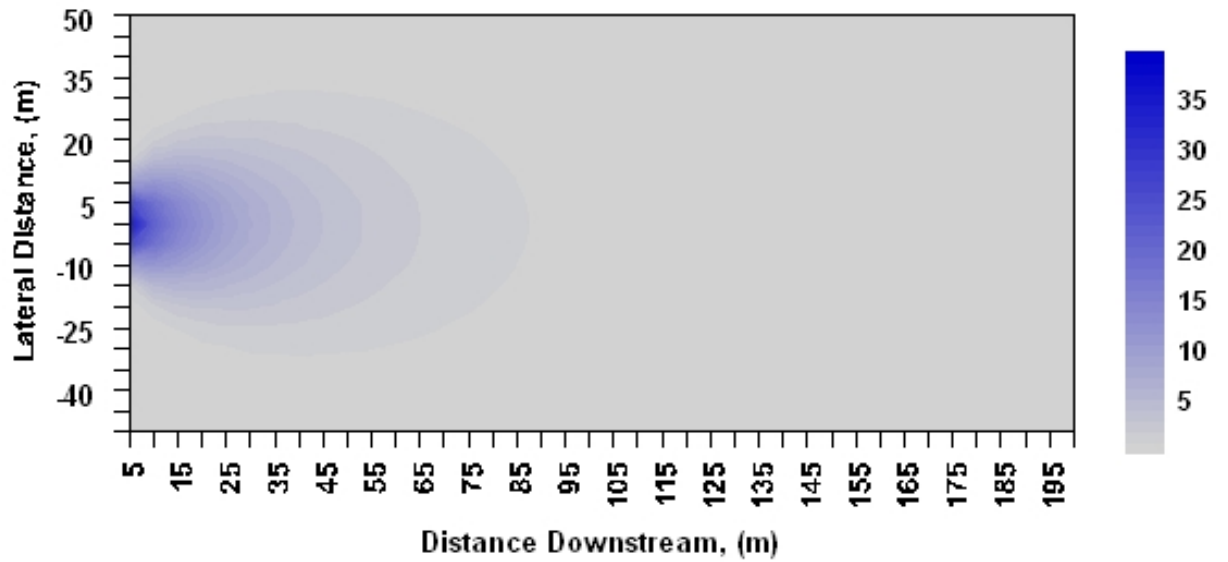
ALCOA 2



### ALCOA 3



### ALCOA 4





**DREDGE numerical output**

**ALCOA 1**

Dredge Type : Open Clamshell  
 Near-Field Model : TGU Method  
 Far-Field Model : Kuo's Model  
 Resuspended Material Selected : TSS

	<b>5</b>	<b>10</b>	<b>15</b>	<b>20</b>	<b>25</b>	<b>30</b>	<b>35</b>	<b>40</b>	<b>45</b>	<b>50</b>	<b>55</b>	<b>60</b>	<b>65</b>	<b>70</b>	<b>75</b>	<b>80</b>	<b>85</b>	<b>90</b>	<b>95</b>	<b>100</b>
-50	0	0	0,001	0,005	0,02	0,044	0,073	0,101	0,125	0,143	0,154	0,159	0,159	0,155	0,148	0,138	0,128	0,117	0,107	0,096
-45	0	0	0,004	0,024	0,065	0,118	0,17	0,212	0,242	0,259	0,264	0,261	0,251	0,236	0,219	0,201	0,182	0,163	0,146	0,129
-40	0	0,001	0,023	0,091	0,189	0,286	0,363	0,412	0,437	0,44	0,428	0,406	0,377	0,345	0,312	0,28	0,248	0,219	0,193	0,168
-35	0	0,013	0,112	0,295	0,483	0,624	0,708	0,741	0,735	0,704	0,656	0,6	0,541	0,483	0,427	0,375	0,327	0,285	0,246	0,213
-30	0,001	0,096	0,433	0,814	1,087	1,229	1,265	1,231	1,155	1,056	0,949	0,842	0,74	0,645	0,56	0,483	0,416	0,357	0,305	0,261
-25	0,018	0,533	1,361	1,923	2,162	2,179	2,068	1,892	1,692	1,49	1,297	1,121	0,964	0,825	0,704	0,599	0,509	0,432	0,366	0,31
-20	0,297	2,174	3,475	3,884	3,795	3,483	3,09	2,689	2,313	1,973	1,675	1,418	1,197	1,008	0,849	0,714	0,6	0,505	0,424	0,356
-15	2,643	6,489	7,204	6,711	5,878	5,015	4,224	3,535	2,949	2,456	2,044	1,701	1,416	1,179	0,982	0,819	0,683	0,57	0,476	0,398
-10	12,609	14,173	12,128	9,918	8,035	6,506	5,28	4,297	3,508	2,871	2,356	1,938	1,597	1,318	1,09	0,903	0,749	0,622	0,517	0,43
-5	32,199	22,649	16,576	12,537	9,692	7,607	6,037	4,832	3,893	3,153	2,566	2,095	1,716	1,409	1,16	0,957	0,791	0,655	0,543	0,451
0	44,011	26,48	18,396	13,556	10,317	8,013	6,313	5,024	4,031	3,253	2,639	2,15	1,758	1,441	1,185	0,976	0,806	0,666	0,552	0,458
5	32,199	22,649	16,576	12,537	9,692	7,607	6,037	4,832	3,893	3,153	2,566	2,095	1,716	1,409	1,16	0,957	0,791	0,655	0,543	0,451
10	12,609	14,173	12,128	9,918	8,035	6,506	5,28	4,297	3,508	2,871	2,356	1,938	1,597	1,318	1,09	0,903	0,749	0,622	0,517	0,43
15	2,643	6,489	7,204	6,711	5,878	5,015	4,224	3,535	2,949	2,456	2,044	1,701	1,416	1,179	0,982	0,819	0,683	0,57	0,476	0,398
20	0,297	2,174	3,475	3,884	3,795	3,483	3,09	2,689	2,313	1,973	1,675	1,418	1,197	1,008	0,849	0,714	0,6	0,505	0,424	0,356
25	0,018	0,533	1,361	1,923	2,162	2,179	2,068	1,892	1,692	1,49	1,297	1,121	0,964	0,825	0,704	0,599	0,509	0,432	0,366	0,31
30	0,001	0,096	0,433	0,814	1,087	1,229	1,265	1,231	1,155	1,056	0,949	0,842	0,74	0,645	0,56	0,483	0,416	0,357	0,305	0,261
35	0	0,013	0,112	0,295	0,483	0,624	0,708	0,741	0,735	0,704	0,656	0,6	0,541	0,483	0,427	0,375	0,327	0,285	0,246	0,213
40	0	0,001	0,023	0,091	0,189	0,286	0,363	0,412	0,437	0,44	0,428	0,406	0,377	0,345	0,312	0,28	0,248	0,219	0,193	0,168
45	0	0	0,004	0,024	0,065	0,118	0,17	0,212	0,242	0,259	0,264	0,261	0,251	0,236	0,219	0,201	0,182	0,163	0,146	0,129
50	0	0	0,001	0,005	0,02	0,044	0,073	0,101	0,125	0,143	0,154	0,159	0,159	0,155	0,148	0,138	0,128	0,117	0,107	0,096

<b>105</b>	<b>110</b>	<b>115</b>	<b>120</b>	<b>125</b>	<b>130</b>	<b>135</b>	<b>140</b>	<b>145</b>	<b>150</b>	<b>155</b>	<b>160</b>	<b>165</b>	<b>170</b>	<b>175</b>	<b>180</b>	<b>185</b>	<b>190</b>	<b>195</b>	<b>200</b>
0,086	0,076	0,068	0,06	0,052	0,046	0,04	0,035	0,03	0,026	0,023	0,02	0,017	0,015	0,013	0,011	0,009	0,008	0,007	0,006
0,114	0,1	0,087	0,076	0,066	0,058	0,05	0,043	0,037	0,032	0,027	0,024	0,02	0,017	0,015	0,013	0,011	0,009	0,008	0,007
0,147	0,127	0,11	0,095	0,082	0,071	0,061	0,052	0,045	0,038	0,033	0,028	0,024	0,02	0,017	0,015	0,013	0,011	0,009	0,008
0,183	0,157	0,135	0,116	0,099	0,085	0,072	0,061	0,052	0,045	0,038	0,032	0,027	0,023	0,02	0,017	0,014	0,012	0,01	0,009
0,222	0,189	0,161	0,137	0,116	0,099	0,084	0,071	0,06	0,051	0,043	0,037	0,031	0,026	0,022	0,019	0,016	0,013	0,011	0,01
0,262	0,221	0,187	0,158	0,134	0,113	0,095	0,08	0,068	0,057	0,048	0,041	0,034	0,029	0,025	0,021	0,017	0,015	0,012	0,011
0,299	0,252	0,212	0,178	0,149	0,126	0,106	0,089	0,075	0,063	0,053	0,045	0,038	0,032	0,027	0,022	0,019	0,016	0,013	0,011
0,332	0,278	0,233	0,195	0,163	0,137	0,115	0,096	0,081	0,068	0,057	0,048	0,04	0,034	0,028	0,024	0,02	0,017	0,014	0,012
0,358	0,298	0,249	0,208	0,174	0,145	0,121	0,102	0,085	0,071	0,06	0,05	0,042	0,035	0,03	0,025	0,021	0,018	0,015	0,012
0,374	0,311	0,259	0,216	0,18	0,15	0,126	0,105	0,088	0,074	0,062	0,052	0,043	0,036	0,03	0,026	0,021	0,018	0,015	0,013
0,38	0,316	0,263	0,219	0,183	0,152	0,127	0,106	0,089	0,074	0,062	0,052	0,044	0,037	0,031	0,026	0,022	0,018	0,015	0,013
0,374	0,311	0,259	0,216	0,18	0,15	0,126	0,105	0,088	0,074	0,062	0,052	0,043	0,036	0,03	0,026	0,021	0,018	0,015	0,013
0,358	0,298	0,249	0,208	0,174	0,145	0,121	0,102	0,085	0,071	0,06	0,05	0,042	0,035	0,03	0,025	0,021	0,018	0,015	0,012
0,332	0,278	0,233	0,195	0,163	0,137	0,115	0,096	0,081	0,068	0,057	0,048	0,04	0,034	0,028	0,024	0,02	0,017	0,014	0,012
0,299	0,252	0,212	0,178	0,149	0,126	0,106	0,089	0,075	0,063	0,053	0,045	0,038	0,032	0,027	0,022	0,019	0,016	0,013	0,011
0,262	0,221	0,187	0,158	0,134	0,113	0,095	0,08	0,068	0,057	0,048	0,041	0,034	0,029	0,025	0,021	0,017	0,015	0,012	0,011
0,222	0,189	0,161	0,137	0,116	0,099	0,084	0,071	0,06	0,051	0,043	0,037	0,031	0,026	0,022	0,019	0,016	0,013	0,011	0,01
0,183	0,157	0,135	0,116	0,099	0,085	0,072	0,061	0,052	0,045	0,038	0,032	0,027	0,023	0,02	0,017	0,014	0,012	0,01	0,009
0,147	0,127	0,11	0,095	0,082	0,071	0,061	0,052	0,045	0,038	0,033	0,028	0,024	0,02	0,017	0,015	0,013	0,011	0,009	0,008
0,114	0,1	0,087	0,076	0,066	0,058	0,05	0,043	0,037	0,032	0,027	0,024	0,02	0,017	0,015	0,013	0,011	0,009	0,008	0,007
0,086	0,076	0,068	0,06	0,052	0,046	0,04	0,035	0,03	0,026	0,023	0,02	0,017	0,015	0,013	0,011	0,009	0,008	0,007	0,006











**ALCOA 4**

Dredge Type : Open Clamshell  
 Near-Field Model : TGU Method  
 Far-Field Model : Kuo's Model  
 Resuspended Material Selected : TSS

	<b>5</b>	<b>10</b>	<b>15</b>	<b>20</b>	<b>25</b>	<b>30</b>	<b>35</b>	<b>40</b>	<b>45</b>	<b>50</b>	<b>55</b>	<b>60</b>	<b>65</b>	<b>70</b>	<b>75</b>	<b>80</b>	<b>85</b>	<b>90</b>	<b>95</b>	<b>100</b>
-50	0	0	0	0.005	0.018	0.042	0.073	0.105	0.135	0.16	0.179	0.191	0.198	0.2	0.198	0.193	0.186	0.177	0.166	0.155
-45	0	0	0.003	0.022	0.061	0.113	0.169	0.22	0.26	0.289	0.306	0.314	0.313	0.306	0.295	0.28	0.263	0.246	0.227	0.209
-40	0	0.001	0.02	0.082	0.175	0.275	0.362	0.427	0.47	0.492	0.497	0.489	0.471	0.448	0.42	0.391	0.36	0.33	0.301	0.273
-35	0	0.01	0.096	0.263	0.447	0.601	0.707	0.768	0.791	0.786	0.76	0.722	0.676	0.626	0.574	0.523	0.474	0.428	0.385	0.345
-30	0	0.079	0.372	0.727	1.008	1.182	1.264	1.276	1.242	1.179	1.1	1.013	0.924	0.836	0.753	0.675	0.603	0.537	0.477	0.423
-25	0.014	0.441	1.17	1.717	2.004	2.096	2.065	1.961	1.82	1.663	1.504	1.349	1.203	1.069	0.947	0.836	0.738	0.649	0.571	0.502
-20	0.237	1.801	2.989	3.468	3.517	3.35	3.086	2.787	2.488	2.203	1.942	1.705	1.494	1.307	1.142	0.997	0.87	0.759	0.662	0.578
-15	2.11	5.378	6.197	5.992	5.448	4.824	4.218	3.664	3.172	2.742	2.369	2.046	1.768	1.528	1.321	1.143	0.99	0.857	0.743	0.644
-10	10.068	11.746	10.432	8.855	7.446	6.259	5.272	4.454	3.774	3.206	2.731	2.331	1.994	1.709	1.466	1.261	1.085	0.935	0.807	0.697
-5	25.709	18.771	14.259	11.194	8.982	7.317	6.028	5.008	4.188	3.521	2.974	2.52	2.143	1.827	1.561	1.337	1.147	0.985	0.848	0.73
0	35.14	21.945	15.825	12.104	9.561	7.709	6.303	5.207	4.336	3.633	3.059	2.587	2.195	1.868	1.594	1.363	1.168	1.002	0.862	0.742
5	25.709	18.771	14.259	11.194	8.982	7.317	6.028	5.008	4.188	3.521	2.974	2.52	2.143	1.827	1.561	1.337	1.147	0.985	0.848	0.73
10	10.068	11.746	10.432	8.855	7.446	6.259	5.272	4.454	3.774	3.206	2.731	2.331	1.994	1.709	1.466	1.261	1.085	0.935	0.807	0.697
15	2.11	5.378	6.197	5.992	5.448	4.824	4.218	3.664	3.172	2.742	2.369	2.046	1.768	1.528	1.321	1.143	0.99	0.857	0.743	0.644
20	0.237	1.801	2.989	3.468	3.517	3.35	3.086	2.787	2.488	2.203	1.942	1.705	1.494	1.307	1.142	0.997	0.87	0.759	0.662	0.578
25	0.014	0.441	1.17	1.717	2.004	2.096	2.065	1.961	1.82	1.663	1.504	1.349	1.203	1.069	0.947	0.836	0.738	0.649	0.571	0.502
30	0	0.079	0.372	0.727	1.008	1.182	1.264	1.276	1.242	1.179	1.1	1.013	0.924	0.836	0.753	0.675	0.603	0.537	0.477	0.423
35	0	0.01	0.096	0.263	0.447	0.601	0.707	0.768	0.791	0.786	0.76	0.722	0.676	0.626	0.574	0.523	0.474	0.428	0.385	0.345
40	0	0.001	0.02	0.082	0.175	0.275	0.362	0.427	0.47	0.492	0.497	0.489	0.471	0.448	0.42	0.391	0.36	0.33	0.301	0.273
45	0	0	0.003	0.022	0.061	0.113	0.169	0.22	0.26	0.289	0.306	0.314	0.313	0.306	0.295	0.28	0.263	0.246	0.227	0.209
50	0	0	0	0.005	0.018	0.042	0.073	0.105	0.135	0.16	0.179	0.191	0.198	0.2	0.198	0.193	0.186	0.177	0.166	0.155

<b>105</b>	<b>110</b>	<b>115</b>	<b>120</b>	<b>125</b>	<b>130</b>	<b>135</b>	<b>140</b>	<b>145</b>	<b>150</b>	<b>155</b>	<b>160</b>	<b>165</b>	<b>170</b>	<b>175</b>	<b>180</b>	<b>185</b>	<b>190</b>	<b>195</b>	<b>200</b>
0.144	0.133	0.122	0.112	0.102	0.093	0.084	0.076	0.069	0.062	0.055	0.05	0.045	0.04	0.036	0.032	0.028	0.025	0.023	0.02
0.192	0.175	0.159	0.143	0.13	0.117	0.105	0.094	0.084	0.075	0.067	0.06	0.053	0.047	0.042	0.038	0.033	0.03	0.026	0.023
0.247	0.222	0.2	0.179	0.16	0.143	0.128	0.114	0.101	0.09	0.08	0.071	0.063	0.055	0.049	0.043	0.038	0.034	0.03	0.027
0.308	0.275	0.245	0.218	0.193	0.171	0.152	0.134	0.119	0.105	0.093	0.082	0.072	0.064	0.056	0.05	0.044	0.038	0.034	0.03
0.374	0.331	0.292	0.258	0.227	0.2	0.176	0.155	0.137	0.12	0.106	0.093	0.082	0.072	0.063	0.055	0.049	0.043	0.038	0.033
0.441	0.387	0.339	0.298	0.261	0.229	0.2	0.176	0.154	0.135	0.118	0.103	0.091	0.079	0.07	0.061	0.053	0.047	0.041	0.036
0.504	0.439	0.383	0.334	0.292	0.255	0.222	0.194	0.169	0.148	0.129	0.113	0.099	0.086	0.075	0.066	0.058	0.05	0.044	0.039
0.559	0.485	0.422	0.366	0.319	0.277	0.241	0.21	0.183	0.159	0.139	0.121	0.105	0.092	0.08	0.07	0.061	0.053	0.047	0.041
0.602	0.521	0.451	0.391	0.339	0.294	0.255	0.222	0.193	0.168	0.146	0.127	0.111	0.096	0.084	0.073	0.064	0.056	0.049	0.042
0.63	0.544	0.47	0.407	0.352	0.305	0.264	0.229	0.199	0.173	0.15	0.131	0.114	0.099	0.086	0.075	0.065	0.057	0.05	0.043
0.639	0.552	0.476	0.412	0.356	0.309	0.268	0.232	0.201	0.175	0.152	0.132	0.115	0.1	0.087	0.076	0.066	0.058	0.05	0.044
0.63	0.544	0.47	0.407	0.352	0.305	0.264	0.229	0.199	0.173	0.15	0.131	0.114	0.099	0.086	0.075	0.065	0.057	0.05	0.043
0.602	0.521	0.451	0.391	0.339	0.294	0.255	0.222	0.193	0.168	0.146	0.127	0.111	0.096	0.084	0.073	0.064	0.056	0.049	0.042
0.559	0.485	0.422	0.366	0.319	0.277	0.241	0.21	0.183	0.159	0.139	0.121	0.105	0.092	0.08	0.07	0.061	0.053	0.047	0.041
0.504	0.439	0.383	0.334	0.292	0.255	0.222	0.194	0.169	0.148	0.129	0.113	0.099	0.086	0.075	0.066	0.058	0.05	0.044	0.039
0.441	0.387	0.339	0.298	0.261	0.229	0.2	0.176	0.154	0.135	0.118	0.103	0.091	0.079	0.07	0.061	0.053	0.047	0.041	0.036
0.374	0.331	0.292	0.258	0.227	0.2	0.176	0.155	0.137	0.12	0.106	0.093	0.082	0.072	0.063	0.055	0.049	0.043	0.038	0.033
0.308	0.275	0.245	0.218	0.193	0.171	0.152	0.134	0.119	0.105	0.093	0.082	0.072	0.064	0.056	0.05	0.044	0.038	0.034	0.03
0.247	0.222	0.2	0.179	0.16	0.143	0.128	0.114	0.101	0.09	0.08	0.071	0.063	0.055	0.049	0.043	0.038	0.034	0.03	0.027

